David P. Knops

# Effects of the foreshore and heterogeneities of the subsoil on the safety analysis of piping

**Master Thesis**

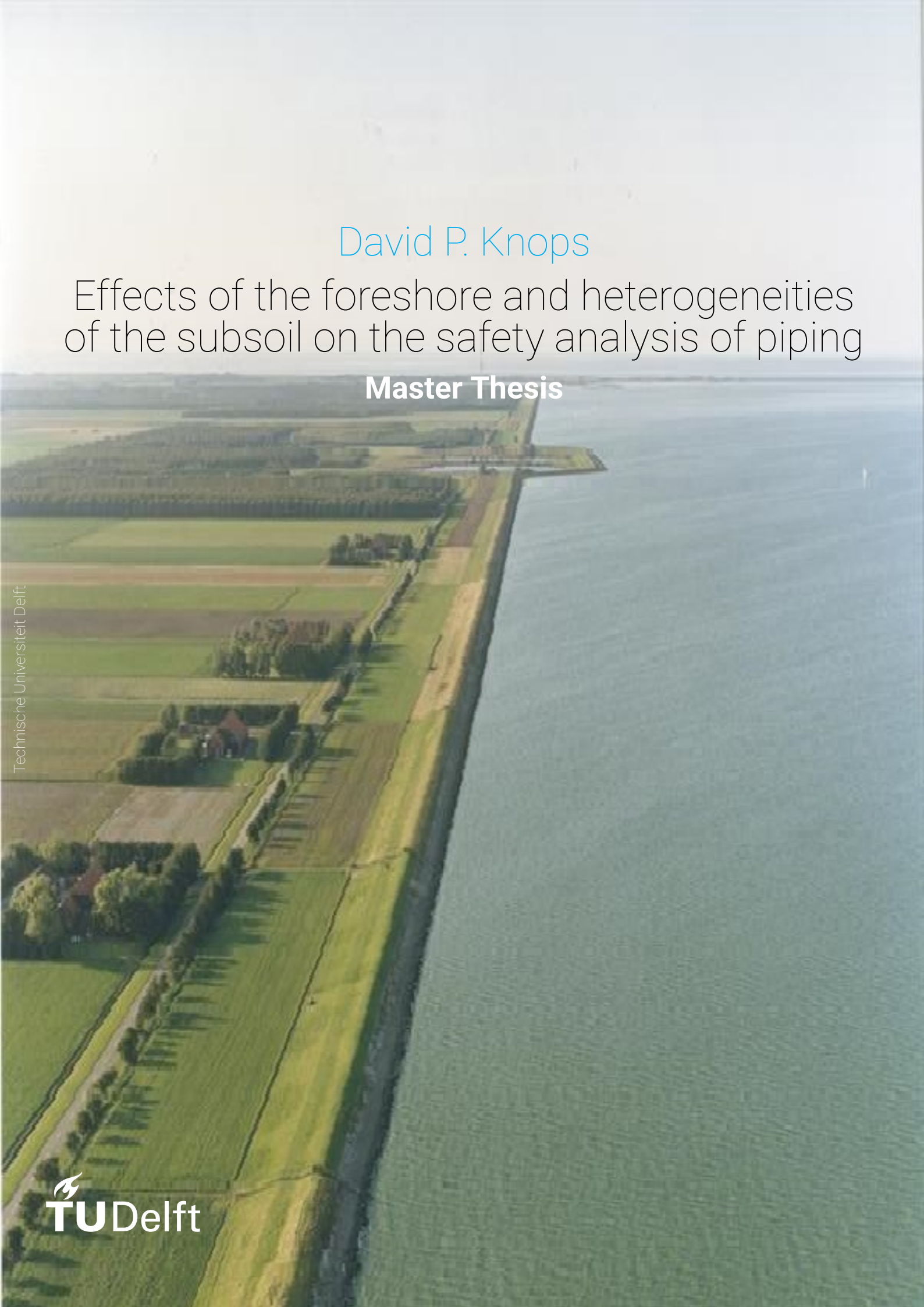

Technische Universiteit Delft

TU Delft

# Effects of the foreshore and heterogeneities of the subsoil on the safety analysis of piping

Master Thesis

by

David P. Knops

To obtain the degree of Master of Science
at the Delft University of Technology,
to be defended publicly on 05-12-2018

| | |
|---|---|
| Student number: | 4218019 |
| Project duration: | February, 2018 – December, 2018 |

| | | |
|---|---|---|
| Chairman committee: | Prof. Dr. Ir. M. Kok | TU Delft |
| Thesis committee: | Dr. Ir. W. Kanning | TU Delft |
| | Dr. Ir. A. P. van den Eijnden | TU Delft |
| | Ir. W. L. A. ter Horst | HKV Lijn in water |
| | Ir. J. J. Heerema | Rijkswaterstaat |

*Cover image: https://beeldbank.rws.nl, Rijkswaterstaat*

TU Delft

HKV LIJN IN WATER

# Preface

This thesis forms the completion of the master track Hydraulic Engineering, with specialization Flood Risk at Delft University of Technology. This research was carried out at HKV Lijn in Water, located at Delft and Lelystad.

As a start I would like to thank my thesis committee for their help, inspiration, motivation and expertise, which guided me through this period of research. I would specially like to thank Ir. W.L.A. ter Horst from HKV, my daily supervisor, for his critical view, his feedback and his advice about the subject during all the meetings we had. Also Dr. Ir. W. Kanning for sharing his knowledge and enthusiasm about the subject. Despite him being abroad, I could always ask for his input or advise by email or during one of our Skype sessions. Ir. J.J. Heerema and Dr. Ir. A.P. van den Eijnden for their critical view at my approach and reports during the committee meetings. Also a big thanks to Prof. Dr. Ir. M. Kok for his advice, guidance and directing the committee meetings as the chair of my thesis committee.

I also would like to thank my colleagues at HKV for the fun conversations we had during coffee breaks or at the lunch table. They were always ready to help if I had a question or a problem. I want to thank my family for always supporting me and last of all my friends for making my study time at Delft University of Technology a great time.

*David P. Knops*
*Delft, December 2018*

# Summary

In this thesis the influence of a foreshore and heterogeneities in the subsoil on the piping safety analysis is researched. The Netherlands is very vulnerable to floods and therefore lots of dikes are present along the shore and main rivers. These dikes can fail in several ways. One way is by means of pipe formation below a dike body. Pipe formation occurs due to eroding particles from the sandy subsoil below the dike. Erosion starts when high water level differences across the dike occur. The eroding particles are transported out of the subsoil to the surface through a fracture in the inland cover layer. This fracture can only occur if the pressures below this cover layer exceed the weight of the cover layer. If the fracture is present, pipe formation starts here and progresses to the outer water at the other side of the dike, leaving a pipe below the dike and thereby eventually leading to an open connection between the outer water and the inside of the dike. When this open connection occurs, the erosion starts to speed up and the dike will collapse after some time.

Piping is a complex problem and is investigated a lot in the last century. In 2006 J. Sellmeijer came up with a design formula. This formula was revised and adapted in 2011. The revised formula from 2011 is the currently used design formula for the piping safety analysis in the Netherlands. The Sellmeijer formula is derived for homogeneous, uniform soil conditions. The subsoil is, however, very heterogeneous and it is therefore expected that the Sellmeijer formula underestimates the resistance against piping of a cross-section. In the current safety analysis, the influence of the foreshore is described in a certain way in which a representative seepage length, which can be put into the Sellmeijer formula, is calculated. This seems a good approach, but the effects of the presence of holes on a foreshore are not incorporated in detail in the safety analysis.

In this thesis the influence of a foreshore and heterogeneities in the subsoil is investigated by use of the numerical D-Geo Flow model. In this numerical model, cross-sections can be created in which heterogeneities and variations in geometry can be applied and results can be generated. D-Geo Flow calculates the groundwater flow, the water flow along the pipe and the limit state equilibrium of the particles in the pipe. The results computed with D-Geo Flow are not verified, as the model is, for now, only validated for simple configurations. This study proves that for more complex geometries, the model approaches the results from the Sellmeijer formula in the limits.

The research in this thesis is done for the two subjects, the foreshore and the subsoil heterogeneities, separately. For both research parts a general study and a case study is done. In the general foreshore study, the influence of the length of the foreshore and the flow resistance of the foreshore cover layer is determined. In the foreshore case study research, local foreshores are modelled and the influence of permeability and holes on these foreshores is determined. In the soil heterogeneity general research, the influence of a resistance layer in the cross-section is determined. This resistance layer is a continuous horizontal layer throughout the whole cross-section. The influence of the depth and flow resistance of this layer is searched for. In the case study heterogeneity research, local subsoil compositions are made based on local and regional data. From these compositions, heterogeneities were identified. The influence of a specific heterogeneity is then searched for.

The current approach of reducing the seepage length if a foreshore cover layer is relatively permeable seems the right approach, based on the findings in this thesis. However, the extent of reduction and the exact approach is questionable, but was not searched for in this thesis. It can, based on the findings in this thesis, be concluded that the influence of a hole on the foreshore is significant and the condition of this hole is very important for the outcome of the safety analysis. If a hole on the foreshore does not reach the aquifer, but some resistance against flow is present, the increases in safety analysis result can be approximately 20-30%, based on the cases and assumptions in this thesis. An improvement on the piping safety analysis would therefore be to assess holes on the foreshore in more detail.

From the heterogeneity research it can be concluded that a heterogeneous subsoil is more resistant to piping than homogeneous soils, as used in the Sellmeijer formula. The identified heterogeneities in this thesis

influenced the critical head result positively as well as negatively. But out of nine identified heterogeneities , only two had a negative influence. The influence of the identified heterogeneities ranged from -26% to +139%. From the general research the conclusion can be drawn that a resistance layer, crossing the whole cross-section, always increases the resistance against piping. It was beforehand expected that this positive influence would increase with increasing flow resistance of the resistance layer until a maximum was achieved when the layer is impermeable. The research proved however that for some geometries, the largest positive influence was found for resistances between 20-500 days, which is not at impermeability. This phenomenon is described as "one-way sealing".

Finally is can be said that the research objective: *"Improve the piping safety analysis by including the effects of the foreshore and soil heterogeneities."* is met, as more knowledge is gained of the influence of a foreshore and heterogeneities in the subsoil. This knowledge can be applied on the decisions which have to be made in the piping safety analysis.

# Contents


**Summary** v

**1 Introduction** 1
- 1.1 Subject introduction . . . 1
- 1.2 Introduction into piping . . . 2

**2 Research description** 3
- 2.1 Problem Statement . . . 3
- 2.2 Research objective . . . 4
- 2.3 Research questions . . . 4
- 2.4 Approach . . . 4

**3 Literature and Background study** 7
- 3.1 Piping . . . 7
  - 3.1.1 Piping mechanism . . . 7
  - 3.1.2 Piping research through history . . . 8
  - 3.1.3 Piping assessment in the Netherlands . . . 9
  - 3.1.4 Historical piping cases in the Netherlands . . . 12
- 3.2 Variabilities in the subsoil . . . 13
  - 3.2.1 Heterogeneity . . . 13
  - 3.2.2 Anisotropy . . . 13
- 3.3 Subsoil study . . . 13
  - 3.3.1 Introduction . . . 13
  - 3.3.2 Dutch subsoil . . . 14
  - 3.3.3 Soil samples . . . 15
  - 3.3.4 Soil characteristics . . . 15

**4 Case selection and standard model set-up** 19
- 4.1 Case introduction: Lekdijk . . . 19
- 4.2 Standard model set-up . . . 20
  - 4.2.1 Standardization of the cases . . . 20
  - 4.2.2 Boundary conditions . . . 20
  - 4.2.3 Geometry of the model . . . 21
  - 4.2.4 Model set-up and validation . . . 22

**I Foreshore** 23

**5 General Foreshore research** 27
- 5.1 Introduction . . . 27
- 5.2 Standard model and approach . . . 27
- 5.3 Results . . . 29
- 5.4 Analysis . . . 29

**6 Case study specific research** 31
- 6.1 Geometry information . . . 31
  - 6.1.1 Foreshore geometry of Salmsteke . . . 32
  - 6.1.2 Foreshore geometry of Honswijk . . . 32
  - 6.1.3 Foreshore geometry of Den Oord . . . 32
- 6.2 Modelling the foreshore . . . 33
  - 6.2.1 Introduction and assumptions . . . 33
  - 6.2.2 Standard foreshore models . . . 33

6.3 Variations of the foreshore . . . 36
6.3.1 Introduction . . . 36
6.3.2 Variations in the models . . . 36
6.4 Sensitivity analysis . . . 38
6.4.1 Hydraulic conductivity of the foreshore . . . 38
6.4.2 Width of the holes on the foreshore . . . 40
6.4.3 Depth of the holes on the foreshore . . . 41
6.4.4 Silting up of the holes on the foreshore . . . 42
6.5 Application general foreshore research on cases . . . 42
6.5.1 Application . . . 42
6.5.2 Adjustment of the application of the general research on the cases . . . 44

**7 Conclusions** **47**
7.1 General research . . . 47
7.2 Case study specific research . . . 47
7.2.1 Hydraulic conductivity of the foreshore . . . 47
7.2.2 Variation of the holes on the foreshore . . . 48
7.2.3 Application general research on case studies . . . 49

**II Soil heterogeneities** **51**

**8 General soil heterogeneity research** **55**
8.1 Introduction and model set-up . . . 55
8.2 Results . . . 57
8.3 Analysis . . . 58

**9 Case study specific soil heterogeneity research** **61**
9.1 Introduction/Approach . . . 61
9.1.1 Creating the cross-section . . . 61
9.2 Heterogeneities in the Case cross-sections . . . 61
9.2.1 Salmsteke cross-section . . . 61
9.2.2 Honswijk cross-section . . . 64
9.2.3 Den Oord cross-section . . . 67
9.3 Modelling the heterogeneities . . . 69
9.3.1 Salmsteke . . . 69
9.3.2 Honswijk . . . 70
9.4 Analysis of the results . . . 71
9.4.1 Analysis Salmsteke results . . . 71
9.4.2 Analysis Honswijk results . . . 73

**10 Conclusions** **77**
10.1 General soil heterogeneity research . . . 77
10.2 Case study specific soil heterogeneity research . . . 77
10.2.1 Heterogeneities in the cross-section . . . 77
10.2.2 Application general research . . . 78

**III Discussion, Conclusions and Recommendations** **79**

**11 Discussion** **81**
11.1 Foreshore . . . 81
11.2 Soil heterogeneity research . . . 85

**12 Conclusions** **89**
12.1 Introduction . . . 89
12.2 Conclusions Foreshore . . . 89
12.3 Conclusions Soil heterogeneities . . . 90

**13 Recommendations and further research** **91**
13.1 Introduction . . . 91
13.2 Implementing the results in the safety analysis . . . 91
13.3 Further research . . . 91

**Glossary** **93**

**List of Symbols** **95**

**List of Figures** **97**

**List of Tables** **101**

**Bibliography** **103**

**IV Appendices** **105**

**A Piping research through history** **107**

**B Appendix: Samples subsoil study** **111**

**C Soil characteristics** **117**

**D D-Geo Flow** **121**
D.1 Introduction . . . 121
D.2 Working with D-Geo Flow . . . 121
D.3 Limitations of D-Geo Flow . . . 123

**E Appendix: Results foreshore sensitivity analysis** **125**
E.1 Hydraulic conductivity of the foreshore . . . 125
E.2 Width of the entry points . . . 127
E.3 Depth of the entry points . . . 130
E.4 Silting up of the entry points . . . 133

**F Appendix: Generic Foreshore results** **137**
F.1 Initial seepage length = 50m . . . 137
F.2 Initial seepage length = 100m . . . 137
F.3 Representative seepage lengths . . . 138

**G Appendix:Case samples** **141**
G.1 Salmsteke . . . 141
G.2 Honswijk . . . 145
G.3 Den Oord . . . 147

**H Appendix: GeoTop model** **149**
H.1 Introduction . . . 149
H.2 Description of the model . . . 149
H.3 Determining the soil types(lithoclasses) . . . 150
H.4 Model uncertainties . . . 152

**I Appendix: Results generic subsoil research** **153**
I.1 Hydraulic conductivity aquifer = 20m/day . . . 153
I.2 Hydraulic conductivity aquifer = 40m/day . . . 157

**J Appendix: Results heterogeneity models** **161**
J.1 Salmsteke . . . 161
J.2 Honswijk . . . 163

# 1 Introduction

## 1.1. Subject introduction

The Netherlands is very vulnerable to floods. Not only because large parts of the Netherlands are located below sea level, but also because it's home to some large rivers like the Rhine and the Meuse. Because of this continuing threat of flooding, the Netherlands has always been busy protecting itself against this threat. To have a consistent and regulated protection against flooding, the rules concerning flood protections are regulated by law.

This law is named the Dutch Water Act. In this act, design and assessment rules for all the flood protections in the Netherlands are stated.

As described above, the Netherlands has a very large flood protection system. This flood protection system consists of "natural defences" like dikes and dunes, but also of "artificial defences" like sluices, locks and barriers. Another separation is made between "primary" and "regional" flood defences. Primary defences protect the land against floods from mainly the North Sea (and its branches), the Wadden Sea and the main rivers (Rhine and Meuse). The Netherlands is protected by around 3500 km of primary defences. Regional defences are all the non-primary defences. Regional dikes protect the land from floods from inland water.

After the flood of 1953, the flood protection system of the Netherlands was changed under the influence of the "Delta-committee". This lead to the Delta-Works, but also to a new insight in flood protection. Flood defences had to be designed and assessed based on the probability of exceedance of a certain water level. This water level was defined based on the consequence in case of flooding. For years this was the standard norm of flood defences [2].

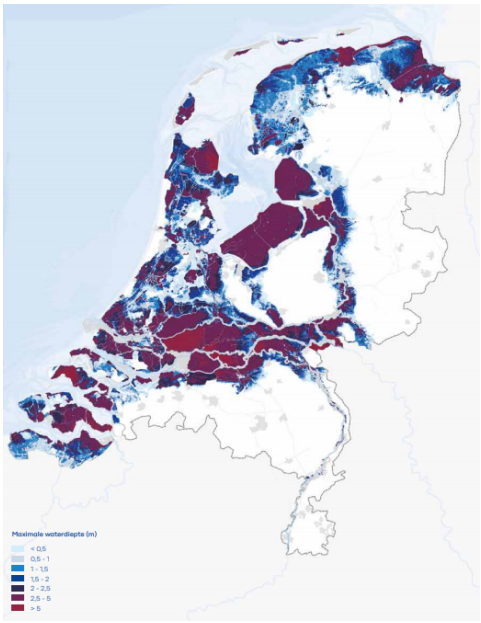


Figure 1.1: Water depth in the Netherlands in case of flooding [1]

In 2017, the philosophy changed. Instead of a norm based on the exceedance of a certain water level, the new norm is based on the risk of flooding. The risk of flooding is a combination of probability and the consequences [1]. Flooding is dependent on failure. Failure is the incapability of a dike to retain the outer water. Flood defences can fail in different ways. These ways are called failure mechanisms. The failure mechanisms can occur separately, but can also influence each other. An overview of the failure mechanisms of a dike can be seen in fig. 1.2.

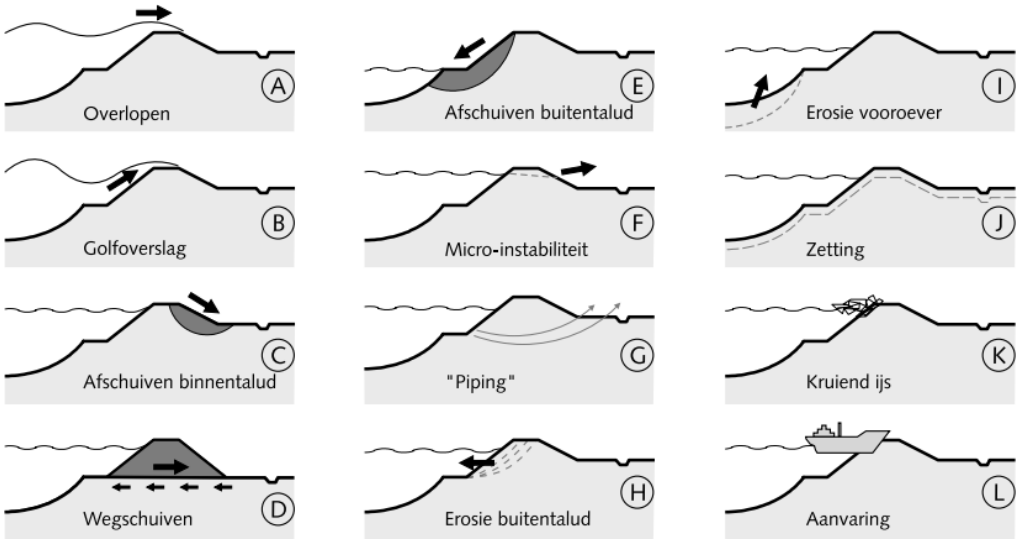


Figure 1.2: Failure mechanisms [3]

## 1.2. Introduction into piping

One of the major failure mechanisms of dikes is piping, particularly Backward Erosion Piping (from now on called piping). Piping consists of 3 main stages: *Uplift*, *Heave* and *Piping*. Piping is the erosion process of sand particles in an aquifer covered by in impermeable cohesive layer (the blanket). An aquifer is a water-bearing permeable layer. When piping occurs, particles are transported from the aquifer to the surface, causing the formation of little channels, the so called *pipes*. The formation of pipes may, eventually, have effects on the stability of the dike and even cause dike failure. Piping is the main subject of this thesis and the process of piping will be explained in more detail in section 3.1.1.

The assessment for piping in the Netherlands is based on rules developed by J.B.Sellmeijer (1988), which were adjusted in 2011. Sellmeijer describes the equilibrium of the soil particles, more information about the method can be found in section 3.1.2. A lot of research has been done to understand the processes of piping, but still a lot is unknown. A major insecurity is the fact that soils are very variable. Because piping depends for a major part on the soil conditions, a lot can be gained when these insecurities are reduced.

In the piping safety analysis, based on the rules of Sellmeijer, some soil characteristics are needed. To make a safe prediction of unknown characteristics, the characteristics of the soil are chosen in a conservative way in the Netherlands. This, on one hand, leads to a safe prediction and could therefore be assumed a good prediction, but on the other hand it leads, most likely, to an underestimation of the actual strength and thereby higher costs.

# 2
# Research description

In this chapter this Thesis will be introduced and described. First the problem will be stated, after which the research objective and research question will be formed.

## 2.1. Problem Statement

Sellmeijer's formula (2011) is the core for the current piping safety analysis for dikes. Although the formula by Sellmeijer describes the erosion process more accurately than the old analysis rule of Bligh (1910), some remarks can be placed.

Sellmeijer's formula is based on a standard geometry: an impermeable cohesive layer covering a permeable homogeneous aquifer. In practice, the shallow subsurface in the Netherlands is strongly heterogeneous[4]. These heterogeneities are present on a micro- and macro-scale. On a micro-scale, the porosity and the grain sizes throughout the layer may vary [4]. Also the placement direction of the grains may vary. Grains are never completely round and, because of their alluvial deposition, they are placed on their flat side. This placement orientation results in an directional inequality in the ease of water flow through the layer. This ease of flowing is called the hydraulic conductivity. The inequality of hydraulic conductivity between the horizontal and vertical direction is called *anisotropy*. On a macro-scale, the aquifer may contain different sub-layers like clay or gravel layers [4]. Another macro-scale heterogeneity is the presence of anomalies in the aquifer, like, for instance, an old river bed [5].

Sellmeijer's formula was based on 2D steady flow and describes the progression of the pipe. Studies [6] [7] revealed that the 2D assumption is incorrect and may lead to unsafe predictions about the critical head/gradient. Assuming steady flow, according to laboratory experiments, is conservative. The response of the aquifer to changes in the hydraulic boundary conditions is timedependent and therefore not completely steady [7].

Unless some remarks can be placed, Sellmeijer's formula is the base of the piping safety analysis in the Netherlands. As the formula acquires several characteristics of the soil and the geometry of the cross-section, data is needed. For the soil , however, the exact composition and characteristics are uncertain. Nowadays the soil is not mapped in enough detail to acquire the enough information to create a cross-section, which is representative enough to give a realistic outcome of the safety analysis. This means some assumptions have to be done. Due to the uncertainty, the soil is assumed to be homogeneous with conservative chosen characteristics.

In the piping safety analysis the geometry of the cross-section, for instance the foreshore, can be of influence on the result of the safety analysis. It is unclear when and under which conditions the foreshore has to be incorporated in the safety analysis. The uncertainty of the influence of the foreshore leads to a safe and conservative choice whether the foreshore has to be included or not. Next to that, the location of the foreshores (outside the dike protection zone), makes it, due to political boundaries, hard to incorporate it in the safety analysis.

Conservative choices are used to overcome uncertainties. Making conservative choices seem to be a good approach, because it leads to safe dikes. However, conservative choices and thereby underestimation of the

strength can lead to an over-designed dike, which lead to unnecessary costs. An increase in the accuracy in the safety analysis for piping would reduce these unnecessary costs.

## 2.2. Research objective

As stated above in the problem statement (section 2.1), the choices in the safety analysis for piping are, due to uncertainties, conservative and can lead to unnecessary costs. The safety analysis can be improved when more knowledge is gained about the influence of the foreshore and heterogeneities in the subsoil and this knowledge can be applied in the safety analysis, resulting in a more realistic outcome. The research objective can therefore be described as:

*"The research objective of this thesis is to improve the piping safety analysis by including the effects of the foreshore and soil heterogeneities."*

## 2.3. Research questions

The main research question of this thesis is:

*"What is the effect of the foreshore and soil heterogeneities on the result of the piping safety analysis?".*

To answer this research question, a research will be conducted by use of case studies. These case studies will be defined later. To give a stepwise approach to answer the research question, sub-research questions are defined in two parts, one with the focus on the foreshore (part I) and one with the focus on the soil heterogeneities (part II):

1. 
   - How can the available data be translated to representative foreshore scenarios?
   - How can these scenarios be modelled in D-Geo Flow?
   - What is the result of the foreshore scenarios from D-Geo Flow?
   - What is the difference between the results from D-Geo Flow and the result from the current safety analysis?
   - How can the influence of the foreshore be incorporated in the safety analysis?
2. 
   - How can the available data be translated to representative soil scenarios with local heterogeneities?
   - What is the result of the soil scenarios from D-Geo Flow?
   - What is the difference between the results from D-Geo Flow and the result from the current safety analysis?
   - How can the influence of the soil heterogeneities be incorporated in the safety analysis?

## 2.4. Approach

The focus of this thesis is to search for the influence of a foreshore and heterogeneities. The first step is understanding the problem. This is done by studying literature. From the literature study, knowledge of the piping mechanism, how it is assessed in the Netherlands and what parameters are of influence, is amassed. This literature study is the start of the research and will be followed by a number of steps to give answer to the research question.

Cases are used as the core of this thesis. The chosen cases have to be relevant for this research and must, at least, include a foreshore. The cases are chosen along the river *Lek*, because of the availability of data from the safety analysis. This availability of data of the safety analysis gives also good insights in which values are used for the parameters in the analysis.

To search for the influence of the foreshore and soil heterogeneities, a model must be used. In this research the model D-Geo Flow is used, which will be explained later on in this thesis. Per case a standard model will be set-up. As in the different cases, different values for certain parameters are used, the outcome of the cases is hard to compare. Therefore the depth of the aquifer, the hydraulic conductivity of the aquifer and the grain size will be transformed to standardized values.

To asses the influence of the foreshore, case specific information of the foreshore must be collected. By use of elevation maps and more local data, the geometry of the foreshore can be determined. After the geometry is

determined, some information about the soil characteristics in the foreshore must be collected. To limit the variability in the foreshore, it is assumed to have a homogeneous composition. For this homogeneous composition, characteristics must be assumed. For all the cases, the same foreshore characteristics will be used to prevent the additional effect on the result when other characteristics are used. When the information about the geometry and the characteristics of the foreshore is known, the standard foreshore models per case can be set-up. Depending on the geometry of the foreshore, some variations on the standard foreshore models are made to see how certain factors influence the result. The variations are made based on the uncertainty in assumptions by setting up the standard foreshore model and on expert judgement.

For the assessment of the influence of the heterogeneities, information about the subsoil is needed. As the soil is very variable and lots of heterogeneities can be present, only the Holocene layer is mapped in more detail. In the assumptions for the standard model a depth of 30m is assumed. The Holocene layer will not reach this depth. Beneath the Holocene layer a Pleistoceen layer is present. The Pleistoceen layer below the Holocene layer will be assumed to be homogeneous. The first step in modelling the subsoil is to determine, per case, the depth of the Holocene-Pleistoceen boundary. After the boundary is known from local data, the subsoil can be mapped. After the soil is mapped, the heterogeneities, on aquifer scale, which can be identified are named. To see how the heterogeneities influence the results, they will be added to the standard model per case one at a time. The geometrical and soil characteristics of heterogeneities will be varied to overcome the uncertainties.

After the results of both focus areas are generated, the results will be analysed and conclusions will be drawn based on the analysis. The limits of this thesis and in the choices made, will be discussed in the discussion, after which recommendation for further research will be made.

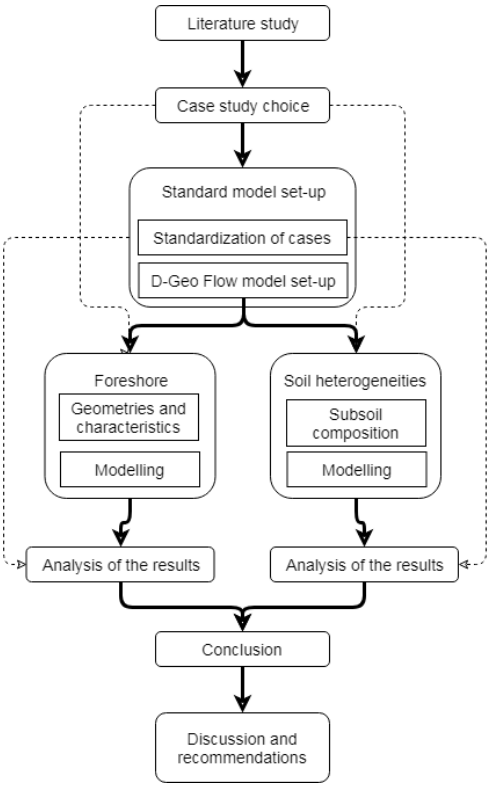


Figure 2.1: The approach depicted in a scheme

# 3

# Literature and Background study

## 3.1. Piping

### 3.1.1. Piping mechanism

Piping is the erosion process of sand particles in an aquifer covered by in impermeable cohesive layer(the blanket). An aquifer is a water-bearing permeable layer. When piping occurs, particles are transported from the aquifer to the surface, causing the formation of little channels, the so called *pipes*. The forming of pipes may, eventually, have effects on the stability of the dike and even cause a dike failure.

For piping to occur, some condition must be present. Firstly, the dike section geometry must be sensitive to piping. Piping can only occur in a aquifer, covered by a cohesive, impermeable layer[4]. The cohesive layer op top of the piping sensitive layer(the aquifer) is needed, because a "roof" must be present to prevent the collapse of the pipe(s)[4],[8].

Secondly, the hydraulic boundary conditions for piping to occur must be present. Transport of particles can only occur if water flow through the aquifer, from the upstream side of the dike(the wet side) to the downstream side(the dry side), is present. The upstream side water level is, for clarity, from now on called the outer water level an the downstream side water level is called the inner water level. The transport of sand particles is caused by a significant hydraulic gradient over the aquifer. The hydraulic gradient is the outer water level minus the inner water level. Dike sections with high outer water levels with a low inner water level are therefore vulnerable to piping.

Pipes below the cohesive layer are formed when sand particles from the aquifer are washed out. For particles to wash out, an open and unfiltered exit must be present[4]. In case of a cohesive impermeable layer on top of the aquifer, the open exit is formed due to hydraulic fracturing. In case of hydraulic fracturing, high water pressures, caused by a high outer water level, cause the blanket to crack under *uplift* pressures[5]. The open, unfiltered exit, the exit channel, allows the water flow to increase and to wash out sand particles from the aquifer. The exit channel is filled with the sand particles from the aquifer, these particles are fluidized[9]. This fluidization is caused by pore pressures exceeding the effective stresses of the particles, turning it into a fluid state[4].

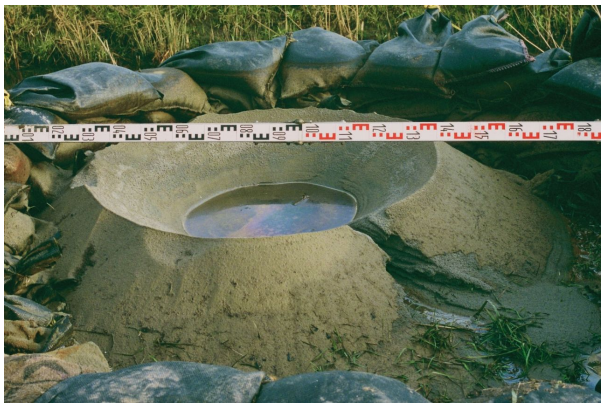

Figure 3.1: Sand boil

When these fluidized particles are washed out, the initiation of the pipe(s) below the blanket have started, this is called *heave*. The washed-out particles are deposited around the exit channel, resulting in sand boils at the surface, as can be seen in fig. 3.1.

After the initiation of the pipe has started, the pipe may progress. The pipe progresses from the inner to the outer side. This process is called *backward erosion piping*. During backward erosion piping, sand particles may continue to erode. This progressive process is more or less uniform, until a length of around 40% of the total seepage path. When this length is reached, the progression will accelerate until it reached the outer side[8]. When the outer side is reached, an open connection is formed through the aquifer between the inner and outer side[5]. When the open connection is present, the resistance of the sand particles disappears. This reduction of resistance, allows the water to flow freely through the pipe(s). Causing a rapid increase in flow velocity[4]. A rapid increase in flow erodes sand particles around the pipe(s), causing a widening of the pipe(s). The formation of these hollow spaces below the dike result in subsidence or fracture of the dike and eventually failure. An overview of the steps in the piping process can be seen in fig. 3.2.

The above described process occurs when the hydraulic gradient is large enough for the pipe(s) to progress. However, after the initiation of the pipe has occurred, the progression of the pipe can form a new equilibrium, depending on the hydraulic gradient throughout the layer. If this new equilibrium is reached, the flow, caused by the gradient, is insufficient to erode particles. When the flow is insufficient, the sand boil will turn into a boil, which produces "clean" water[9], [10]. This equilibrium situation will hold until the flow is strong enough to erode the sand particles again. Reaching the equilibrium situation before failure also implies that the presence of sand boils do not always indicate a critical situation[11].

The conditions for and the process of piping, explained above, can often be found at river levees[4]. Studies show that piping has been an important failure mechanisms for river dikes in the USA, China and the Netherlands[12].

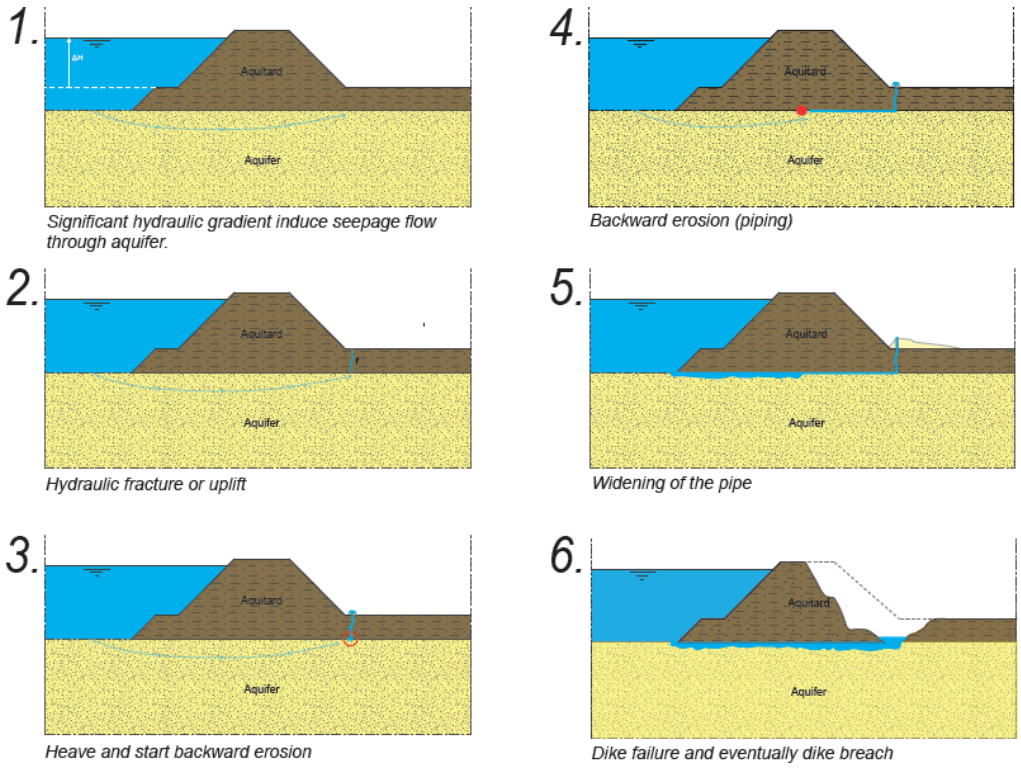


Figure 3.2: Piping process [13]

### 3.1.2. Piping research through history

Throughout the years, a lot of research has been done for piping.In this section the most important research will be named and explained. At the beginning of the 1900's, people became aware of the occurrence of piping. Several researchers have investigate the phenomenon of piping. A short explanation what they did is described in appendix A. The most important researcher, for this thesis, was Sellmeijer in 1998 and 2011.

**Sellmeijer(1988 & 2011)**
The method by Sellmeijer (1988) was the first method that theoretically accounted for the processes of piping [14]. He combined the equation for groundwater flow with flow equations in a pipe. The model of Sellemeijer is basically an equilibrium model that checks whether a critical development of the piping channel is reached [5]. To develop a model, he assumed a simplified situation. In his simplification he assumed a standard, simple geometry in which a permeable, homogeneous aquifer is covered by an impermeable (clay) blanket and/or levee. He assumed steady state seepage and a constant upper and lower head boundary. Sellmeijer assumed that the sediment transport in the pipe is dominated by erosion of particles at the bottom of the pipe [4]. The erosion of the particles is based on White's(1940) equilibrium approach [7]. The flow through the pipe is described as Poiseuille flow between two parallel boundaries.
Curve fitting on numerical calculations resulted in a formula, relating sand characteristics to geometric properties of the sand bed [15]. His model was was calibrated with large scale tests in the Delta Flume [16].

In 2011, the approach by J.B. Sellmeijer, was revised because of renewed knowledge. Through a multivariate analysis based on numerous conducted tests, the influence of various sand characteristics was determined [17]. Based on this analysis , the formula was adjusted in 2011. This adjusted design rule is the design standard for dikes(or levees) in the Netherlands. The adjusted design rule describes the critical hydraulic head as a product of three contributors: a resistance $F_R$, a scale $F_S$ and a geometry factor $F_G$ [8]:

$$\Delta H_c = L \cdot F_R \cdot F_S \cdot F_G \tag{3.1}$$

$$F_R = \eta \cdot \frac{\gamma_p^{'}}{\gamma_w} \cdot \tan\theta \left(\frac{RD}{RD_m}\right)^{0.35} \tag{3.2}$$

$$F_S = \frac{d_{70_m}}{\sqrt[3]{\kappa L}} \cdot \left(\frac{d_{70}}{d_{70_m}}\right)^{0.4} \tag{3.3}$$

$$F_G = 0.91 \cdot \left(\frac{D}{L}\right)^{\frac{0.28}{\left(\frac{D}{L}\right)^{2.8}-1}+0.04} \tag{3.4}$$

In which [13]:

| | |
|---|---|
| $\Delta H_c$ | = critical hydraulic head $[m]$ |
| $L$ | = Horizontal seepage length $[m]$ |
| $\eta_{'}$ | = White's constant $[-]$ |
| $\gamma_p^{'}$ | = unit weight of the soil particles $[kN/m^3]$ |
| $\gamma_w$ | = unit weight of water $[kN/m^3]$ |
| $\theta$ | = bedding angle[°] |
| $RD$ | = Relative density $[-]$ |
| $RD_m$ | = mean relative density from the small scale tests (=0.725) $[-]$ |
| $d_{70_m}$ | = mean $d_{70}$ in the small scale tests $(= 2.08 * 10^{-4})$ $[m]$ |
| $\kappa$ | = intrisic permeability $[m^2]$ |
| $d_{70}$ | = grain diameter for which 70% of the particles are smaller $[m]$ |

### 3.1.3. Piping assessment in the Netherlands
The assessment of the dikes in the Netherlands for piping consists of a multi staged approach[7] and is described in *"Bijlage iii, Sterkte en veiligheid regeling primaire waterkeringen 2017"*[18]. The first step is a check to determine if a dike section is sensitive to piping, this is the elementary assessment. If a section is sensitive to piping the section is subjected to a detailed assessment. In this detailed assessment, the three main stages of piping (uplift, heave and progression) are checked on their probability of occurrence.

**Elementary assessment**
In the elementary assessment, the dike section is checked on its piping sensitivity. Multiple characteristics of the dike section are assessed on their presence or absence. The check consists of 5 steps:

| | |
|---|---|
| Step 1: | Is the flood defence a dike or a dam? |
| Step 2: | Is the dike or dam made of clay on a sandy foundation? |
| Step 3: | Does the subsoil consist of only natural elements? |
| Step 4: | Does the dike or dam suffices the time-dependency conditions? |

Step 5: Does the dike or dam geometry suffices the geometry conditions?

If all these questions can be answered with "*YES*", the assessment can continue to the detailed assessment. If one of the first three questions can be answered with "*NO*", the dike section is not sensitive to piping. If the last two questions are answered with "*NO*"[1], the dike sections must be assessed with a "situation specific assessment" or "toets op maat". This "situation specific assessment" is an assessment, specifically designed for this dike section.

**Detailed assessment**

In the detailed assessment, the failure probability of a dike section for piping is determined by combining the lowest failure probabilities of the three main mechanisms(uplift, heave and progression). How these failure probabilities are determined will now be explained.

***Uplift***

The failure probability for *Uplift* is calculated using a stability factor $F_u$. This factor is calculated by dividing the critical head difference across the dike $\Delta\phi_{c,u}$ by the occurring head difference across the dike $\Delta\phi$. The translation from the stability factor to the failure probability will not be addressed, but can be seen in *"Bijlage iii, Sterkte en veiligheid regeling primaire waterkeringen 2017"*[18]. The critical head difference can be seen as the resistance against uplift and the occurring head difference as the load. The critical head difference is calculated according to eq. (3.5).

$$\Delta\phi_{c,u} = \frac{D_{blanket} \cdot (\gamma_{sat} - \gamma_{water})}{\gamma_{water}} \tag{3.5}$$

In which:

$D_{blanket}$ = Blanket thickness $[m]$
$\gamma_{sat}$ = Saturated unit weight of the blanket $[kN/m^3]$
$\gamma_{water}$ = unit weight of water $[kN/m^3]$

The occurring head difference is calculated according to eq. (3.6).

$$\Delta\phi = (h - h_{exit}) \cdot r_{exit} \tag{3.6}$$

In which:

$h$ = Hydraulic head at the outer side of the dike $[m]$
$h_{exit}$ = Hydraulic head at the exit point(ground level) $[m]$
$r_{exit}$ = Damping- or response-factor at exit point $[-]$

***Heave***

The failure probability for *Heave* is calculated using a stability factor $F_h$. This factor is calculated by dividing the critical heave gradient$i_{c,h}$ by the calculated heave gradient $i$. The translation from the stability factor to the failure probability will not be addressed, but can be seen in *"Bijlage iii, Sterkte en veiligheid regeling primaire waterkeringen 2017"*[18]. The critical heave gradient is assumed to be 0.3 in the assessment. The calculated heave gradient is calculated using eq. (3.7):

$$i = \frac{(h - h_{exit}) \cdot r_{exit}}{D_{blanket}} \tag{3.7}$$

In which:

$h$ = Hydraulic head at the outer side of the dike $[m]$
$h_{exit}$ = Hydraulic head at the exit point(ground level) $[m]$
$r_{exit}$ = Damping- or response-factor at exit point $[-]$
$D_{blanket}$ = Blanket thickness $[m]$

[1] The conditions for step 4 and 5 can be found in *"Bijlage iii, Sterkte en veiligheid regeling primaire waterkeringen 2017"*[18]

***Progression***
The failure probability for *Heave* is calculated using a stability factor $F_p$. The stability factor for progression is calculated using eq. (3.8):

$$F_p = \frac{\Delta H_c}{h - h_{exit} - r_c \cdot D_{blanket}} \tag{3.8}$$

In which:

| | |
|---|---|
| $\Delta H_c$ | = Critical head difference across the dike $[m]$ |
| $h$ | = Hydraulic head at the outer side of the dike $[m]$ |
| $h_{exit}$ | = Hydraulic head at the exit point(ground level) $[m]$ |
| $r_c$ | = Reduction factor for the exit head loss (=0.3, see intermezzo) $[-]$ |
| $D_{blanket}$ | = Blanket thickness $[m]$ |

**Intermezzo: 0.3d-rule [13]**
The hydraulic gradient used in the rule of Sellmeijer is reduced by a factor of 0.3 times the thickness of the blanket($D_{blanket}$) in situations with a covering layer (e.g. clay and / or peat) on a piping-sensitive sand or soil layer. By this reduction, The additional resistance of the fluidized sand grains in the uplift channel is taken into account. This reduction is known as the *"0.3d-rule"*.

The critical head difference across the dike($\Delta H_c$) is calculated using the rules of Sellmeijer (eq. (3.1)).

**Including foreshore in the safety assessment**
Including a foreshore in the safety analysis has effect on the seepage length, which is included in the Sellmeijer formula. However, due to seepage through the foreshore and presence of dips, its length can not just be added to the initial seepage length. Two aspects has to be examined in the use of the foreshore in the safety analysis:

1. The presence of a possible entry point on the foreshore;
2. The representative foreshore length.

*1. Presence of holes*
In the analysis, the presence of holes on the foreshore must be determined. These holes could be dips or waterways in the foreshore, where water penetrates through the foreshore into the aquifer or. If this is the case, the seepage length has to be chosen from this entry point to the exit point.

*2. Representative seepage length*
In the safety analysis the representative seepage length is determined by use of fig. 3.3. In this figure, $\lambda_1$ is the representative foreshore length.

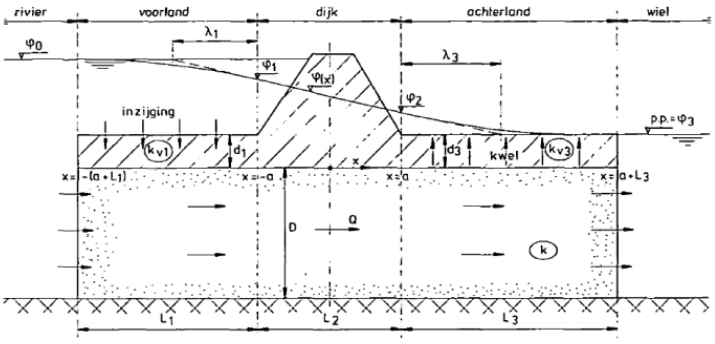


Figure 3.3: Determine the representative seepage length, foreshore[19]

This representative foreshore length ($\lambda_1$) is determined using the following formula:

$$\lambda_1 = \sqrt{k_{h_{aq}} * D_{aq} * \frac{d_f}{k_{f_v}}} \tag{3.9}$$

In which:

| | |
|---|---|
| $k_{h_{aq}}$ | = horizontal hydraulic conductivity of the aquifer; |
| $D_{aq}$ | = thickness aquifer; |
| $d_f$ | = thickness foreshore; |
| $k_{f_v}$ | = vertical hydraulic conductivity of the foreshore. |

$$L_{seep_{fic}} = \lambda_1 * \tanh \frac{L_1}{\lambda_1} \tag{3.10}$$

### 3.1.4. Historical piping cases in the Netherlands

In the Netherlands, no recent cases of dike failure due to piping occurred, although signs of pipe formation were observed in the form of sand boils. In the Netherlands, three dike failures due to piping are known and documented [9, 13]:

- Dike breach at Nieuwkuijk (1880)
- Dike breach at Tholen (1894)
- Dike breach at Zalk (1926)

The three dike failures are documented by laymen, unaware of the phenomenon piping. Piping was also not known at that time, the information about these cases is therefore questionable and is therefore not explained in more detail[9, 13].

Other cases in the Netherlands do not describe failure due to piping, but describe the formation of sand boils. During the high waters of 1993 and 1995, around 300 sand boils were observed along the main rivers (Rhine, Waal, IJssel and Meuse)[9].

Figure 3.4: Ringing of a sand boil[20]

In **1993**, high discharges through the Rhine and Meuse caused extremely high waters in the rivers. At around 120 places, sand boils were noticed: 40 along the Rhine, 40 along the Waal, 30 along the IJssel and 10 along the Meuse. As no dike failed, the sand boils didn't indicate a failure situation. This also due to the effectiveness of emergency mitigation measures, like boil ringing (see fig. 3.4)[20].

In **1995**, extremely high water levels occurred again. The water level of the Meuse was lower than in 1993, but the water level of the Rhine was higher. Sand boils, noticed in 1993, returned and some more were noticed. Around 180 sand boils were noticed during this high water. Most of them along the Rhine, Waal and Lek. Just like in 1993, no failures occurred, as emergency measure were taken to prevent dangerous situations [21].

## 3.2. Variabilities in the subsoil

In soils, lots of variabilities are present at different scales. Not only the composition of the soil can differ from place to place, also the characteristics of the soil can vary throughout a soil layer. In this part, some variabilities of the subsoil below a dike are explained.

### 3.2.1. Heterogeneity

Heterogeneity is a very wide concept. In general is the heterogeneity of a material referred to as non-uniform in the composition or one of the characteristics of this material.
In this case, large scale heterogeneity is referred to as a inhomogeneous composition of the subsoil. A heterogeneous subsoil is defined as a soil with two or more elements or layers. The soil in these layers or elements vary in characteristics. Small scale heterogeneity is referred to as varying characteristics throughout the same soil type. This can, for example, mean grain size differences in a soil type. A heterogeneous subsoil can, because of large and small scale heterogeneities, have more than one variation.

### 3.2.2. Anisotropy

When an element or body is anisotropic, it means that it has directional-dependent properties [13]. In this thesis, anisotropy is referred to as the directional difference of the hydraulic conductivity in a soil element or layer. The two directions which are dominant in this thesis are the vertical and horizontal direction.

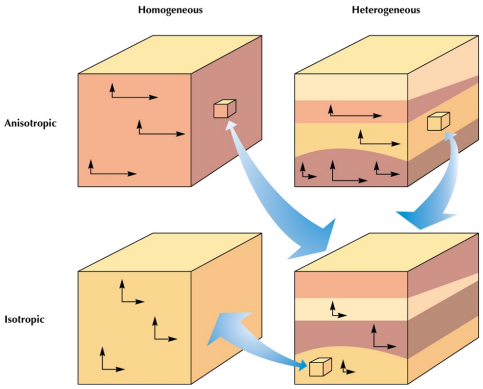

Figure 3.5: Anisotropy and Heterogeneity [22]

Anisotropic behaviour is therefore defined as an inequality in the horizontal and vertical component of the hydraulic conductivity.

Anisotropy, as defined above, is governed by the placing of the soil particles. As most of the particles are not perfect spheres, but prismatic, columnar or plate-shaped particles, the placement orientation affects the hydraulic conductivity [23]. Soil is mainly deposited by sedimentation processes, this sedimentation causes the particle arrangement to be more parallel than random[24]. From this, in combination with the fact that during sedimentation particles tend to land on their flat side, it can be concluded that the horizontal hydraulic conductivity is higher than the vertical hydraulic conductivity.

Anisotropy on a small scale can lead to anisotropy on a large scale. A subsoil, composed of multiple soil types can be anisotropic, even though most of the layers are isotropic. The magnitude of anisotropy of a subsoil therefore depends on the spatial variations in the subsoil, as well as the soil types composing this subsoil. In addition, the weight of the overlying material, the *"geostatic pressure"*, tends to reduce the hydraulic conductivity with depth [13].

The anisotropic conditions of a soil type are not very well known. Anisotropy is expressed in an anisotropy coefficient, dividing the horizontal hydraulic conductivity by the vertical hydraulic conductivity. In literature ranges are given, but no clear numbers. The value for the anisotropy coefficient, clearly, depends on the soil type. Soil types with more rounded particles, like sand and gravel, will have a lower coefficient than soils with plate-shaped particles, like clay. The choice for the anisotropy coefficient for the different soil types will be addressed later.

## 3.3. Subsoil study

### 3.3.1. Introduction

In this section the Dutch subsoil will be examined. The composition of the subsoil of the regions useful for this thesis will be analysed. This composition must be known to create models which are representative for the situation in practice. In this part, the areas of interest are the main river, lakes and coastal areas. As this thesis focusses on piping, the first 30-40m of the subsoil is of interest. The first 30-40m of the subsoil is

determined by Pleistoceen and Holocene deposits, on these will be focussed in this section.

### 3.3.2. Dutch subsoil

As stated in the introduction, flood defences are present near the coast, rivers and lakes. The subsoils in these areas are different due to their deposition. To make a distinction between the different areas in the Netherlands, a classification in made based on the parent material. Parent material is the upper layer of sediment. The different parent materials in the Netherlands, as can be seen in fig. 3.6, are:

- Fluviatile clay
- Marine clay
- Sand
- Peat
- Loess (Löss)

For the areas of interest, fluviatile clay and marine clay are the most important parent materials.

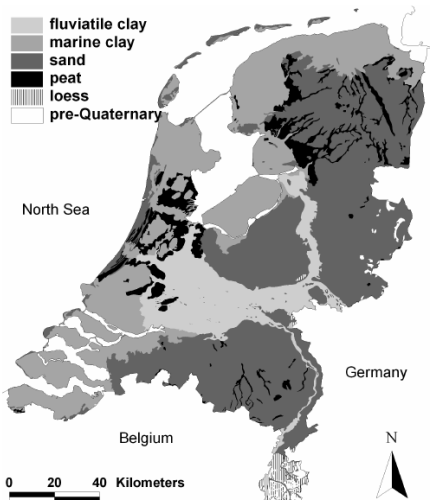


Figure 3.6: Parent material in the Netherlands [25]

**Fluviatile clay**

Fluviatile clay formations consist mainly of sand and clay deposited by the rivers Rhine, Meuse and IJssel. For the fluviatile clay district, two distinctions can be made based on their origin: the *Meuse valley* and the *River lands*. In both these areas the lower subsoil is dominated with coarse sand deposits from the Pleistoceen, these are linked to the Kreftenheye formation [26]. Locally also deposits of peat and loam can be present, these are deposited in the Boxtel formation [27], but in general it can be assumed that the lower subsoil consist of pleistoceen coarse sand.

For the *Meuse Valley* the subsoil mainly consists of sand, which gradually becomes finer going upward. In the Meuse Valley are also gravel deposits below a thin layer of sand are present [28]. The Meuse Valley is determined by deposits in the Beegden formation [29].

For the *River lands* the subsoil is determined by the formations of Echteld [30] and Naaldwijk [31]. However, the Naaldwijk formation is more a marine than a fluviatile formation. This also implies that the River Lands, as examined here, do not cover the whole area of the main rivers, but only cover the area of the Echteld formation, as can be seen in fig. 3.7. The River Lands subsoil is governed by fine to medium sand deposits with, locally, thin layers of clay.

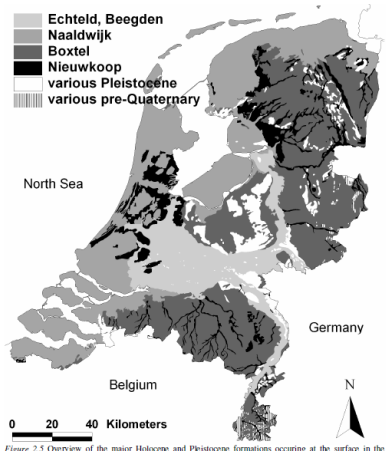


Figure 3.7: Holocene Formations [25]

**Marine clay**

The subsoils in the marine clay area consist mostly of Holocene deposits by the North Sea. Below the Holocene deposits, Pleistoceen deposits of coarse sand are present. As in fig. 3.7 can be seen, the main formation is the Naaldwijk formation [31]. Locally, the Nieuwkoop formation [32] is present. The Naaldwijk formation mainly consists of fine sand to heavy clay deposits. As the Naaldwijk formation covers a large area, variations are present in this area. To make a distinction based on the location, the Naaldwijk formation district is divided in the following regions:

- The *Delta* area: covering the south-west part of the Netherlands
- The *IJsselmeer* area: covering the area around the IJssel lake
- The *Waddenzee* area: covering the north east part of the Netherlands along the Wadden Sea

### 3.3.3. Soil samples

To verify the compositions of the soil as described above. Soil samples are analysed. These samples are collected from '*Dinoloket*' [33]. To have a good view of the subsoil, the samples had to be at least 20m below ground level and had to be on or very close to the dike. To give an image, the following samples are taken for the following areas:

- Fluviatile clay district:
  - Meuse Valley
  - River Lands
  - IJssel
- Marine clay district:
  - Delta
  - IJsselmeer
  - Waddenzee

The sample locations can be seen in fig. 3.8. The samples itself can be seen in appendix B. From these samples it can be concluded that the descriptions above meet the situations in practice, as the layers, described above, are indeed present in the samples. The samples contain all sorts of different layers and are very different, but looking at the general trend of these samples, it can be concluded that the above described compositions are indeed a representation of the situation in practice. The problem, however, is that the samples are taken at one location. To translate the samples to a cross section, assumptions for the progression of the layer through the subsoil are needed. The development of the models and therefore the cross sections will be explained at a later stage in this thesis.


Figure 3.8: Sampling of the different areas

### 3.3.4. Soil characteristics

In the previous section (3.3.3), samples of the subsoil are examined. In this part the different soil in these samples are named and are characterized, as the characteristics of the soil types are important in modelling the subsoil. In the samples, the following soil types are distinguished [33]:

- Gravel
- Sand
  - Coarse sand
  - Medium sand
  - Fine sand
- Clay
  - Clay
  - Clayey sand or sandy clay
- Peat

Because soil is more variate than the variations named above, the characteristics of the different soil types will be given as a range of values. As not all the soil characteristics are needed in this thesis, only the characteristics needed for the models will be discussed. For the models (in D-Geo Flow) the following soil characteristics are needed:

| | |
|---|---|
| Horizontal hydraulic conductivity $K_x$ | $[m/day]$ |
| Vertical hydraulic conductivity $K_y$ | $[m/day]$ |
| Particle diameter $D_{70}$ | $[m]$ |
| Porosity $n$ | $[-]$ |
| Compressibility $\alpha$ | $[m^2/N]$ |

As the horizontal hydraulic conductivity is, mostly, named as the hydraulic conductivity, the vertical hydraulic conductivity is mostly undefined and chosen as the same as the horizontal hydraulic conductivity. However, this thesis focusses, partly, on the influence of the anisotropy. Therefore the hydraulic conductivity will be named as one (the horizontal component) and a anisotropy coefficient ($C_A = \frac{K_x}{K_y}$) will also be discussed as a soil parameter. As the vertical hydraulic conductivity is dependent on both the horizontal hydraulic conductivity and the anisotropy coefficient it will from now on not be named as a separate characteristic.

The sources and the different values of the soil characteristics can be seen in appendix C. In the following a summary and conclusion of this research to soil characteristics is given.

**Summary**

The characteristics for the soil types which will be used in the models are based on different literature. As the literature mainly gave ranges of values, the chosen characteristics are an assumption. For this thesis it is chosen to determine all the values by assumptions based on literature except for the hydraulic conductivity. As this is the most influential characteristic. The characteristics of the different soil types can be seen in the table below:

Table 3.1: Summary soil characteristics

| Soil types<br>- | Hyd. conductivity<br>$K$ - $[m/day]$ | Particle diameter<br>$D_{70}$ - $[m]$ | Porosity<br>$n$ - $[-]$ | Compressibility<br>$\alpha$ - $[m^2/N]$ |
|---|---|---|---|---|
| Gravel | 50.0-100.0 | $1.5 * 10^{-2}$ | 0.30 | $1.0 * 10^{-8}$ |
| Coarse sand | 20.0-50.0 | $1.0 * 10^{-3}$ | 0.39 | $1.0 * 10^{-7}$ |
| Medium sand | 5.0-20.0 | $3.0 * 10^{-4}$ | 0.39 | $1.0 * 10^{-7}$ |
| Fine sand | 1.0-5.0 | $1.5 * 10^{-4}$ | 0.39 | $1.0 * 10^{-7}$ |
| Clayey sand/Sandy clay | 0.1-0.5 | $2.0 * 10^{-5}$ | 0.40 | - |
| Clay | 0.002 - 0.15 | $2.0 * 10^{-6}$ | 0.41 | |
| Peat | 1.0 - 5.0 | - | - | - |

The characteristics in this table, based on the literature, must be applied to the models made in D-Geo Flow. However, in D-Geo Flow, not all values for the different characteristics are allowed. In the user manual [34] the ranges for the different characteristics are given. For the relevant characteristics these are summarized in table 3.2. Instead of the hydraulic conductivity, the intrinsic permeability is used. The relation between the hydraulic conductivity (K)$[m/day]$ and the intrinsic permeability ($\kappa$)$[m^2]$ is: $K = \frac{3600*24*\kappa}{1.35*10^{-7}}$.

Table 3.2: Characteristics ranges in D-Geo Flow

| Parameter | Particle Diameter | Intrinsic permeability | Hydraulic conductivity | Porosity | Compressibility |
|---|---|---|---|---|---|
| Symbol | $D_{70}$ | $\kappa$ | $K$ | $n$ | $\alpha$ |
| Minimum | $1 * 10^{-4}$ | $10^{-16}$ | $6.40 * 10^{-5}$ | 0.20 | $10^{-10}$ |
| Maximum | $8 * 10^{-4}$ | $10^{-6}$ | $6.40 * 10^{5}$ | 0.90 | $10^{-5}$ |

Combining the values from the literature and the allowed values from the user manual, the values which will be used in the models can be seen in table 3.3.

Table 3.3: Summary definitive soil characteristics

| Soil types<br>- | Hyd. conductivity<br>$K$ - $[m/day]$ | Particle diameter<br>$D_{70}$ - $[m]$ | Porosity<br>$n$ - $[-]$ | Compressibility<br>$\alpha$ - $[m^2/N]$ |
|---|---|---|---|---|
| Gravel | 50.0 - 100.0 | $8.0 * 10^{-4}$ | 0.30 | $1.0 * 10^{-8}$ |
| Coarse sand | 20.0 - 50.0 | $8.0 * 10^{-4}$ | 0.39 | $1.0 * 10^{-7}$ |
| Medium sand | 5.0 - 20.0 | $3.0 * 10^{-4}$ | 0.39 | $1.0 * 10^{-7}$ |
| Fine sand | 1.0 - 5.0 | $1.5 * 10^{-4}$ | 0.39 | $1.0 * 10^{-7}$ |
| Clayey sand/Sandy clay | 0.1 - 0.5 | $1.0 * 10^{-4}$ | 0.40 | $1.0 * 10^{-6}$ |
| Clay | 0.002 - 0.15 | $1.0 * 10^{-4}$ | 0.41 | $1.0 * 10^{-6}$ |
| Peat | 1.0 - 5.0 | $2.0 * 10^{-4}$ | 0.50 | $1.0 * 10^{-6}$ |

# 4

# Case selection and standard model set-up

As described in the approach, the influence of the foreshore and heterogeneities in the soil is searched for by use of case studies. From these cases, scenarios will be modelled in D-Geo Flow. In this chapter a general introduction into the case choice, the cases and the standard model set-up is given.

Figure 4.1: The river Lek ([35])

## 4.1. Case introduction: Lekdijk

The *Lek* is a branch of the Rhine, flowing through the middle of the Netherlands, as can be seen in fig. 4.1. The Lek is located in the River Land and continues the *Nederrijn* westerly and is followed by the *Nieuwe Maas*. The river is part of the main steam of the Rhine. The water levels of the Lek are therefore directly dependent on the discharge of the Rhine.

As the Lek is located in the River Lands, soil compositions typically for this area, as described in section 3.3 can be expected along the Lek: A Pleistocene coarse sand layer, covered by Holoceen medium to fine sands with a gradually fining in upward direction and thin layer(s) of clay and peat. From the soil sampling it can be concluded that this assumption is right.

Along the Lek, three cases are chosen for this thesis. The cases are chosen based on the available data and the relevance for this thesis, as a foreshore must be present. The cases which will be evaluated are:

1. Salmsteke (DP15,102);
2. Honswijk (DP44,225);
3. Den Oord (DP44,154).

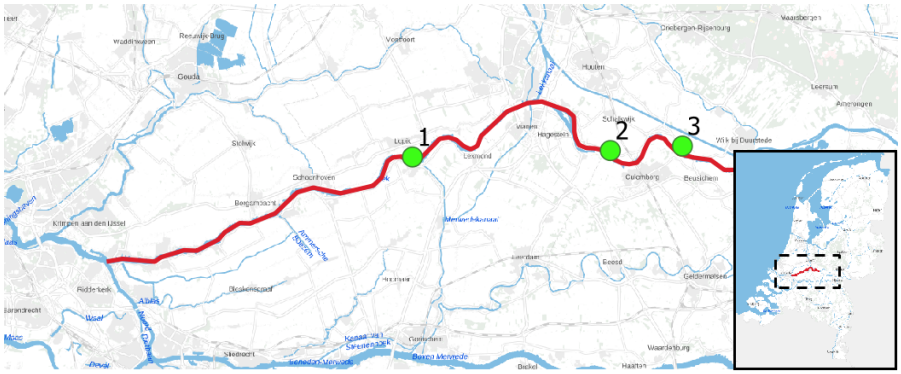


Figure 4.2: Location of the case studies along the Lek

The location of these cases can be seen in fig. 4.2. At the location of these cases a safety analyses is done. Some assumptions from these analyses is used in this thesis and the results are used as comparison material. In the safety analysis the following values are used:

Table 4.1: Input characteristics of the safety analysis and the result (Crit. Head) of the safety analysis

| Case | Seep. length $[m]$ | Thick. aq. $[m]$ | Hyd. cond. aq. $[m/day]$ | Part. diam. $[m]$ | Crit. head $[m]$ |
|---|---|---|---|---|---|
| Salmsteke | 58.09 | 40.83 | 22 | $1.63 * 10^{-4}$ | 3.09 |
| Honswijk | 121.72 | 55 | 45 | $2.00 * 10^{-4}$ | 4.31 |
| Den Oord | 100.82 | 50 | 40 | $2.00 * 10^{-4}$ | 3.89 |

In the safety analysis these cases were assessed following the standard pipint safety analysis in the Netherlands, see section 3.1.3. For each case counts that the strength against piping was insufficient. The result in terms of critical head from the safety analysis can be seen in the last column of table 4.1.

## 4.2. Standard model set-up

In this section the standard models per case will be set-up. Standard characteristics for the models will be chosen, geometry determined and boundary conditions defined.

### 4.2.1. Standardization of the cases

From the safety analysis it became clear that all the case sections do not fulfil the current standards. The influence of the foreshore and heterogeneities is determined for standardized models. In these standardized models the hydraulic conductivity, the thickness of the aquifer and the grain size are chosen to be equal for all the case sections.

**Thickness of the aquifer**

For the thickness of the aquifer 30m is chosen. This 30m is chosen, because by the verification by Stoop(2018)[13], based on the findings of Robbins and van Beek(2015)[36], it became clear that for this depth the model is valid.

**Hydraulic conductivity of the aquifer**

The hydraulic conductivity is chosen to be 20 $m/day$. This value is chosen based on the report by Deltares [37]. The values for the hydraulic conductivity is chosen just above the average of the median values for dike section 15. As dike section 15 contains the Salmsteke case and is located next to the dike section of the other cases, this value is assumed to be a good representation on these locations.

**Grain size of the aquifer**

The grain size, the $D_{70}$, is 0.0002m and this is equal to the values of the grain size of the cases at Honswijk and Den Oord and is a usual used value for the grain size in the piping safety analysis.

---

With the assumptions for the parameters above, the cases are standardized. The result from the safety analysis is also changed, as the input parameters are changed. The "new" results according to the approach of the safety analysis, the Sellmeijer formula, can be seen in column 4 of table 4.3.

### 4.2.2. Boundary conditions

The boundary conditions in D-Geo Flow models describe the influence of the surroundings around the model. In Stoop(2018)[13] an explanation of the different boundary conditions is given. As the approach for the models in this thesis is similar to the models used by *Stoop(2018)*, the same boundary conditions will be assigned. An overview of the assigned boundary conditions in the models can be seen infig. 4.3.


Figure 4.3: Standard boundary conditions which will be used for all models, a detail is shown for the exit point configuration

The boundaries in fig. 4.3 are:

Table 4.2: Standard model Boundary Conditions

| Line | Boundary condition type |
|---|---|
| A-B-C-D | Submerged Boundary |
| D-E-F | Seepage Boundary |
| F-G | Constant Head Boundary [1] |
| G-H-I | Seepage Boundary |
| I-J | Constant Head Boundary |
| J-K-L-M-N-O-A | No-Flow Boundary |

The two boundary conditions where input is needed are the Submerged boundary condition and the Constand head boundary conditions. For the Submerged boundary condition the input changes with every model. The only thing held constant with this boundary condition is the increase in head per time step. The step size is chosen to be 0.1m/time-step. This means when an increase in head of 10m is chosen, 100 time-steps have to be done. To limit the calculation time, the minimum amount of steps is chosen to be desirable. But as the exact critical head is unknown, this can be an iterative process. If the model is overloaded (a much higher head is chosen than the actual critical head), the model gives no wrong answers, this is due to the instantaneous connection between the head along the pipe and the applied head (see [34]).

The constant head boundary is chosen at ground level to create no other effect on the result. This means that water is free to flow out of the exit point.

### 4.2.3. Geometry of the model

In Stoop(2018)[13] it is already stated that the length of hinterland is of influence on the result. As stated in Stoop(2018), the influence is minimized when the hinterland length is *sufficient*. The influence of the hinterland is minimized when the distance is at 4 times the thickness of the aquifer, as the aquifer is standardized at a depth of 30m, the hinterland should be at least 120m.

The exit configuration, as can be seen in fig. 4.5 is taken from Stoop(2018). Stoop looked at the differences when the exit configuration is changed. This was of very little influence, so this configuration is chosen to be governing.

Blanket and levee geometry, the parts "above" the pipe are of minor influence on the critical head result, as Stoop concluded. To limit the influence they have to be impermeable. The hydraulic conductivity is therefore, similar to the findings of Stoop chosen at 0.002m/day. The height of the dike is chosen differently per case and the height of the blanket is chosen to be 0.5m.

The only residual geometry parameter is the seepage length (or in D-Geo Flow the pipe length). The seepage length follows from the safety analysis from the cases and is, thereby, for each case different. An overview of the seepage lengths which are used in the safety analyses can be seen in table 4.1.

[1] A heave boundary could be used, but in the comparison with the results from the models with the Sellemijer formula results, an additional calculation step must be done. It is therefore chosen not to use a heave boundary. Next to that requires D-Geo Flow the advanced computations for a heave boundary, increasing the calculation time for the computations.

### 4.2.4. Model set-up and validation

Now the geometry, the standardized soil characteristics and the boundary conditions are known, the standard models can be set up. As the models of the different cases are very similar, except for the seepage length and dike height, only one standard model is depicted below(Salmsteke). The exit configuration is the same for each case.

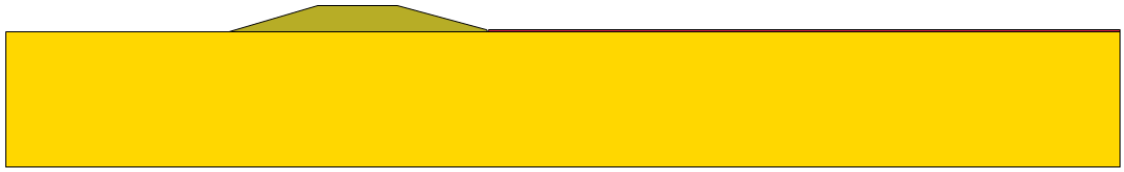

Figure 4.4: Standard model in D-Geo Flow for the Salmsteke case, overview

The validity of the standard models is checked according to the approach in the safety analysis, with the Sellmeijer formula. In the table below the old results from the safety analysis are depicted next tot the results of the standardized models and the new results according to the safety analysis. In the last column the difference between the results according to the safety analysis and the results from the standard models is depicetd.

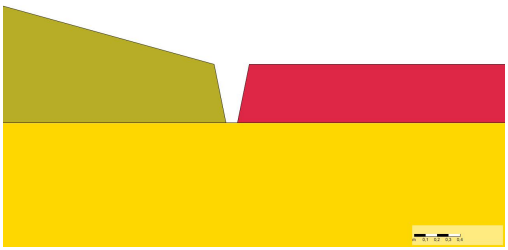

Figure 4.5: Standard model in D-Geo Flo for the Salmsteke case, exit configuration

As can be seen in table 4.3 the differences between the results from the standard model and the results from the Sellmeijer rules are very small. From this it can be assumed that the standard model can be used as a representation of the approach according to the safety analysis, based on the Sellmeijer formula.

Table 4.3: Difference Safety Analysis-Standard Model and results from Sellmeijer

| Case: | Saf. ana. result(old) | Std. models result | Validity check on standard model (new) | |
|---|---|---|---|---|
| | Critical head [m] | Critical head [m] | Critical head [m] | Difference with std. model |
| Salmsteke | 3.09 | 3.40 | 3.37 | 0.03 m |
| Honswijk | 4.31 | 6.2 | 6.27 | 0.07 m |
| Den Oord | 3.89 | 5.3 | 5.42 | 0.12 m |

# I

# Foreshore

# Introduction

The foreshore is an elevated piece of land, next to a water body and outside of the dike protection area. This means that during high water levels on the river, the foreshore could be flooded. From safety point of view it is the area which is unprotected. As the foreshore is a higher elevated piece of land than the river bed it, most likely, covers the aquifer, but it is uncertain whether the foreshore seals the aquifer. Therefore more research on the influence of a foreshore on piping is useful.

The foreshore research in this Thesis is conducted two ways. First a general research is conducted to understand how and to what extend a foreshore can influence the critical head result. Secondly a case study research is conducted at the case study locations determined in section 4.1. In this case study research, local foreshores will be modelled and analyses will be done to determine the influence of variations of and on the foreshore on the critical head result. After the case study research, the application of the general research on the cases will be checked.

# 5

# General Foreshore research

## 5.1. Introduction

To give a general advise about the use of the foreshore in the safety analysis, a general research is conducted. The conclusions from this general research will be applied and verified with the case studies in the next chapter. In this chapter the effects of the foreshore with respect to its resistance and length on the critical head result are searched for.

## 5.2. Standard model and approach

To search for the effects of the resistance and length of the foreshore, a standard model is created. This standard model is then varied to give some insights in the effects. The standard model is the basic set-up as is mentioned before in this report, with the following characteristics:

- The aquifer is 30m thick;
- The hydraulic conductivity of the aquifer is 20 m/day;
- The seepage length, **without foreshore**, is 50m;
- The exit configuration is similar to fig. 4.5.

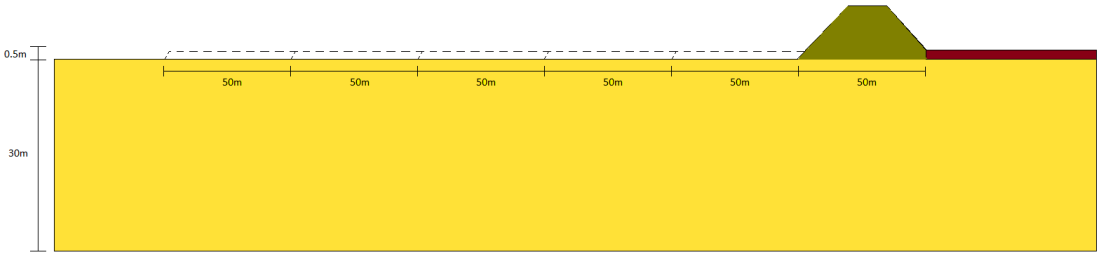


Figure 5.1: Schematic cross-section of the varied foreshore length, not on scale, river located on the left

To search for the effects of the resistance and the length, the foreshore length is varied from 50m to 250m with steps of 50m, see fig. 5.1. For each step the resistance of the foreshore is varied. This variation gives, per foreshore length, a graph in which the increase in critical head, in percentages, can be seen. In this way, the increase in critical head can easily be determined when the foreshore characteristics are known. The resistance of the foreshore is determined by the following formula:

$$c = \frac{D_{foreshore}}{K_{foreshore}} \tag{5.1}$$

As the hydraulic conductivity of the foreshore cover layer $K_{foreshore}$ can be varied more easily than the cover layer thickness, the cover layer thickness $D_{foreshore}$ is held constant. It must, however, be verified that

if the *c* value is constant, but the combination of cover layer thickness and hydraulic conductivity is different, the model gives the same results. The results of the verification can be seen below:

Table 5.1: Verification of influence of varying combinations of the foreshore thickness and hydraulic conductivity on the critical head result

| Cov. Lay. thickness D | Hyd. cond. Cov. Lay. K | Resistance c | Critical head |
|---|---|---|---|
| 0.5 m | 0.002 m/day | 250 days | 5.30m |
| 1.0 m | 0.004 m/day | 250 days | 5.30m |
| 2 m | 0.008 m/day | 250 days | 5.20m |
| 4 m | 0.016 m/day | 250 days | 5.20m |

As can be seen in table 5.1 the differences between the configurations are not significant, it can be assumed that the c-value, independent of the combination of D and K, gives a steady outcome.

The model with a seepage length of 50m and no foreshore, gives a critical head result of 3.0m, this is the reference level for the computations with the foreshore.

For the computations, the c-value is varied from 2000 to 0.025 days. It is assumed that the foreshore resistances in reality will fit in this range. The boundaries can be determined by the standard model and the Sellmeijer formula. The lower boundary represents the case without foreshore, where only the initial seepage length contributes to the critical head result, which is 3.0m. The lower boundary is determined by the standard model with a seepage length of 50m and no foreshore. The upper boundary is the boundary in which the foreshore is incorporated in the seepage length. The upper boundary results are calculated by use of the Sellmeijer formula. A summary of the boundaries can be seen in table 5.2. The results of the research can be verified with these boundaries.

Table 5.2: Lower and upper boundaries from the foreshore model computations (see fig. 5.1). Lower boundaries are calculated with the standard model, upper boundaries are calculated with the Sellmeijer formula

| Foreshore length[$m$]: | Seepage length[$m$]: | Lower bound. in crit. head [$m$] | Upper bound. in crit. head [$m$] |
|---|---|---|---|
| 50 | 100 | 3.0 | 5.4 |
| 100 | 150 | 3.0 | 7.7 |
| 150 | 200 | 3.0 | 10.0 |
| 200 | 250 | 3.0 | 12.2 |
| 250 | 300 | 3.0 | 14.4 |

## 5.3. Results

The computations in D-Geo Flow with the different foreshore lengths give the results depicted in fig. 5.2. It is good to notice that the $L_{voor}$ in the graph is the foreshore length, this is not the total seepage length as the initial seepage length of 50m has to be added to the foreshore length. The results are depicted in the graph below (fig. 5.2). The numerical results can be seen in appendix F.

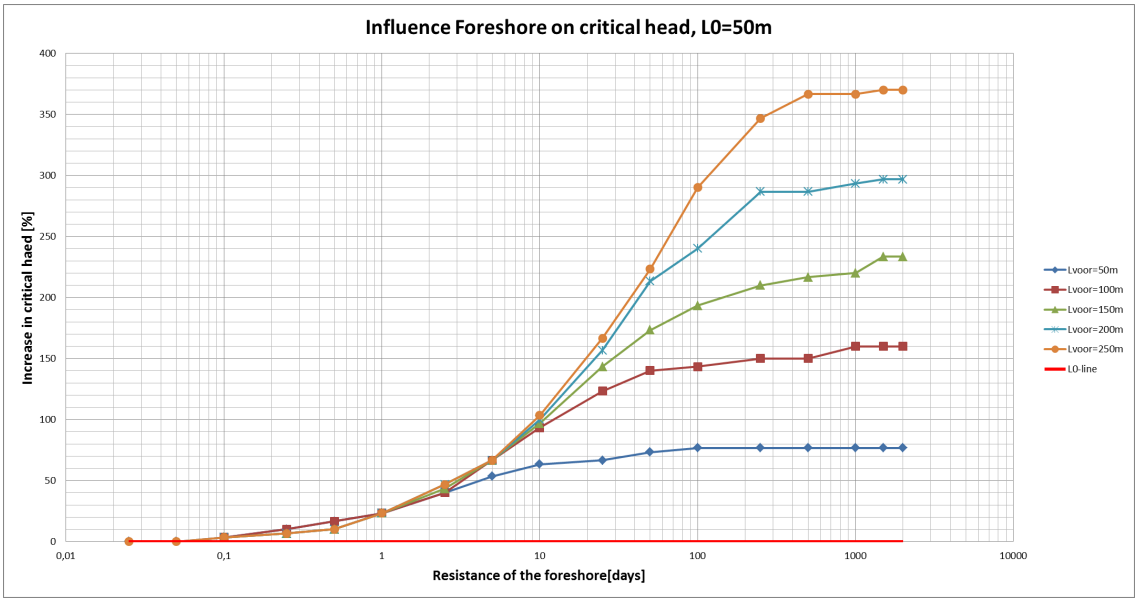


Figure 5.2: Results of the general foreshore research in terms of increase in critical head with respect to the standard model, with a starting seepage length of 50m

## 5.4. Analysis

The graph, as can be seen in fig. 5.2, is the visual representation of the results in table F.1 and table F.2 in appendix F. To conclude on these results, they have to be analysed. This will be done in this section.

As explained before, the results could be tested against the "expected boundaries", calculated with the Sellmeijer formula, which can be seen in table 5.2. The results from the computations are compared with these boundaries, to see if they are similar. The results for low resistances are located on the L0-line, this indicated that the results are in line with the lower boundaries from table 5.2. The upper limit, as already explained is not constant over the different seepage lengths. As the graph only shows the increase in critical head, the absolute value has to be extracted from table F.1 in appendix F . The "expected" and the "computed" boundaries are put next to each other in the table below (table 5.3). The difference is also shown in green if the difference is less than 5% (which is assumed to be acceptable) and in red if the difference is larger than 10%.

Table 5.3: Comparison "expected"(Sellmeijer) and "computed"(D-Geo Flow) Lower and upper boundaries

| Foreshore length [$m$] | Lower bound. expected- computed (in crit. head) [$m$] | Upper bound. expected- computed (in crit. head) [$m$] |
|---|---|---|
| 50 | 3.0 - 3.0 0% | 5.4 - 5.3 1.9% |
| 100 | 3.0 - 3.0 0% | 7.7 - 7.8 1.3% |
| 150 | 3.0 - 3.0 0% | 10.0 - 10.0 0% |
| 200 | 3.0 - 3.0 0% | 12.2 - 11.9 2.5% |
| 250 | 3.0 - 3.0 0% | 14.4 - 14.1 2.1% |

In table 5.3 it can be seen that the differences are very small, this means the computations are similar to the expected results, calculated with the Sellmeijer formula. This, firstly, verifies the model, and , secondly, shows that the Sellmeijer formula can be applied on the cases with a foreshore if the foreshore conditions are similar to the the boundary limit conditions.

It also becomes clear that the "zone of influence", the range in which the largest variability can be seen, is from ± 2.5 to ± 100 days. Outside this zone, the results are more or less constant. A foreshore will, most likely, have a resistance in the same order.

The differences between the results for other foreshore lengths are for resistances smaller than 2.5 days very small, even almost 0. This means that for resistances of 2.5days and smaller, the effect of the foreshore length is negligible. However, a small increase in comparison with the L0-line can be seen.

The diverging differences in results with increasing resistance, is due to the effect that the lower boundary is the same for each foreshore length and the upper boundary is very variable due to the total seepage length variation.

The graph as can be seen above is with a initial seepage length of 50m. To see if the effect of adding a foreshore with several hydraulic conductivities is similar with a different initial seepage length, the same computations are done, but with a initial seepage length of 100m. The results of these computations can be seen below (fig. 5.3).

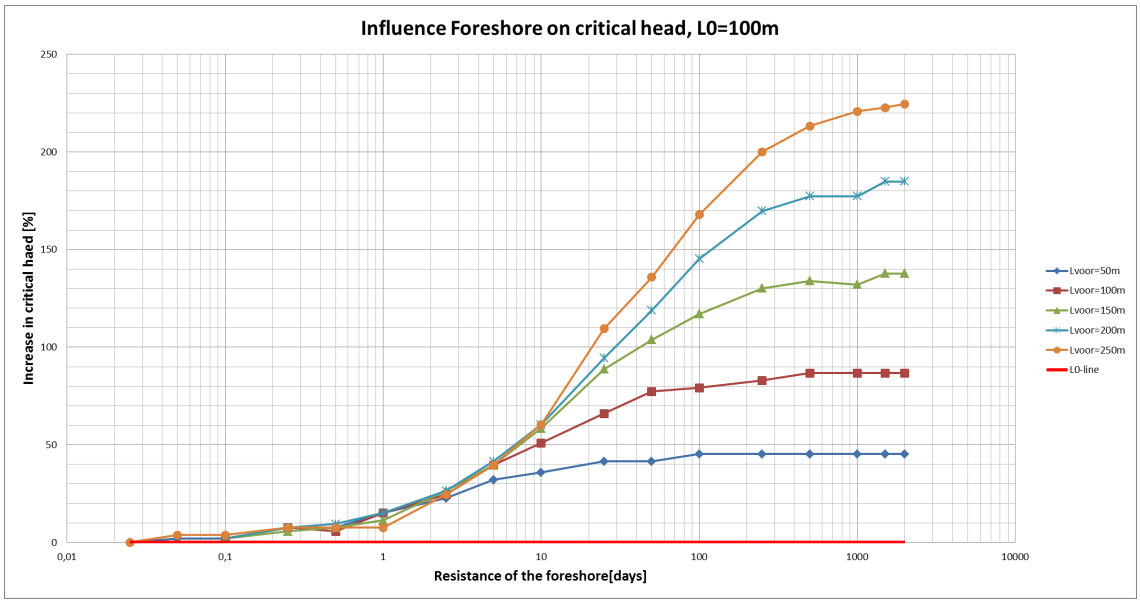


Figure 5.3: Results of the general foreshore research in terms of increase in critical head with respect to the standard model, with a starting seepage length of 100m

As can be seen in the figure above, the similarities with fig. 5.2 are clear. However, the values are a lot lower. This means that for different initial seepage lengths, the increase in critical head is also different. This has to be taken into account in the application of the general research on the cases.

# 6

# Case study specific research

## 6.1. Geometry information

As the foreshore is an elevated piece of land next to the river with a certain height and thickness, these parameters are necessary to create a model. The first step in creating a foreshore model is to create a height profile of the cross-sections at the case study locations.

Tp create the height profile of the cross-sections, the AHN is used. The AHN (Actueel Hoogtebestand Nederland) is a digital height map of the Netherlands[38]. The height map is created by laseraltemetry: Helicopters and airplanes are used to fly over an area and map the height profile with a laser pointed at the surface, this creates a detailed result. The last AHN measurement cycle is the AHN3, this cycle is started in 2014 and will be finished in 2019. The area of interest, the area around the *Lek*, is mapped in 2014-2015. This means the data is relatively up-to-date and therefore applicable in this Thesis. An overview of the AHN3 data for the area of interest can be seen in fig. 6.1.

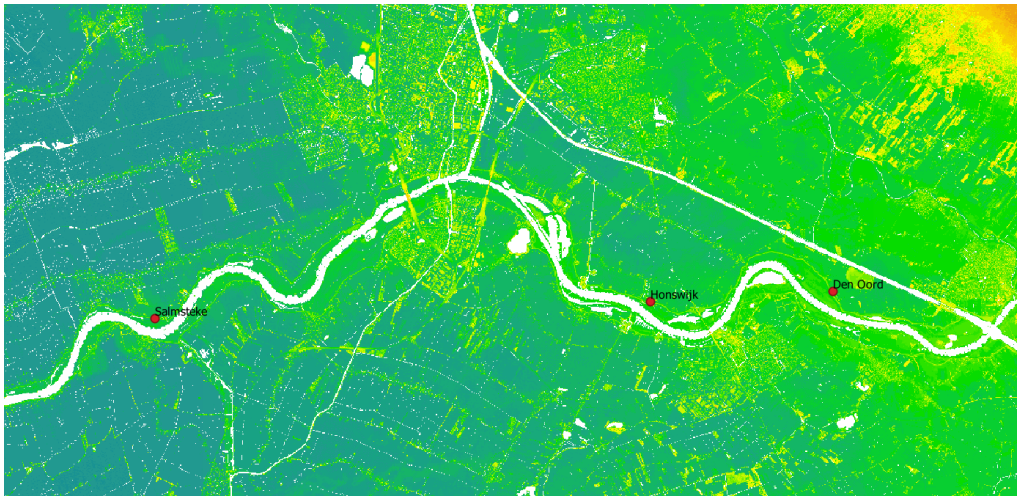


Figure 6.1: Height profile along the Lek

The foreshore geometry will be determined using the AHN. From the AHN data a cross-sectional height profile is created at the locations of the cases. This cross-sectional height profile is then modelled in D-Geo Flow. The modelling approach is explained further on in this Thesis. Per case a height profile is created from the AHN and can be seen below. For clarity, the river side is located on the right side of the height profile, where a rapid decrease in height can be seen.

### 6.1.1. Foreshore geometry of Salmsteke

The cross-sectional height profile can be seen in fig. 6.2. This profile will be the base of the foreshore model.

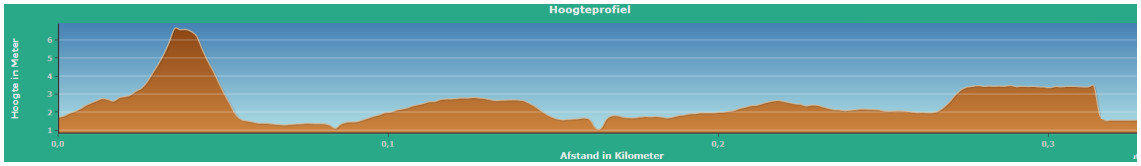


Figure 6.2: Cross-sectional height profile of Salmsteke, river is located at the right

As the model requires a horizontal separation between the foreshore cover layer and the aquifer, a lower boundary level for the foreshore cover layer must be chosen, this is the horizontal separation line between the foreshore cover layer and the aquifer. For the model, a separation level of NAP+1m is chosen, this is the lowest point in the cross-sectional height profile.

### 6.1.2. Foreshore geometry of Honswijk

The cross-sectional height profile can be seen in fig. 6.3. This profile will be the base of the foreshore model.

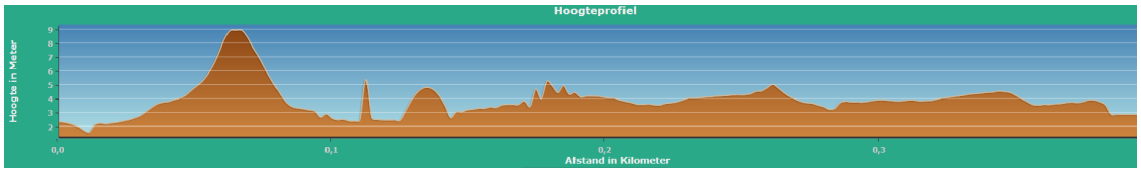


Figure 6.3: Cross-sectional height profile of Honswijk, river is located at the right

The horizontal separation level between the foreshore cover layer and the aquifer is chosen to be at NAP+2.25m. This is the lowest point on the foreshore.

### 6.1.3. Foreshore geometry of Den Oord

The cross-sectional height profile can be seen in fig. 6.4. This profile will be the base of the foreshore model.

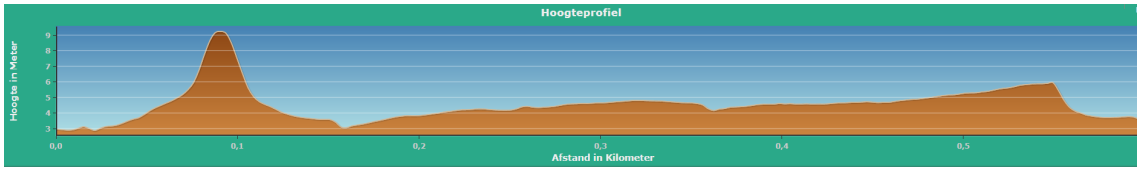


Figure 6.4: Cross-sectional height profile of Den Oord, river is located at the right

The horizontal separation level between the foreshore cover layer and the aquifer is chosen to be at NAP+3m. This is the lowest point on the foreshore.

## 6.2. Modelling the foreshore

### 6.2.1. Introduction and assumptions

Before the models can be set-up some assumptions must be done. As already explained, the foreshore will be added to the standard models, as introduced in section 4.2. In section 6.1 it was already explained that the foreshore cover layer is separated from the aquifer by a horizontal line. The level of this separation line is already determined.

For the geometry of the foreshore, linear interpolation between two points is used in D-Geo Flow. As input, D-Geo Flow requires boreholes, consisting the local soil information and heights. The geometry of a model in D-Geo Flow is the result of interpolation between these boreholes. To create a representative model, the boreholes are chosen at the locations where rapid changes in height can be seen.

In the cross-sectional height profiles of the cases, see fig. 6.2 to fig. 6.4, holes can be seen on the foreshore. At the location of these holes, the cover layer on the foreshore is not present or thin. These holes define, in the models in D-Geo Flow, the possibilities where a pipe could form. As a first assumption, the holes are assumed to reach to the aquifer, so no foreshore cover layer is present. This is, however, a first assumption and will be analysed in more detail. As the exact geometry of a hole is hard to determine from the AHN data, it is, for now, assumed that the geometry is similar to the geometry of the exit point in the standard model (see fig. 4.5).

As the composition of the foreshore is still unknown, assumptions have to be done for the hydraulic conductivity and the grain size. As the foreshore, most likely, is formed by river deposits in low flow velocity areas, the deposits are fine grained and not very permeable, therefore a hydraulic conductivity of 0.1m/day is assumed. The influence of the hydraulic conductivity of the foreshore on the results is analysed later on. The grain size is assumed to be 0.0002m.

Now the assumptions above are defined, the standard foreshore model per case can be set-up.

### 6.2.2. Standard foreshore models

**Salmsteke standard foreshore model**

To define the holes, the cross-sectional height profile must be analysed. In this profile, two "dips" in the foreshore can be seen, these are the lowest points on the foreshore. Together with the location for the exit point, the holes define the possible seepage lengths in the models. For this case the holes can be defined as can be seen in fig. 6.20.

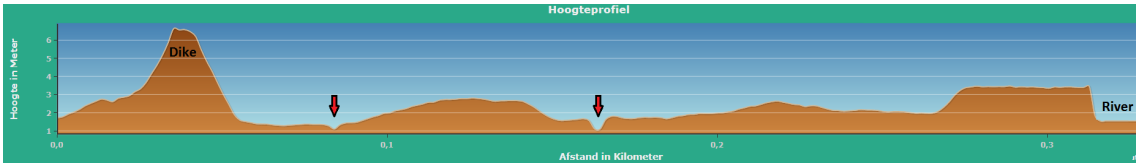


Figure 6.5: Cross-section of Salmsteke, pointing out the holes in the foreshore.

The corresponding seepage lengths with these holes can be seen in fig. 6.6. When no holes are present, the distance between the exit point and the river is the seepage length, this is 300m. In the standard model a foreshore hydraulic conductivity of 0.1m/day is used. A schematic figure of the standard foreshore model, in which all the holes reach to the aquifer(are open), can be seen in fig. 6.6.

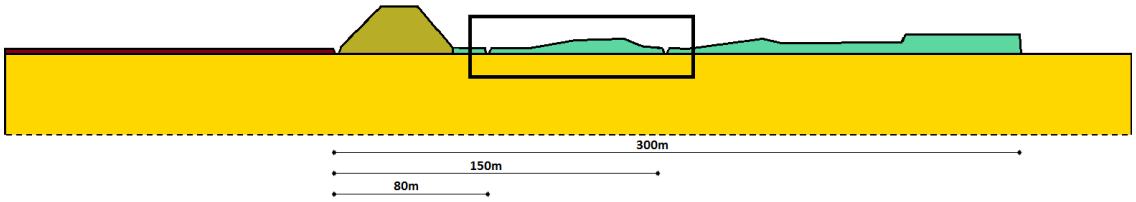


Figure 6.6: Schematic representation of the standard foreshore model for Salmsteke, river located at the right, not on scale

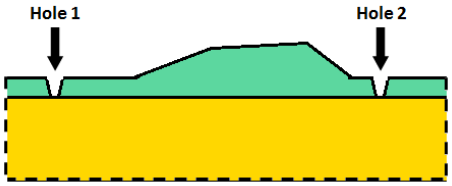


Figure 6.7: Schematic representation of the detail from fig. 6.6, holes pointed out

Now the standard model is set-up, the first computation can be done. The result of the standard foreshore model will be used as a reference level. As the foreshore hydraulic conductivity is defined at 0.1 m/day, there will be seepage through the foreshore into the aquifer, this will affect the result, which makes it hard to compare the results with the Sellmeijer formula. The critical head result of the standard foreshore model is 4.8m.

**Honswijk standard foreshore model**

The holes in the foreshore for the cross-section of Honswijk are determined at the locations which can be seen below, the arrows indicate the locations of the holes in the foreshore.

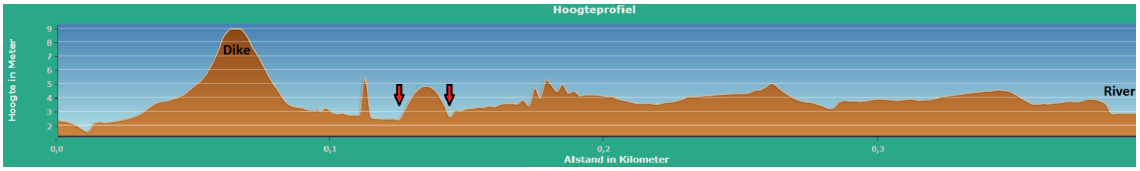


Figure 6.8: Cross-section of Honswijk, pointing out the holes in the foreshore

The corresponding seepage lengths of these holes are 105m and 125m. The distance between the river and the exit point is 360m. The standard foreshore model can now be set up.

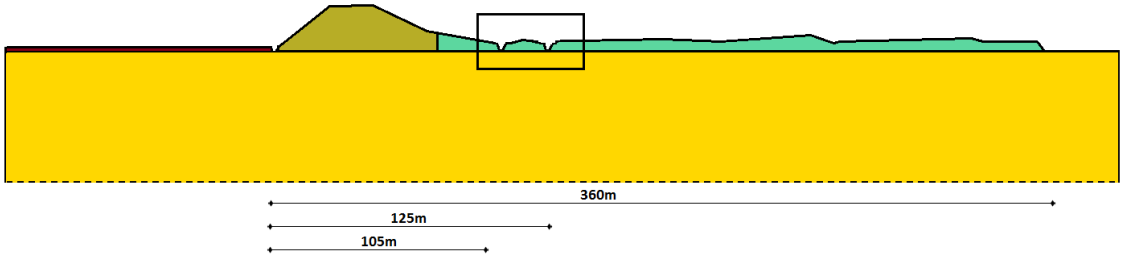


Figure 6.9: Schematic representation of the standard foreshore model for Honswijk, river located at the right, not on scale

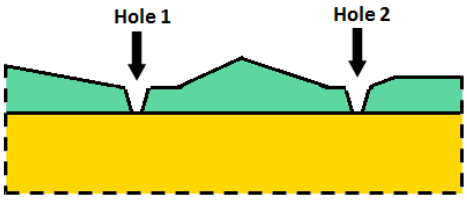


Figure 6.10: Schematic representation of the detail from fig. 6.9, holes pointed out

The critical head result of the standard foreshore model is 6.2m. This computation is done with the assumption of the hydraulic conductivity of the foreshore of 0.1m/day.

**Den Oord standard foreshore model**

The holes on the foreshore for the cross-section of Den Oord are determined at the locations which can be seen below:

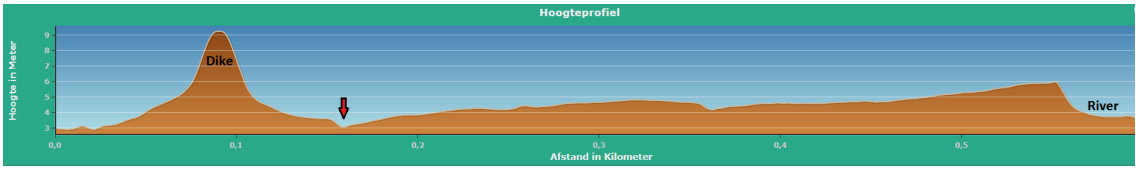


Figure 6.11: Cross-section of Den Oord, pointing out the holes in the foreshore

The corresponding seepage length of the hole is 135m. The river side is located at 545m from the exit point. The standard foreshore model set-up can be seen in fig. 6.12.

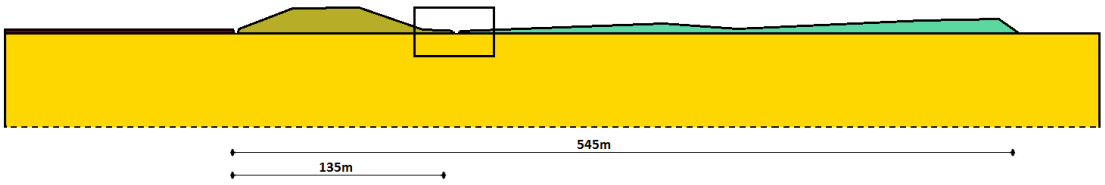


Figure 6.12: Schematic representation of the standard foreshore model for Den Oord, river located at the right, not on scale

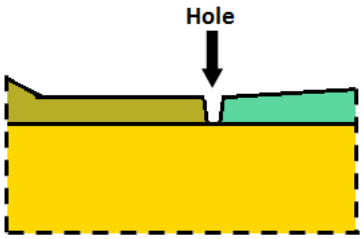


Figure 6.13: Schematic representation of the detail from fig. 6.12, holes pointed out

The critical head result of the standard foreshore model is 7.5m. This computation is done with the assumption of the hydraulic conductivity of the foreshore of 0.1m/day.

The critical head results of the standard foreshore models are the base for the case specific foreshore research. These results will also be the reference level for the research. Because the results of the standard foreshore models differ from the results of the standard models from section 4.2, this difference is depicted below. The results can be seen in table 6.1.

Table 6.1: Critical head results of the standard foreshore models(with holes) and the results from the standard model(no foreshore)

| | Salmsteke | Honswijk | Den Oord |
|---|---|---|---|
| Standard foreshore model [$m$]: | 4.8 | 6.2 | 7.5 |
| Standard model [$m$]: | 3.4 | 6.2 | 5.3 |
| Difference [$m$]: | 1.4 | 0.0 | 2.2 |

## 6.3. Variations of the foreshore

### 6.3.1. Introduction

Modelling the foreshore leads to several assumptions, this decreases the certainty. To decrease the uncertainty of the results, several assumptions are varied. In this section the variations will be named and a sensitivity analysis is done to see what the effect of the assumptions is on the result. This improves the understanding of several components on the safety analysis. The results are expressed in an increase in critical head with respect to the results of the standard foreshore models models from table 6.1

### 6.3.2. Variations in the models

As previously said, several assumptions in the modelling phase will be varied. The effects are determined by a sensitivity analysis, this means wide ranges of values are used. In all the cases, the same variations are used to create a good image of the effects on the results. The following variations are done:

1. Hydraulic conductivity of the foreshore;
2. Width of the hole on the foreshore;
3. Depth of the hole on the foreshore;
4. Silting up of the hole on the foreshore.

For the cases of Salmsteke and Honswijk, where two holes are present on the foreshore, the variations are done for the first hole. However, two situations will be computed, variations **hole 1**, given hole 2 is open (as in the standard configuration, see fig. 4.5) and variations given hole 2 is closed. In this case the hole is assumed to be absent on the foreshore.

Good to note is that an open hole is a hole which creates an open connection of the surface with the aquifer. So in case of an open hole, no resistance is present in the hole and the water can flow into the aquifer.

**Hydraulic conductivity of the foreshore**

In the set-up for the standard foreshore model, the hydraulic conductivity of the foreshore was assumed to be 0.1m/day. To say more about the effect of variations in hydraulic conductivity of the foreshore, the value of the hydraulic conductivity of the foreshore is varied with standard steps: 0.001 m/day - 0.01 m/day - 0.1 m/day - 1.0 m/day - 10 m/day.

**Width of the holes on the foreshore**

The holes on the foreshore, as defined in section 6.2.2, are in fact dips in the foreshore where pools will be formed or a creek is present. As a first assumption, the geometry of the holes is chosen to be the same as the exit point geometry, so a width of 0.1m and walls of 0.1m wide. In reality the holes can be much wider. The effect of the width of a hole on the critical head result is searched for. As the width of the holes is uncertain and it is even more uncertain which width reaches to the aquifer, the bottom width of the holes is varied. To limit the amount of variations, the width and the slope of the walls are not varied. The values the bottom width of the holes is varied with is: 0.1m - 0.5m - 1.0m - 5.0m. the wide range of values result in a good understanding in how bottom widths of holes on the foreshore affect the critical head result. As more than one hole can be present on the foreshore, the effect of more holes will be examined.

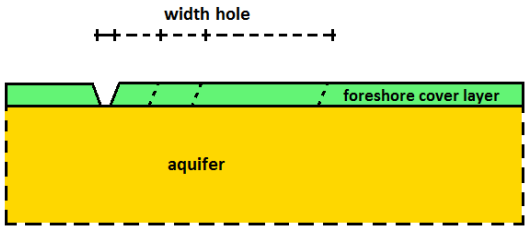


Figure 6.14: Schematic figure of the width variation of the holes

**Depth of the holes on the foreshore**

The assumption for the standard model was that the holes reach to the aquifer. As it is uncertain whether this is actual true, the effects of less deep holes are searched for. To search for this effect, the depth of the holes is decreased as an percentage of the initial depth of 0.5m, so for 10% - 25% - 50% - 75%. The material in the holes is the same as the cover layer on the foreshore, with a hydraulic conductivity of 0.1m/day. As more than one hole can be present on the foreshore, the effect of more holes will be examined.

Figure 6.15: Foreshore variations

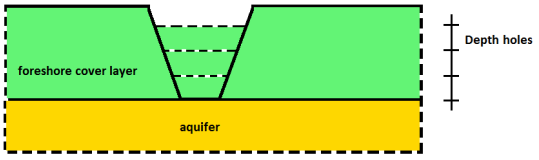


(a) Schematic figure of the depth variation in the entry points

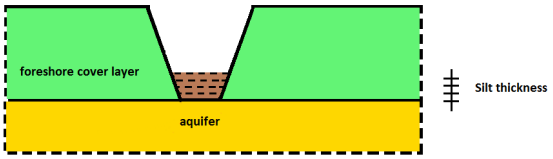


(b) Schematic figure of the silting up variation in the entry points

**Silting up of the holes on the foreshore**

The phenomenon of silting up is added to the sensitivity analysis by expert judgement. When water is flowing over the foreshore, the flow velocity can be very low, as the river flowing area is very wide. When the flow velocity drops, sediment is deposited on the foreshore. This sediment, or silt, can be deposited in the holes and seal the aquifer, this can influence the critical head result. A range of silt deposit thickness is added. The range is: 0.05m - 0.10m - 0.15m -0.20m. The hydraulic conductivity of the silt is assumed based on expert judgement and research on sediment deposits [39]. De Lange states in his article that the hydraulic conductivity can be assumed as 0.001m/day. However, after consulting de Lange about the case study locations, it is assumed that the hydraulic conductivity of silt is 0.01m/day.

## 6.4. Sensitivity analysis

In the sensitivity analysis the effects of the above named variabilities are presented, explained and analysed. The reference levels for the results from the analyses are the results of the standard foreshore models. This standard foreshore model has the following characteristics (see section 6.2.2):

- The holes are "open";
- The bottom of the holes reach to the aquifer;
- The hole geometry is as described in fig. 4.5;
- The foreshore has a hydraulic conductivity of 0.1m/day.

The results of the standard foreshore models are:

Table 6.2: Standard foreshore model critical head results

| | Salmsteke | Honswijk | Den Oord |
|---|---|---|---|
| Standard foreshore model result: $[m]$ | 4.8 | 6.2 | 7.5 |

### 6.4.1. Hydraulic conductivity of the foreshore

The results are depicted as an in-/decrease in critical head with respect to the critical head result of the standard foreshore model (see table 6.2). In the configurations, the holes on the foreshore are open. To create an image of the influence of the hydraulic conductivity of the foreshore on the critical head, the results, which can be seen in appendix E.1, are plotted in the graph below.

An increase in hydraulic conductivity of the foreshore cover layer means water can flow with more ease through this layer. Increasing hydraulic conductivities will therefore lead to a decrease in critical head. Decreasing hydraulic conductivity lead to more resistance to flow through the cover layer, which will lead to an increase in critical head. In fig. 6.16 this trend can also be seen. It can however be seen that the graph is not symmetrical for all three cases.

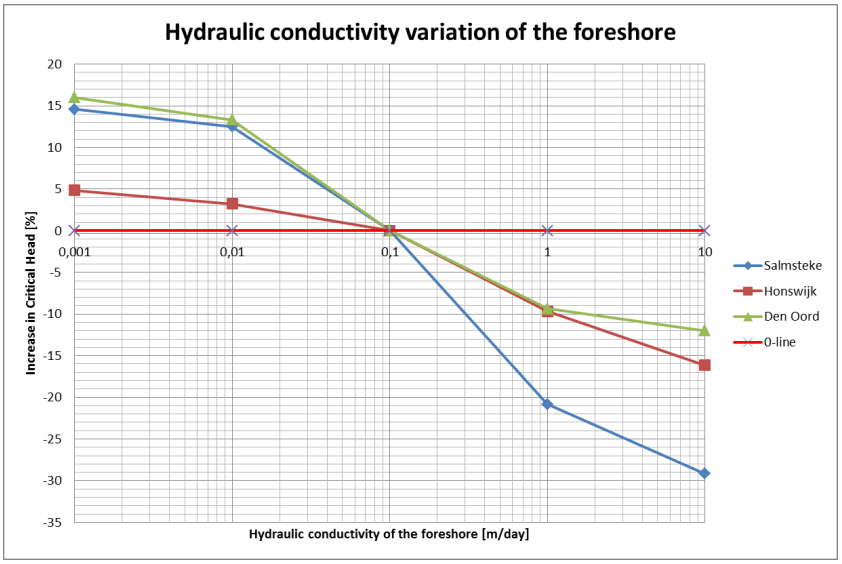


Figure 6.16: Influence on the critical head result of the variation of the hydraulic conductivity of the foreshore cover layer, in comparison with table 6.2. The red line indicated the standard foreshore model, with a hydraulic conductivity of the foreshore cover layer of 0,1 m/day.

An explanation for the asymmetry can be found in the geometry of the foreshore. The location and number of holes in the foreshore, as well as the thickness of the foreshore influence the results and thereby the shape of the graph. The results of the three cases are explained separately.

In the Salmsteke case, two holes are present on the foreshore on a distance of 80m and 150m from the exit point. The average thickness of the foreshore cover layer is around 2m. It can however be seen in fig. 6.20 that this thickness is very variable. In fig. 6.16, the results of Salmsteke are depicted with the blue line. It can be seen that increasing hydraulic conductivity has more effect on the critical head result than decreasing hydraulic conductivity. This can be explained by the fact that the holes on the foreshore are assumed to reach to the aquifer. so water can penetrate into the aquifer via these holes. An increase in hydraulic conductivity of the foreshore cover layer has more effect than a decrease, because with a decrease the water still reaches

the aquifer via the holes. With an increase, this also occurs, but at a low hydraulic conductivity of the foreshore cover layer, the water also penetrates through this cover layer. The presence of holes limits the effect of decreasing hydraulic conductivity more than it limits the effect of increasing hydraulic conductivity of the foreshore cover layer.

For the Honswijk case, two holes are present on the foreshore at distances of 105m and 125m from the exit point. The average thickness of the foreshore cover layer is around 1m. The same trend as for the Salmsteke case can be seen. The effect of a decrease in hydraulic conductivity of the foreshore cover layer has less effect than an increase. The above described influence of the presence of two holes in the foreshore define this difference in in-/decrease, as the presence of holes limits the effect of decreasing hydraulic conductivity more than it limits the effect of increasing hydraulic conductivity of the foreshore cover layer.

In the case of Den Oord, where one hole is present on the foreshore at a distance of 135m from the exit point and the average thickness is around 2m, a different trend can be seen than for the two other cases. This can be explained by two things, the presence of only one hole and the absence of foreshore cover layer between the dike and the hole, as can be seen in fig. 6.12. The absence of more holes cause a less asymmetric shape of the graph above.

The different shapes of the lines in graph 6.16 are now explained. For Salmsteke and for Honswijk the same explanation was found for the shape of the graph. However, it can be seen that the amount of in-/decrease the two cases is different. This difference originates in the the position of the holes and the thickness of the foreshore cover layer. As already said, the holes limit the effect of increasing/decreasing hydraulic conductivity of the foreshore. This effect is limited even more when the holes are located close to each other. In the Honswijk case, the distance between these holes is very small compared to the distance which can be seen in the Salmsteke case. The very low increase in critical head with decreasing hydraulic conductivity for Honswijk can be explained by this fact. This also holds for the increase in hydraulic conductivity, but the thickness of the foreshore cover layer strengthens this effect. Therefore a larger difference between the two cases can be seen for an increase in hydraulic conductivity of the foreshore cover layer than for a decrease.

### 6.4.2. Width of the holes on the foreshore

The variation in width of the holes in the foreshore cover layer will affect the critical head result, as the area of contact of the outer water with the aquifer will change. For the cases of Salmsteke and Honswijk, two holes in the foreshore cover layer were defined. In the introduction of this section it was explained that two computations will be done if two holes are present on the foreshore:

1. Width variations of **hole 1**, given hole 2 is open;
2. Width variations of **hole 1**, given hole 2 is closed.

Good to note is that hole 1 is the hole most close to the dike, see fig. 6.7 and fig. 6.10. The influence of the hole width variation for the three cases on the critical head result can be seen below. For the cases in which 2 holes were present on the foreshore, two lines are depicted.

In fig. 6.17 the influence of the hole width on the critical head result can be seen. As can be seen in the graph the influence with an increase in width of 50x is only 8%, in comparison with the standard foreshore model. In the graph it can be seen that the lines flatten. In other words: the increase in influence decreases with increasing width. It can however be seen that for the case of Den Oord, the line flattens less than for the other cases, which have more or less the same shape. This can be explained by the absence of a second hole in the foreshore of Den Oord, which is present at Salmsteke and Honswijk.

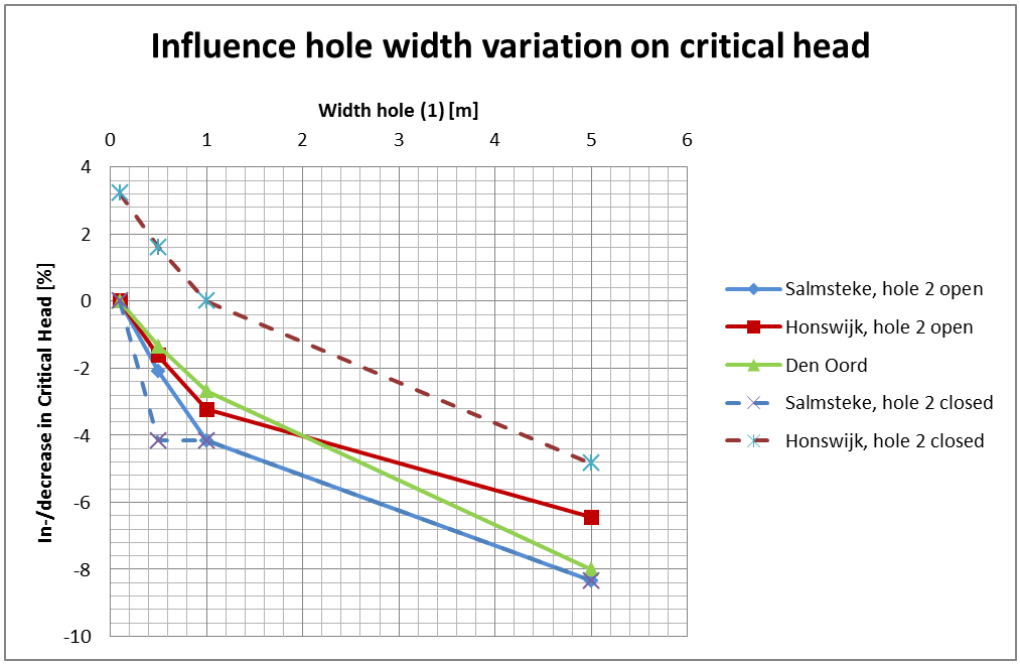


Figure 6.17: Influence on critical head results of the variation of the hole width on the foreshore for the three cases, in comparison with table 6.2

The influence of the second hole can be seen by comparing the two lines of Salmsteke or Honswijk. For Salmsteke it becomes clear that the influence of the presence of the second hole is negligible. For Honswijk it can be seen that closing the second hole leads to an increase in critical head. The difference between these cases is explainable by the location of the two holes. As for Salmsteke the distance between the holes is very large, resulting in hardly any influence of the second hole on the first hole. For Honswijk the holes are very close to each other, resulting in more influence of the second hole.

### 6.4.3. Depth of the holes on the foreshore

The depth of the holes will affect the result of the critical head, because of more resistance on the foreshore against seepage into the aquifer. It was in the standard foreshore model assumed that the holes on the foreshore were "open", this meant the holes reached to the aquifer, resulting in an open connection between the aquifer and the outer water.

For the cases of Salmsteke and Honswijk, two holes in the foreshore cover layer were defined. In the introduction of this section it was explained that two computations will be done if two holes are present on the foreshore:

1. Depth variations of **hole 1**, given hole 2 is open;
2. Depth variations of **hole 1**, given hole 2 is closed.

Good to note is that hole 1 is the hole most close to the dike, see fig. 6.7 and fig. 6.10. In the graph below, the results for the depth variation of the hole on the foreshore can be seen. As said, for the cases of Salmsteke and Honswijk, two computations are done.

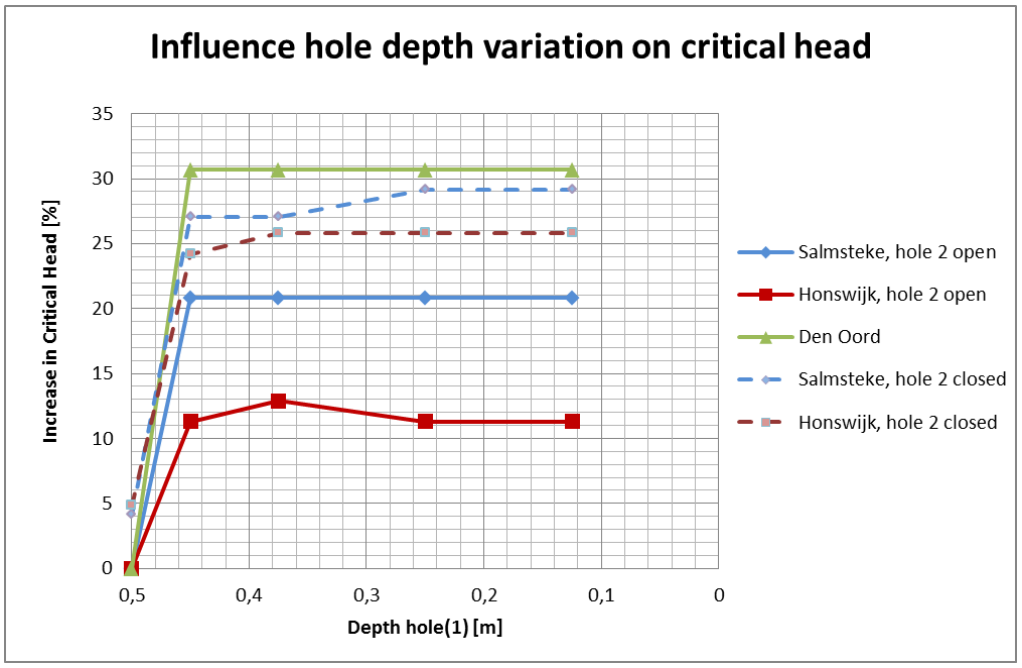


Figure 6.18: Influence on critical head results of the variation of the hole depth on the foreshore for the three cases,in comparison with table 6.2

In fig. 6.18 it can be seen that for all the cases, the same shape appears: A rapid increase with a little decrease in depth, after which the increase remains constant for other variations. This means that if the depth of a hole is a little bit decreased, the resistance in this hole is enough to resist the water from flowing through this hole. Another way of explanation is that if a hole does not reach to the aquifer, the pipe will not be formed at that location and the length of the pipe increases, leading to an increase in critical head. The amount of increase is determined by the length at which a next possibility of pipe formation is present, so or at the river side or at a next hole. This immediately explains the difference within the cases, as for an open hole 2, the next possibility is relatively close by, in comparison with the case where this hole is also closed.

### 6.4.4. Silting up of the holes on the foreshore

If a hole is silted up, a thin layer of silt is deposited in the hole. This thin silt layer increases the resistance on the foreshore and will thereby affect the critical head result, as in the standard foreshore models the holes were assumed to reach to the aquifer.

For the cases of Salmsteke and Honswijk, two holes in the foreshore cover layer were defined. In the introduction of this section it was explained that two computations will be done if two holes are present on the foreshore:

1. Silting up variations of **hole 1**, given hole 2 is open;
2. Silting up variations of **hole 1**, given hole 2 is closed.

Good to note is that hole 1 is the hole most close to the dike, see fig. 6.7 and fig. 6.10. In the graph below, the results for the silting up variation of the hole on the foreshore can be seen. As said, for the cases of Salmsteke and Honswijk, two computations are done.

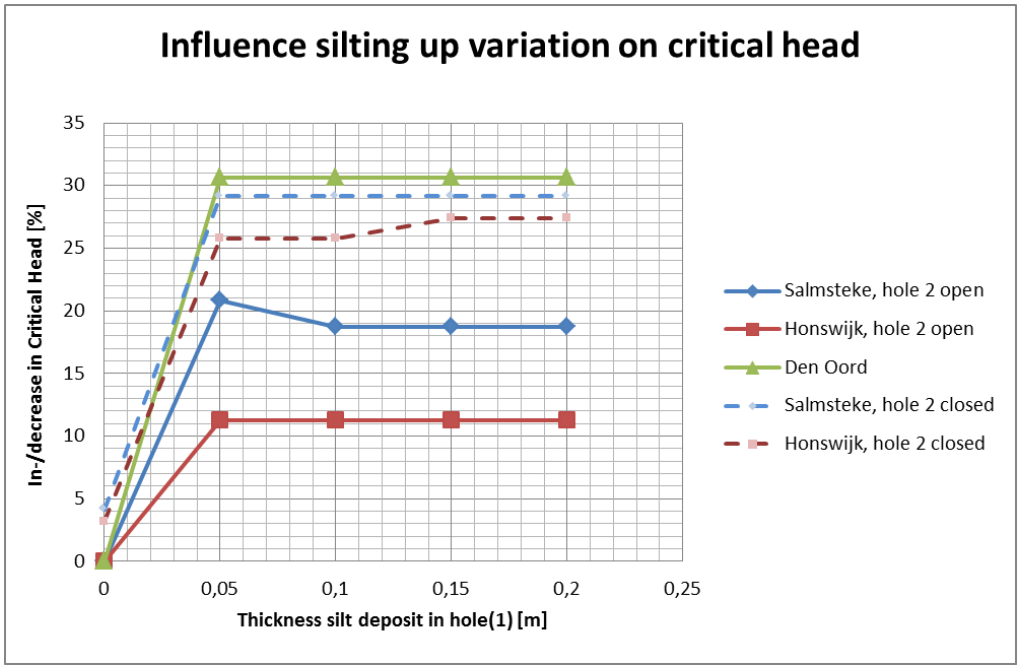


Figure 6.19: Influence on critical head results of the variation of the silt deposit thickness in the holes on the foreshore for the three cases, in comparison with table 6.2

From the graph above, the same can be concluded as from the depth variations of the holes. If a little resistance is present in the holes, the critical head increases rapidly. After this rapid increase in critical head, the critical head value remains constant. A little resistance in a hole, even only 5cm of silt, can cause a large increase in critical head. The difference in the amount of increase for the different lines is the cause of the location of the other possibility where a pipe can be formed from. This is or another hole in the foreshore or the river.

## 6.5. Application general foreshore research on cases

### 6.5.1. Application

To see if the results from the general foreshore research can be applied on case studies, the results of the general research chapter 5 are applied on the cases to see if the results from the case study research can be approached. All the cases, if possible, will be used.

The generic research is based on a foreshore cover layer with no holes and a constant thickness. To compare the results of the general research and the case study research, additional computations are done for the cases with a situation where no holes on the foreshore are present. These results can be seen below:

Table 6.3: Critical head results of the cases when no holes on the foreshore are would be present

| Case: | Salmsteke | Honswijk | Den Oord |
|---|---|---|---|
| Foreshore with no holes | 6.2m | 7.7m | 9.8m |

To compare these results, an assumption for the case study foreshore thickness must be done , based on the geometry. The average, or representative, thickness must be determined to determine the representative resistance of the foreshore.

**Salmsteke case application**

The Salmsteke case has an initial seepage length of 58.09m and a total seepage length(with foreshore included) of 300m. The graph from the general research with the seepage length of 50m will be used to approach the case study result. The 250m line will be used, as the foreshore length (=total length - initial seepage length) is around 250m.

The average thickness for the Salmsteke case is determined based on the AHN-height profile, see the figure below.

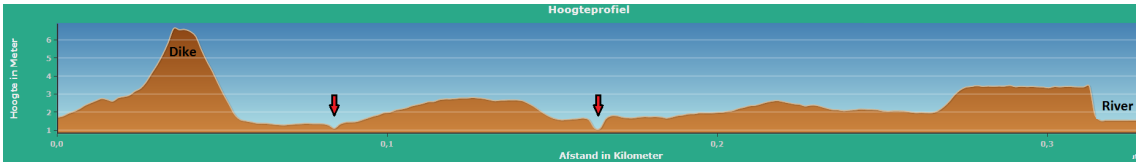


Figure 6.20: Cross-section of Salmsteke with the holes and the river pointed out

As a first estimate, the foreshore cover layer thickness is determined on 1.5m. This will be evaluated later on. As the foreshore hydraulic conductivity was assumed to be 0.1m/day, the resistance is determined at 15 days. When looking at fig. 5.2 at the 250m line at a resistance of 15 days, the increase in critical head should be 140%. As the result of the standard model was 3.4m (see section 4.2), the result is expected to be 8.16m. The result from the computation of the case foreshore without holes is 6.2m, see table 7.1. This is a difference of 1.96m in critical head. As this difference is quite large, en explanation must be found.

The difference in critical head can be caused by several factors. One is the difference in initial seepage length, the difference between between the initial seepage lengths for both computations is around 8m. When looking at the two graphs from the general foreshore research, it can be concluded that an increase in seepage length leads to a decrease in the increase percentage in critical head.

Another cause can be the choice of thickness of the foreshore. Another approach could be to choose the thinnest part of the foreshore as representative thickness. This would result in a thickness of the foreshore for Salmsteke of 0.5m, leading to a representative resistance of 5 days. According to the graph in fig. 5.2, the increase in critical head would be 70%, this leads to a critical head of 5.8m, which underestimates the critical head result from the case study.

**Honswijk case application**

The case study location at Honswijk gives an initial seepage length of 121.72m and a total seepage length of 360m (foreshore included). This makes that the foreshore has a length of around 240m. The best choice of graph from the general research for this case would be the graph with the initial seepage length of 100m and a hydraulic conductivity of 20 m/day. The correct line which should be used is the 250m foreshore line.

The average thickness is estimated based on the AHN-height profile, which can be seen in fig. 6.21.

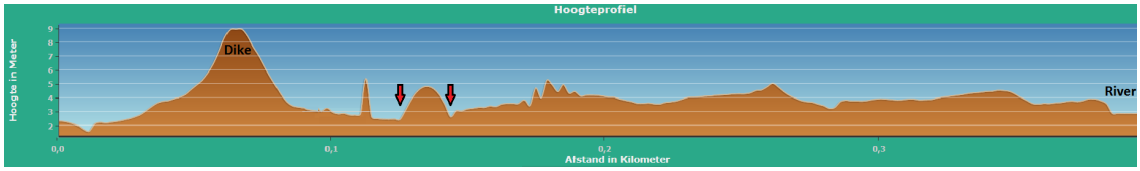


Figure 6.21: Cross-section of Honswijk with the holes and the river pointed out

As the first estimate, an average foreshore cover layer thickness is chosen to be 1m. This will be evaluated in a later stadium. As the hydraulic conductivity of the foreshore is 0.1m/day. The average resistance is 10days. Using the graph in fig. 5.3 and following the 250m foreshore line to a resistance of 10days, the increase in critical head is 60%. The result of the standard model of Honswijk, which should be used as reference level, was 6.2m (see section 4.2. An increase of 60% leads than to a critical head of 9.9m. From the results from table 7.1, it can be seen that for a foreshore without holes in the cover layer, the result is 7.7m. An explanation for this will be searched for.

Several factors can cause the difference in critical head. The initial seepage length was proven to be of large influence on the increases in critical head. When comparing the graphs from the general research for 50 and 100m it can be concluded that with increasing initial seepage length, the increase in critical head decreases. Because of the initial seepage length difference of 21.72m between the Honswijk case and the general research the increase in critical head can be less.

Another cause can be a wrong estimation of the representative thickness of the foreshore. Previously the average thickness was chosen to be the representative thickness. Another approach would be to choose the thinnest part of the foreshore as representative. The thinnest part has a thickness of 0.5m, this would lead to a foreshore resistance of 5 days. Looking at the graph in fig. 5.3, the increase in critical head for a 5 days resistance is 40%. This would lead to a critical head of 8.7m, this also overestimates the result from the case study.

**Den Oord case application**

The Den Oord case has an initial seepage length of the standard model of 100.82m and a total seepage length, in which the foreshore is included, of 545m. Because of the computational choices in the general research the maximal foreshore length was chosen to be 250m. The case of Den Oord therefore falls out of the scope of the results of the general research. Comparing and drawing conclusion is therefore difficult and would lead to uncertain answers. The Den Oord case is therefore not evaluated in the application.

### 6.5.2. Adjustment of the application of the general research on the cases

In the application of the general research on the cases it became clear that the results are different. These differences in results are due to differences in initial seepage length and cover layer thickness. By empirical ways an approach is developed to use the general research results to predict the influence of the foreshore in cases, if it is in the scope of the general research (foreshore lengths to 250m).

The following problems arose in the application:

1. The initial seepage lengths are not similar. Initial seepage lengths have a large influence in the progression of the graphs;
2. The foreshore does not have a continuous thickness, therefore the representative foreshore cover layer thickness is hard to estimate.

To come up with a solution to these problems, the following is suggested:

1. To solve the problem of different seepage lengths, a factor is added to the result. This factor, $C_{seep}$, is the ratio between the initial seepage length from the general research and the initial seepage length from the case study: $C_{seep} = \frac{L_{init_{gen}}}{L_{init_{case}}}$;
2. To solve the problem of the representative thickness, the increase of the critical head for the average thickness(average resistance) and for the minimum thickness(minimum resistance) is determined.

This is translated to a critical head, by multiplying the initial critical head with the increase. This two critical heads are then averaged to come up with the representative critical head.

This results in the following formula and input:

$$H_{cr_{rep}} = \frac{H_{cr_{cav}} + H_{cr_{c_{min}}}}{2}$$
$$H_{cr_{new}} = H_{cr_{rep}} * C_{seep} \tag{6.1}$$

The parameters will be explained by using them on the cases:

**Adaptation on Salmsteke**

The average thickness of the Salmsteke case was 2.0m and the minimum thickness was 0.5m. With a hydraulic conductivity of 0.1m/day, this leads to resistances of 20 and 5 days. Looking at graph fig. 5.2, this gives increases in critical head of 140% and 70%. When these increases are added to the initial head of 3.4m, the new critical head become 8.16 and 5.8m. The representative critical head then becomes:

$$H_{cr_{rep}} = \frac{H_{cr_{cav}} + H_{cr_{c_{min}}}}{2} = \frac{8.16+5.8}{2} = 6.98m$$

The next step is determining the $C_{seep}$ , this is done in the following formula, using the case seepage length of 58.09m and the general research seepage length of 50m:

$$C_{seep} = \frac{L_{seep_{gen}}}{L_{seep_{case}}} = \frac{50}{58.09} = 0.86$$

The final result then becomes

$$H_{cr_{new}} = H_{cr_{rep}} * C_{seep} = 6.98 * 0.86 = 6.00m$$

The result of the formula above, 6.00m, is very close to the "desired" result of 6.2m from the computations in table 7.1. The result slightly underestimates the result from the case study computation, which makes it a safe estimation.

**Adaptation on Honswijk**

The average thickness of the Honswijk case was 1.0m and the minimum thickness was 0.5m. With a hydraulic conductivity of 0.1m/day, this leads to resistances of 10 and 5 days. Looking at graph fig. 5.3, this gives increases in critical head of 60% and 40%. When these increases are added to the initial head of 6.2m, the new critical head become 9.9 and 8.7m. The representative critical head then becomes:

$$H_{cr_{rep}} = \frac{H_{cr_{cav}} + H_{cr_{c_{min}}}}{2} = \frac{9.9+8.7}{2} = 9.3m$$

The next step is determining the $C_{seep}$ , this is done in the following formula, using the case seepage length of 121.72m and the general research seepage length of 100m:

$$C_{seep} = \frac{L_{seep_{gen}}}{L_{seep_{case}}} = \frac{100}{121.72} = 0.82$$

The final result then becomes:

$$H_{cr_{new}} = H_{cr_{rep}} * C_{seep} = 9.3 * 0.82 = 7.64m$$

The result of the formula above, 7.64m, is very close to the "desired" result of 7.7m from the computations in table 7.1. The result slightly underestimates the result from the case study computation, which makes it a safe estimation.

# 7
# Conclusions

## 7.1. General research

The results from the general research, as depicted in fig. 5.2 and fig. 5.3, show that the influence of the foreshore, for one initial seepage length, is equal for different foreshore lengths if the resistance of the foreshore is less than 2.5 days. This means that if the foreshore is significantly permeable the foreshore can not be included in the seepage length for the safety analysis. It must however be noticed that for a resistance of 2.5 days or less, a slight increase in critical head is present. To translate this in terms which can be used in the safety analysis, fig. F.1a and fig. F.1b, in appendix F show representative seepage lengths, which can be included in the safety analysis.

If the resistance of the foreshore exceeds the 2.5 days value, an increase in critical head can be seen. This increase gains effect by increasing foreshore length. This increase continues to larger resistance values, until a equilibrium situation is present. The foreshore resistance value at which this equilibrium starts is dependent on the length of the foreshore. At lower foreshore length, this equilibrium is reached in an earlier stadium than for larger foreshore lengths. The critical head value of this equilibrium state is comparable with the critical head calculated with the Sellmeijer formula, see table 5.3.

In the models, assumptions are done for the characteristics of the dike and the blanket. From the computations, it can be concluded that, for the assumed characteristics, a little seepage through the dike into the aquifer is present. This can be seen in fig. F.1a and fig. F.1b. In these figures it can be seen that for very resistant foreshores, the representative seepage length is different from the actual seepage length. This indicates seepage through the dike. In reality this seepage can also be present, based on the characteristics of the material used in the dike, although in the analyses the dike is always assumed to be impermeable.

## 7.2. Case study specific research

In the previous sections, the influence of the foreshore on the critical head result in the cases of Salmsteke, Honswijk and Den Oord have been evaluated. After varying several properties of or on the foreshore, conclusions can be drawn. These conclusions should lead to more insights in the way of incorporating the foreshore in the safety analysis for piping.

### 7.2.1. Hydraulic conductivity of the foreshore

The in-/decrease in critical head as a result of the variation of hydraulic conductivity of the foreshore can be seen in fig. E.1. In this figure can be seen that the variations can result in a change in critical head of 30%. In section 6.4.1 an explanation of the in-/decreases was given. The changes in critical head can be explained with the amount and location of the holes and the geometry of the foreshore.

In reality the hydraulic conductivity of the foreshore will never reach a value of 10 m/day, as in that case the foreshore will be neglected. The same holds for a hydraulic conductivity of 0.001m/day. This value will not be present in the whole foreshore as this is a value for compacted clay, which is not present on the foreshore. The influence of the hydraulic conductivity is thereby limited to an **in**crease of 13% and a **de**crease of 20% for the Salmsteke case, an **in**crease of 3% and a **de**crease of 10% for the Honswijk case and an **in**crease of

13% and a **de**crease of 9% for the Den Oord case.

From this analysis it can be concluded that the case whether a foreshore can be included or not also has to address the hydraulic conductivity of the foreshore, as this is clearly of influence. This is already incorporated in the safety analysis in a specific way, it must however be evaluated if this approach is the right one.

### 7.2.2. Variation of the holes on the foreshore

The holes were in the analysis varied on several aspects:

- Width;
- Depth;
- Silting up.

The variations in width of the holes on the foreshore leads, in general, to a decrease in critical head. As more area of the aquifer is in direct contact with the outer water. The influence is limited to a maximum value of 6-8% decrease in critical head, for an increase in hole width of 50x (from 0.1m to 5m). The influence of a second hole, if present, is only significant if the second hole is very close to the first hole.

For the variation in depth and in silt thickness in the holes, the general conclusion is: When a hole is present on the foreshore, it has to be ensured that this hole reaches to the aquifer, is this not the case then the hole can be neglected as a starting point for a pipe and the next possible option must be assessed. Even a very small layer in a hole between the aquifer and the outer water can seal the aquifer, which results in a longer seepage length.

This conclusion can be drawn based on the following comparison between the results from the cases and computations of the foreshore where no holes are present for all the cases. The results of these computations can be seen below:

Table 7.1: Critical head results of the cases when no holes on the foreshore are would be present

| Case: | Salmsteke | Honswijk | Den Oord |
|---|---|---|---|
| Foreshore with no holes | 6.2m | 7.7m | 9.8m |

Drawing these results in the graphs of the variations in depth and silt thickness, the following graphs result:

Figure 7.1: Foreshore variations including the "no hole computations"

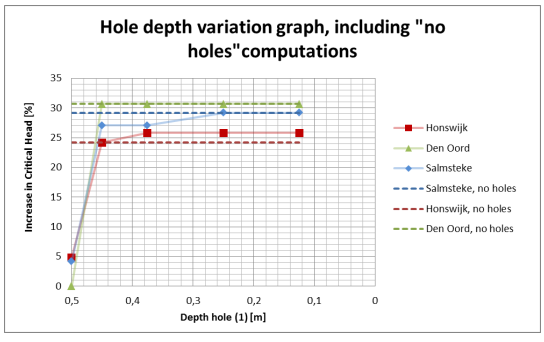


(a) Hole depth variation, including the lines for the "no hole computations"

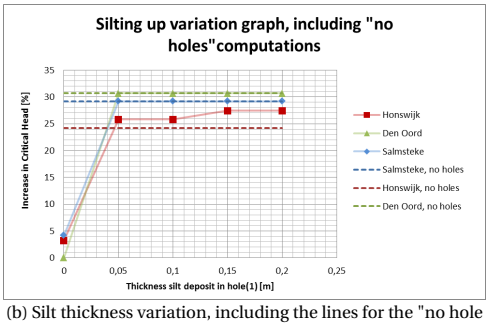


(b) Silt thickness variation, including the lines for the "no hole computations"

In the graphs above, it can be seen that the "no hole computations" approach the horizontal parts of the graphs very closely. Hereby the above stated conclusion holds: "When a hole is present on the foreshore, it has to be ensured that this hole reaches to the aquifer, is this not the case then the hole can be neglected as a starting point for a pipe."

In the safety analysis the presence of a hole could lead to the choice to neglect the foreshore and calculate the critical head with the seepage length from this hole. From the analysis it became clear that it is very useful

to check whether this hole indeed is in contact with the aquifer, as this could influence the safety analysis significantly.

### 7.2.3. Application general research on case studies

After applying the findings from the generic research it can be concluded that the results from the general research are useful in the prediction of the influence of a foreshore. However, two significant differences between the general research and the case study research arose: The resistance of the foreshore and the difference in initial seepage length.

The resistance of the foreshore is, in practical situations, like in the case study, hard to predict. The actual thickness and the hydraulic conductivity of the foreshore cover layer are no determined values, so estimations must be done. To simplify this, two values are required, a minimal and an average resistance. For both these values the expected increase in critical head must be determined and then averaged. This average value can then be used.

To account for the difference in initial seepage length, the initial seepage length from the general research divided by the initial seepage length from the case study, results in a correction factor for the difference.

The two values are multiplied to come to the final result. This final results slightly underestimates the critical head, but it is assumed to be a safe first estimation.

# II

# Soil heterogeneities

# Introduction

With soil heterogeneities, layers in a cross-section other than normal sand, are meant. The scope of this Thesis is to focus on heterogeneities in the Holocene layer, as this is the most variable deposit in the subsoil. Heterogeneities in the cross-section affect the flow of water though the cross-section, thereby influencing the critical head result.

The research to soil heterogeneities is done in two parts. A general part, in which the general effect of a continuous heterogeneity thought the whole cross section is determined. After which a case study specific research is done. In the case specific part, local data is used to identify local heterogeneities. The influence of the identified heterogeneities on the critical head result is then determined. If is is possible, the general research will be applied to see if it is possible to approach the results of the case specific research.

# 8

# General soil heterogeneity research

## 8.1. Introduction and model set-up

When a constant horizontal layer throughout the whole, from now on called **"resistance layer"**, is present in the aquifer, with a hydraulic conductivity lower than the aquifer's hydraulic conductivity, three flow scenarios can occur. Before the flow scenarios are named, an overview of the parameters which will be used in this chapter will be named by use of the figure below (see fig. 8.1).

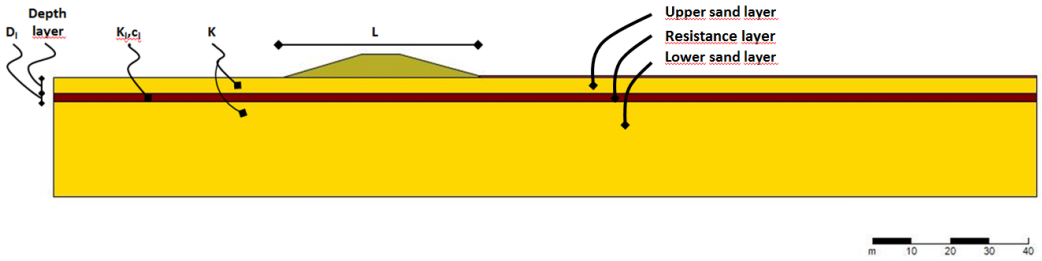


Figure 8.1: Overview of the parameters in an example model

The three flow scenarios are described below, in fig. 8.2 a visual representation of the scenarios is given.

**Flow scenario 1** :Water can flow through the resistance layer downwards and upwards, in this case the water will penetrate in the lower sand layer and eventually flow back through the resistance layer upward (fig. 8.2a);

**Flow scenario 2** :Water can flow through the resistance layer downwards, but is stopped from flowing upward, in this case the lower sand layer will drain the water from the upper sand layer(fig. 8.2b);

**Flow scenario 3** :Water can't flow through the resistance layer to the lower sand layer, in this case the lower layer is sealed and water only flows through the upper sand layer(fig. 8.2c).

Figure 8.2: Three flow scenarios

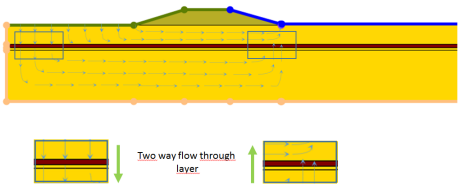


(a) **Flow scenario 1**:2 way flow through resistance layer

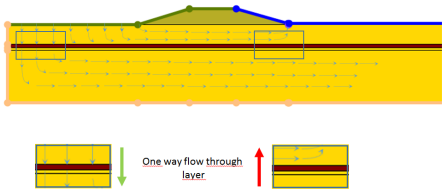


(b) **Flow scenario 2**:1 way flow through resistance layer

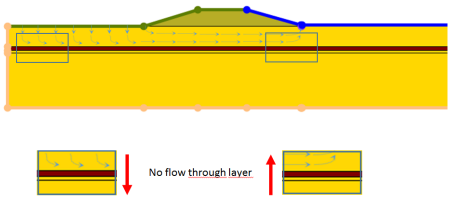


(c) **Flow scenario 3**: No flow through resistance layer

To see how a resistance layer influences the result of the piping safety analysis, the scenarios as described above are computed. To see when which scenario occurs, the thickness, hydraulic conductivity and placing height of the resistance layer is varied. Because working with three unknown parameter is difficult, the factor "c" is introduced. The c-factor can be explained as the resistance a layer gives to vertical flowing of water through the layer.

$$c_l = D_l / K_l \tag{8.1}$$

In which $c_l$ is the resistance in days, $D_l$ the thickness of the resistance layer and $K_l$ the hydraulic conductivity of the resistance layer.

As one value of "$c_l$" can have different meanings: a high $D_l$ and low $K_l$ value or a low $D_l$ and high $K_l$ value. To check if, for one $c_l$-value, the results are the same with different computations a verification is done, as can be seen in table 8.1. If these computations result in the same critical head, it can be concluded that the composition of the $c_l$-factor ($D_l$-$K_l$ value ratio) does not affect the result.

Table 8.1: Verification

| Thickness $D_l$ | Hydraulic conductivity $K_l$ | Resistance $c_l$ | Critical head |
|---|---|---|---|
| 0.5 m | 0.00025 m/day | 2000 days | 4.05 m |
| 1.0 m | 0.0005 m/day | 2000 days | 4.05 m |
| 2 m | 0.001 m/day | 2000 days | 4.05 m |
| 4 m | 0.002 m/day | 2000 days | 4.05 m |

To see when which scenario occurs, the $c_l$-value is varied. It is chosen to use a thickness of the resistance layer of 0.5m. In this way only the hydraulic conductivity and the placing height are varied. To limit the amount of computations, a seepage length and a hydraulic conductivity of the aquifer (sand layers) is chosen. The seepage length is chosen to be 50m and the hydraulic conductivity of the aquifer is chosen at 20 m/day.

Two limit states, most likely, limit the results when the $c_l$-value is varied per depth:

- The lower stateundary is computed by deleting the resistance layer and see what the result of the computation is;: When the whole aquifer will be used for water flow. This bo
- The upper state: When only the aquifer part above the resistance layer will be used for water flow. This boundary is computed by deleting the sand layer below the resistance layer and the resistance layer, resulting in a relatively thin sand layer.

The results for the boundaries can be seen in the table below (see table 8.2). The "upper" boundary is a continuous result, as the thickness of the whole model doesn't change per placing height of the resistance layer. The results are depicted in the critical head.

Table 8.2: Limit states for the different heights of the resistance layer

| Depth layer [m] | Lower state ($\Delta H_{cr}$) [$m$] | Higher state ($\Delta H_{cr}$) [$m$] |
|---|---|---|
| 2 | 3.0 | 6.4 |
| 3 | 3.0 | 5.6 |
| 4 | 3.0 | 5.0 |
| 5 | 3.0 | 4.8 |
| 6 | 3.0 | 4.4 |
| 7 | 3.0 | 4.2 |
| 8 | 3.0 | 4.0 |
| 9 | 3.0 | 3.9 |
| 10 | 3.0 | 3.8 |

## 8.2. Results

Per depth, the hydraulic conductivity($K_l$) for the resistance layer is varied(and so the c-value). To do this in a structured way, with workable numbers, the results for each depth are computed with the same numbers, which can be seen in the tables in appendix I. These table depict all the results of the computations as a increase in critical head in comparison with the standard model, with a critical head of 3m. As a summary of these results a graph is computed in which the increase(or decrease) in critical head is depicted in percentages per depth and $c_l$-value. This percentage is relative to the "lower" boundary, as the current safety analysis uses a continuous hydraulic conductivity for the aquifer.

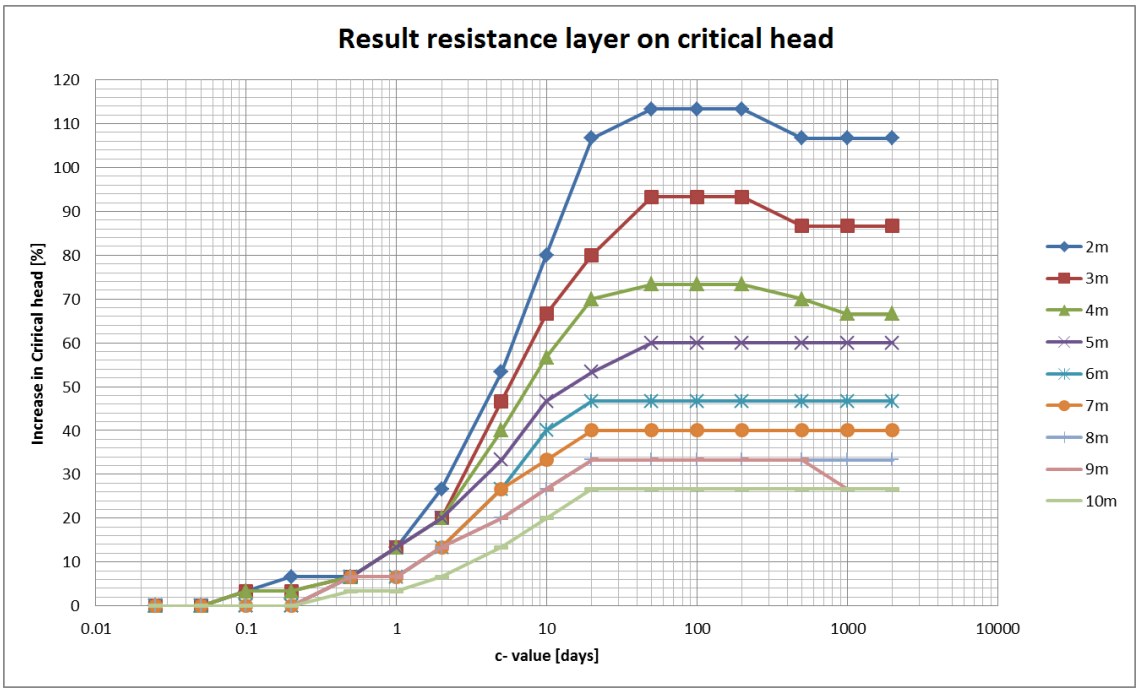


Figure 8.3: Results for L=50m, K=20m/day

To give more insights in how a layer influences the critical head, more models are set-up. The following models are set-up:

- Hydraulic conductivity of the aquifer (K)= 20m/day;
  - Seepage length (L)= 25m;
  - Seepage length (L)= 50m;
  - Seepage length (L)= 100m.
- Hydraulic conductivity of the aquifer (K)= 40m/day;
  - Seepage length (L)= 25m;
  - Seepage length (L)= 50m;
  - Seepage length (L)= 100m.

The results of these models can be seen in appendix I.

## 8.3. Analysis

The three flow scenarios as described in section 8.1 should be clear in the graphs. In this section the results will be analysed to see whether this is true.

The three flow scenarios, as described in section 8.1 are in order of increasing hydraulic conductivity of the resistance layer:

**Flow scenario 1:** The "normal" situation in which the flow progresses in both ways through the resistance layer , this results in lower critical heads, but increasing with increasing resistance of the resistant layer;

**Flow scenario 2:** One way flow through the layer(only downward), this results in an even higher critical head, as the water is drained to the lowest part of the aquifer and the flow area is small;

**Flow scenario 3:** No flow through layer, this results in a high critical head, as there is less aquifer area through which the flow can progress.

As the trend of the graphs, for different seepage lengths and hydraulic conductivities of the aquifer, is relatively similar, the results will be analysed by looking at one particular graph. The analysis below is done based on the graph for an initial seepage length of 50m and a hydraulic conductivity of the sand layer of 20m/day. This graph can be seen in fig. 8.3.

Looking at fig. 8.3 it can be concluded that for small depths flow scenario 2 occurs. For larger depths this flow scenario remains absent. The absence of flow scenario 2 is the result of the lower increases in critical head for deeper layers. If the difference in critical head between the case in which the resistance layer is very permeable and the case in which it is impermeable is not very large, the transition between flow scenario 1 and 3 is very rapid, resulting in the absence of flow scenario 2.

In fig. 8.4 the transitions between the flow scenarios are shown. It must be noted that the flow scenario 2 does not occur for every depth of the resistance, but only if this depth is small. For resistance layer depths for which flow scenario 2 does not occur, the boundary between flow scenario 1 and 2, becomes the boundary of flow scenario 1 and 3. In other words, flow scenario 3 replaces flow scenario 2, see the dashed part of the boundary line.

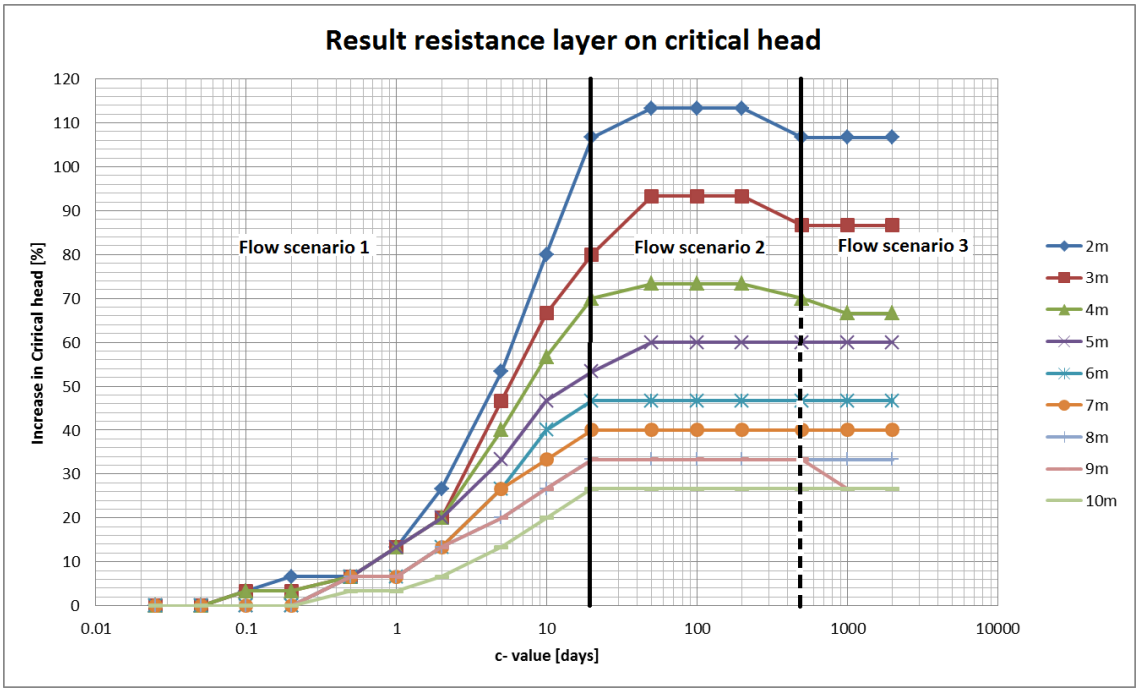


Figure 8.4: The 3 mechanisms showed as 3 zones for L=50m, K=20m/day

# 9

# Case study specific soil heterogeneity research

## 9.1. Introduction/Approach

In section 2.4 it was stated that the influence of the heterogeneities in the **Holocene** layer would be investigated. To determine the separation between the Holocene and Pleistocene depostits, the *Regis-model* is used. Regis is a hydro-geological model which describes, among other things, the deposits. As the Holocene deposit is, in the Regis model, identified as one deposit, the Holocene boundary can easily be determined.

Heterogeneities in the cross-section can be identified if the subsoil of the cross-section is mapped. Mapping the cross-section can be done based on the available data. Data about the soil can be present in for example, the form of core-drillings, CPT-tests or other methods to identify soil layers. There are also subsoil models available based on stochastic interpolation, like the GeoTop model.

### 9.1.1. Creating the cross-section

To create the best possible cross-section, local data is preferred, but this data is scarce. A collection of local data samples can be seen at Dinoloket [33]. From Dinoloket, local samples can be extracted to map the soil. In this Thesis, the focus has been placed on the heterogeneities in the Holocene layer, as is could be possible that the samples do not cover the whole reach of the Holocene layer, they have to be completed. As an assumption, the GeoTop model, which is explained in appendix H, is used to complete the local samples, if necessary. As this model is not very certain on local level it is only used as a completion source for the local data from samples. Completing the local samples with GeoTop is done with much care, because of the uncertainty of the GeoTop model.

Per case the mapping of the soil, as a preparation for the model set up, will be done in the following order:

1. Determine the Holocene depth boundary from Regis;
2. Collect all the samples close to the case location;
3. Complete the samples, if necessary, with the GeoTop model;
4. Determine the cross-section of the case;
5. Identify the heterogeneities in the cross-section;

## 9.2. Heterogeneities in the Case cross-sections

### 9.2.1. Salmsteke cross-section

**Holocene boundary**

As explained in the introduction of this chapter, the Holocene depth boundary is determined by use of the Regis model. From the Regis model, the cross-section of the case can be extracted, containing several deposit layers, see fig. 9.1. As can be seen in the figure, the Holocene depth boundary is at a height of around NAP-10m. The boundary is more or less horizontal and it can therefore be assumed that the boundary throughout the cross-section, which is also depicted in the figure, is constant.

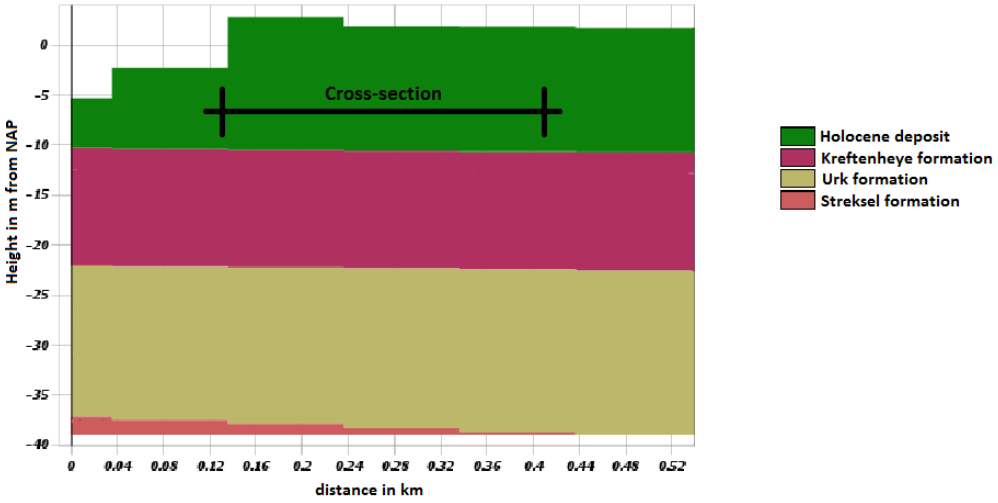


Figure 9.1: Cross section Salmsteke case, deposit layers[33]

**Samples**

As explained in the introduction of this chapter, samples will form the base of the cross-section. As a start, the available samples from Dinoloket[33], close to the cross-section, will be collected. However, in this case, additional samples are taken for the safety analysis. In appendix G the collection of these samples can be seen. The collection of samples consist of samples from Dinoloket and boreholes and probing samples from the additional research for the safety analysis. An overview of the sample locations can be seen in fig. 9.2. The red line in this figure depicts the location of the cross-section.

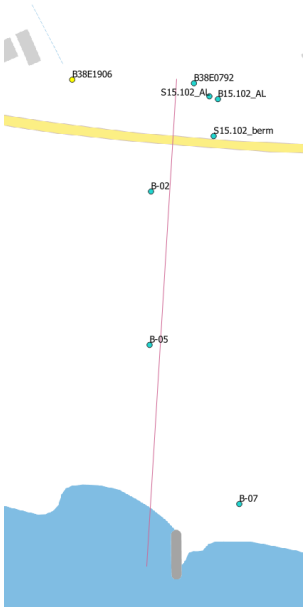


Figure 9.2: Location of the samples for the Salmsteke case

To create a useful cross-section out of the samples, the samples are transformed to the same format. The probing samples, therefore, have to be interpreted [40]. The interpreted samples and the boreholes have to be combined to create a cross-section, however, when looking at the samples it can be seen that they do not cover the whole Holocene layer.

To create a total cover of the Holocene layer, the samples have to be completed. The completion of the samples is, because of lack of data, done with the data from the GeoTop model. The GeoTop model is explained in more detail in appendix H. The downside of the GeoTop model is that the information in this model is in voxels of 100x100x0.5m (length x width x depth). This means that in horizontal way, the precision is on scale of 100m. In vertical way the precision is on scale of 0.5m. The soil types in the GeoTop model are added to the voxels by stochastic interpolation based on the available data from samples at several locations. An overview of the GeoTop model at the location of the Salmsteke case can be seen in fig. 9.3.

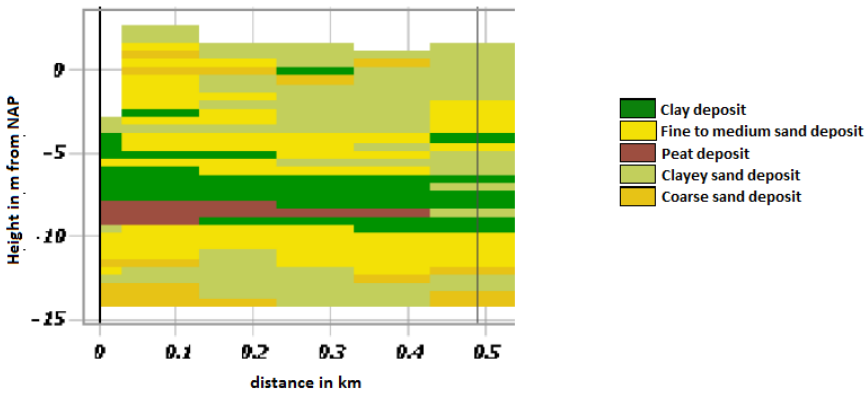


Figure 9.3: Cross section Salmsteke case, soil type layers according to GeoTop[33]

Because the GeoTop model is not very accurate, the information must be handled with care. It is therefore assumed that only the heterogeneities which are present on more or less the same height in 3 voxels in a row are used to complete the boreholes, this covers the whole cross-section. From fig. 9.3, the following heterogeneities are identified:

- A clay layer with the bottom on NAP -10m with a thickness of 0.5-1.0m throughout the whole cross-section;
- A peat layer with the bottom on NAP -9m with a thickness of 0.5-1.0m throughout the whole cross-section;
- A clay layer with the top on NAP -7 m with a thickness of 1.0-2.0m throughout the whole cross-section.

**Soil model**

These heterogeneities, identifies from the GeoTop model, are added to the samples from Dinoloket, if these samples do not cover this range in height. The remaining "spaces" in the boreholes are assumed to be sand as was used in the standard models. The completed boreholes can are put in D-Geo Flow in the form of boreholes. D-Geo Flow creates, according to these boreholes a cross-section, based on linear interpolation between the specific layers in these boreholes. The cross-section from D-Geo Flow can be seen in fig. 9.4.

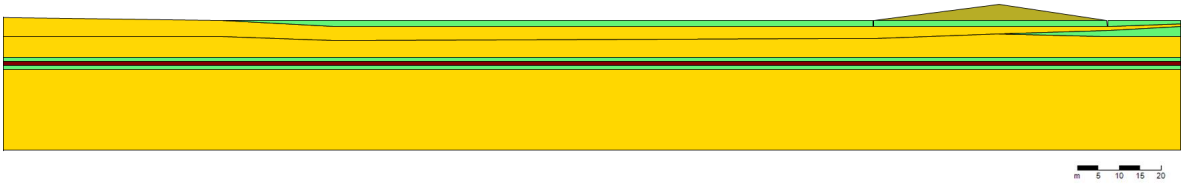

Figure 9.4: Cross section from D-Geo Flow, from boreholes and GeoTop, case Salmsteke

From the model,generated directly from the boreholes, a workable model must be made. In section 4.2, the set-up for the standard model is explained. As the results are compared with the results from the standard model, the current model must be adapted to the standard model form. This means, the foreshore is not entirely included and the hinterland is added, with the same properties as in the standard model. This results in the model which can be seen below.

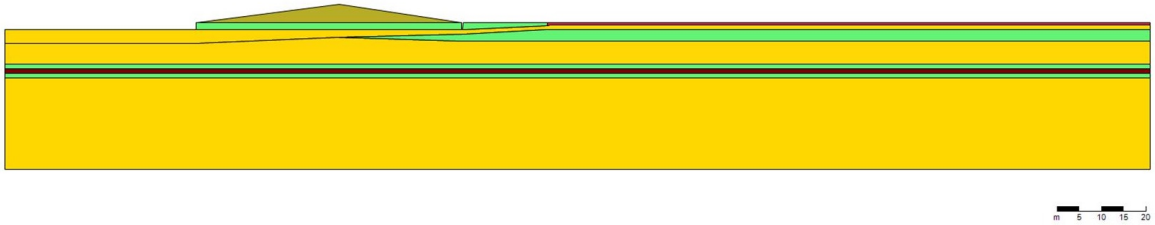

Figure 9.5: Workable cross-section from D-Geo Flow, simplified from fig. 9.4 case Salmsteke

In the cross-section above, four heterogeneities can be seen, these are numbered with their corresponding model numbers:

**Model 1:** A clay layer at the inner toe of the cross-section with a thickness of 2.5m, placed at 1.5m below the toe, reaching from the centre of the dike to the end of the cross section;
**Model 2::** A clay layer with the top on NAP -7 m with a thickness of 1.0-2.0m throughout the whole cross-section;
**Model 3:** A peat layer with the bottom on NAP -9m with a thickness of 0.5-1.0m throughout the whole cross-section;
**Model 4:** A clay layer with the bottom on NAP -10m with a thickness of 0.5-1.0m throughout the whole cross-section.

These heterogeneities will be added to the standard model one by one to see how a specific heterogeneity influences the critical head result. The characteristics of the soil types which will be added can be seen in table 3.3.

### 9.2.2. Honswijk cross-section

**Holocene boundary**
The Holocene depth boundary for the Honswijk case, as can be seen in fig. 9.6, can be assumed at NAP-7.5m. Also in this case the layer can be assumed to be horizontal throughout the cross-section.

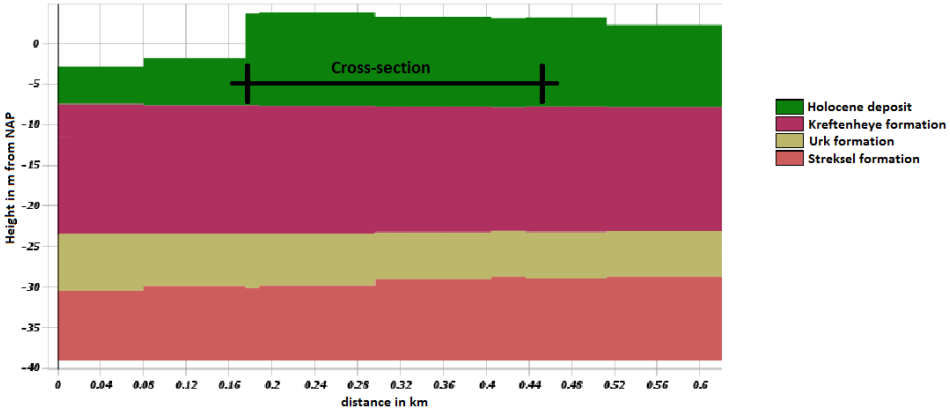


Figure 9.6: Cross section Honswijk case, deposit layers[33]

**Samples**

The collection of samples, as depicted in fig. 9.7 can be seen in appendix G. The samples are collected from Dinoloket. The cross-section is depicted with the red line. As in this case all the samples are taken from Dinoloket([33]), the samples already have the same format. The samples can be seen in appendix G. From the samples a cross-section must be made. However, the samples do not cover the whole reach of the Holocene layer. This means they have to be completed. As described before, the GeoTop model is, carefully, used to complete the samples. The GeoTop cross-section of the Honswijk case can be seen in fig. 9.8. The GeoTop model is used only when clear heterogeneities can be seen, in other words, if the heterogeneities are present in 3 voxels in a row, with this choice the uncertainty is limited. The voxels of the GeoTop model are 100x100x0.5m (length x width x depth). The GeoTop model is described in more detail in appendix H.

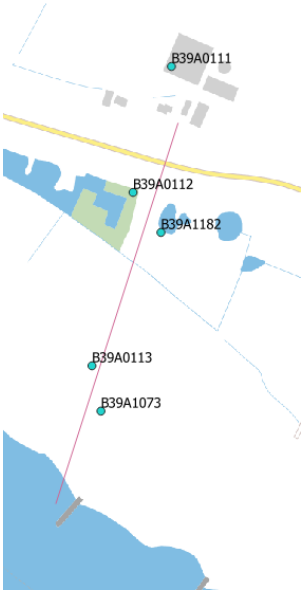


Figure 9.7: Location of the samples for the Honswijk case

As described before, the GeoTop model must be handled with care. This means that only the heterogeneities which can be seen in 3, sequential, voxels are used in this analysis. From the GeoTop model in fig. 9.8, the following heterogeneities can be seen:

- A clay layer at a height of NAP-5m with a thickness of 1-1.5m, located from the left boundary of the cross-section(foreshore included) to 150m to the right;
- A coarse sand layer at a height of NAP-4m, with a thickness of 0.5-1.0m, located in the middle of the cross-section between 100m and 320m in fig. 9.8.

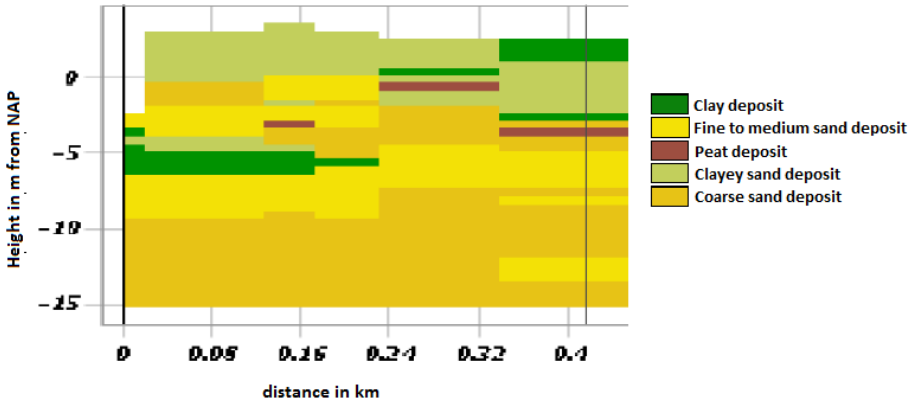


Figure 9.8: Cross section Honswijk case, soil type layers according to GeoTop[33]

**Soil model**

These heterogeneities from GeoTop are added to the samples from Dinoloket, if they do not conflict with the data from the samples. in this case the clay layer heterogeneity does not conflict with the data from the samples, but the coarse sand layer does. This means only the clay layer heterogeneity is included in the samples. The remaining "spaces" are assumed to be sand as it was used in the standard models. The

completed samples are put in D-Geo Flow in the form of boreholes and D-Geo Flow creates a cross-section, based on linear interpolation between the specific soil layers in the boreholes. As the dike was not included in the amples, it is added according to the data from the AHN. The cross-section from D-Geo Flow can be seen in fig. 9.9.

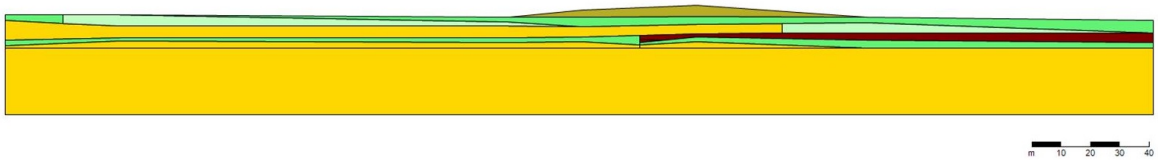


Figure 9.9: Cross section from D-Geo Flow, from boreholes and GeoTop, case Honswijk

As can be seen in the figure above, the model is very variable, in other words, a lot of layers can be seen. To make the model workable, it is transformed by use of the standard model, as the result of the standard model is compared with the results of the model with the heterogeneities. The adapted model can be seen in fig. 9.10. In this model the foreshore is not entirely included, an exit point is created and a hinterland with a blanket is added.

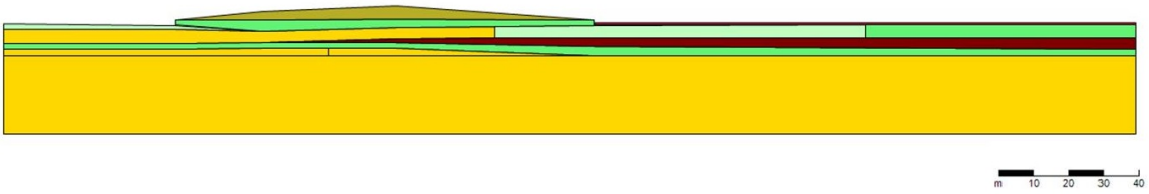


Figure 9.10: Workable cross-section from D-Geo Flow, simplified from fig. 9.4 case Honswijk

In fig. 9.10 the simplified cross-section can be seen. This cross-section will now be used to identify the heterogeneities in the cross-section. The heterogeneities which are not horizontal will be assumed to be horizontal with variations in height to simulate the skewed orientation. The identified heterogeneities are:

**Model 1:** A clayey sand layer at ground level with a thickness of 1.5m and located between the left boundary and the middle of the outer slope of the dike;

**Model 2:** A clayey sand layer below at ground level, but below the blanket in the hinterland with a thickness of 3.5m and located at the middle of the inner slope of the dike with a length of 100m;

**Model 3:** A clay layer below the blanket in the hinterland with a thickness of 3.5m and located at the right boundary with a length of 75m;

**Model 4:** A peat later at a depth of NAP-2.5m with a thickness of 2.5-3.0m. and located from the right boundary to the middle of the inner slope of the dike;

**Model 5:** A clay layer at a depth of NAP -4 to -5m with a thickness of 1.5-2.5m throughout the whole cross-section.

### 9.2.3. Den Oord cross-section

**Holocene boundary**

The Holocene boundary can be determined by looking at fig. 9.11. In this figure it can be seen that the holocene boundary can be drawn around NAP-7 to -7.5m. Because a boundary must be chosen to model the case in the right way, NAP -7.5m is chosen to be the Holocene boundary in this case.

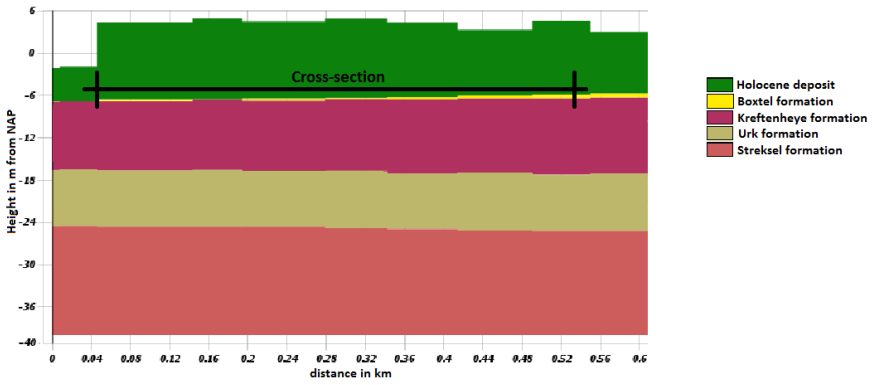


Figure 9.11: Cross section Den Oord case, deposit layers[33]

**Samples**

The collection of samples, as depicted in fig. 9.12 can be seen in appendix G. The samples are collected from Dinoloket. The cross-section is depicted with the red line. In this case all samples are collected from Dinoloket [33], all the samples have therefore the same format. An overview of the samples can be seen in appendix G.3. As not all the samples cover the whole Holocene layer, the samples have to be completed. For this, as in the previous case, the GeoTop model is used.

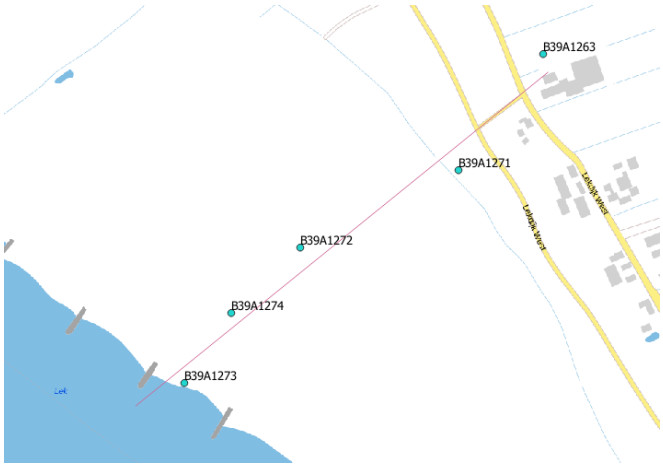


Figure 9.12: Location of the samples for the Den Oord case

With the use of the GeoTop model, the same approach as in the previous case is used. Only the heterogeneities which can be seen in 3 voxels in a row, horizotally and vertically, are used. The voxels of the GeoTop model are 100 x 100 x 0.5m (length x width x height).

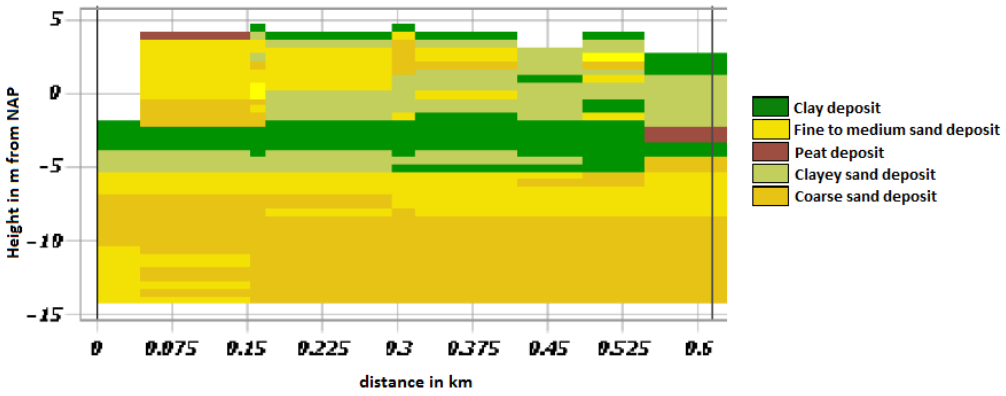


Figure 9.13: Cross section Den Oord case, soil type layers according to GeoTop[33]

**Soil model**

From the GeoTop cross-section of the Den Oord case, see fig. 9.13,only one clear heterogeneity is identified, this is the clay layer at a depth of NAP -2.5 - -4m, with a thickness of around 1.5 - 2.0m. This heterogeneity is added to the samples from Dinoloket, if it does not conflict with the data from the samples. Combining the findings from GeoTop with the samples, it becomes clear that a clay layer of at least, 6m is present. This clay layer is present at ground level to a depth of around NAP-3 to -4m. This layer can therefore be identified as a cover layer.

In the safety analysis, cover layers are assessed against heave and uplift, this is however outside the scope of this Thesis. Therefore this case study location is not relevant for the research to heterogeneities in the subsoil.

## 9.3. Modelling the heterogeneities

The heterogeneities described in the previous section will be modelled in this section. The results will be presented and analyses will be done. Because of uncertainty, the hydraulic conductivity is not used as a determined value in the computation, but a range of values is used. These ranges, for the different soil types, can be seen in table 3.3 .

### 9.3.1. Salmsteke

As described in the previous section, the cross-section, determined from local data, holds the following heterogeneities and corresponding models:

**Model 1:** A clay layer at the inner toe of the cross-section with a thickness of 2.5m, placed at 1.5m below the toe, reaching from the centre of the dike to the end of the cross section;

**Model 2:** A clay layer with the top on NAP -7 m with a thickness of 1.0-2.0m throughout the whole cross-section;

**Model 3:** A clay layer with the bottom on NAP -10m with a thickness of 0.5-1.0m throughout the whole cross-section;

**Model 4:** A peat layer with the bottom on NAP -9m with a thickness of 0.5-1.0m throughout the whole cross-section.

(a) Model 1, Salmsteke

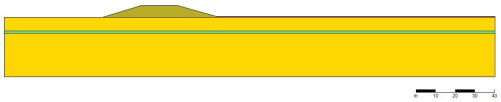

(b) Model 2, Salmsteke

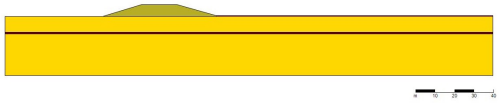

(c) Model 3, Salmsteke

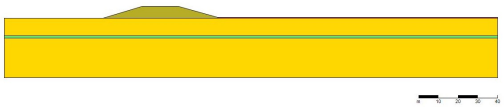

(d) Model 4, Salmsteke

These heterogeneities will be added one by one to the standard model from section 4.2, in the sequence as can be seen above. The resulting 4 models can be seen in appendix J.1. The results from these models will be compared to the result of the standard model(see section 4.2), this critical head result was 3.4m. In the following the results will be presented as an in-/decrease in critical head with respect to the result of the standard model..

As an overview, the results are presented in a histogram which can be seen in fig. 9.15. The numerical results can be found in tables J.1 to J.4 in appendix J.1.


Figure 9.15: Summary of the results of modelling the heterogeneities for the Salmsteke case, results depicted as an in-/decrease in critical head in percentages

In fig. 9.15 the results can be seen. In this histogram the results of the different models can be seen in which the corresponding heterogeneities were added. The results of the models are a range of values because of the variation in input of the hydraulic conductivity, placing height and depth of the heterogeneities.

### 9.3.2. Honswijk

The heterogeneities identified in the Holocene layer of the Honswijk cross-section, as described before, are:

**Model 1:** A clayey sand layer at ground level with a thickness of 1.5m and located between the left boundary and the middle of the outer slope of the dike;

**Model 2:** A clayey sand layer below at ground level, but below the blanket in the hinterland with a thickness of 3.5m and located at the middle of the inner slope of the dike with a length of 100m;

**Model 3:** A clay layer below the blanket in the hinterland with a thickness of 3.5m and located at the right boundary with a length of 75m;

**Model 4:** A peat later at a depth of NAP-2.5m with a thickness of 2.5-3.0m. and located from the right boundary to the middle of the inner slope of the dike;

**Model 5:** A clay layer at a depth of NAP -4 to -5m with a thickness of 1.5-2.5m throughout the whole cross-section.

(a) Model 1, Honswijk

(b) Model 2, Honswijk

(c) Model 3, Honswijk

(d) Model 4, Honswijk

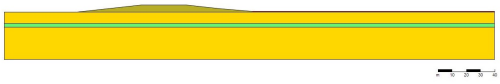

(e) Model 5, Honswijk

As in the Salmsteke case, the heterogeneities, as named above, will be added to the standard model for Honswijk from section 4.2. The critical head result of this standard model from section 4.2 is 6.2m. This result will be used as the reference level to determine the in-/decrease in critical head when the heterogeneities are added to the model.

In fig. 9.17 the results are presented in a histogram per model. The model numbers are in the same sequence as the heterogeneities are explained above. The numerical results can be seen in tables J.5 and J.9 in appendix J.2.

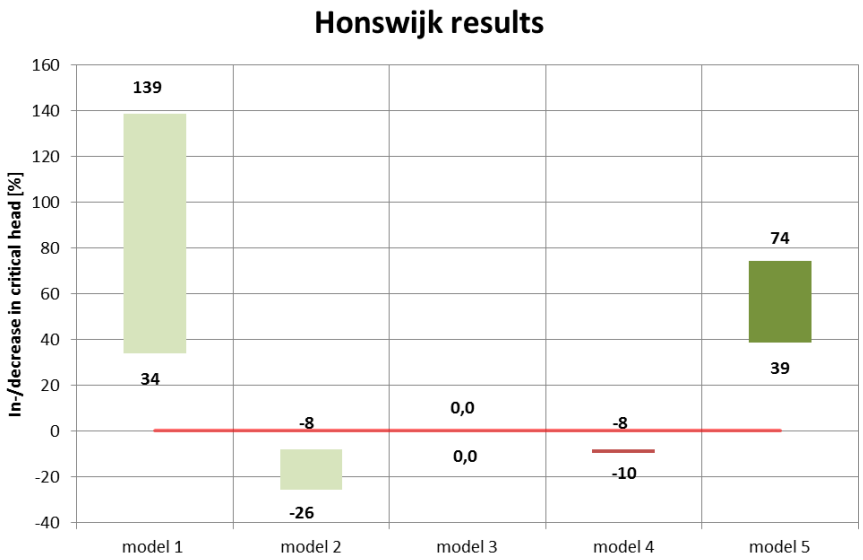


Figure 9.17: Summary of the results of modelling the heterogeneities for the Honswijk case, results depicted as an in-/decrease in critical head in percentages

In fig. 9.17 the results can be seen. In this histogram the different models can be seen in which the corresponding heterogeneities are added. The results of the models are a range of values because of the variation in input of the hydraulic conductivity, placing height and depth of the heterogeneities.

## 9.4. Analysis of the results

In the previous section the heterogeneities were modelled and the results were presented. In this section the results will be interpreted and analysed.

### 9.4.1. Analysis Salmsteke results

In fig. 9.15 the results can be seen. The band width of the diagram represents the results of the models is because of the variation in input of the hydraulic conductivity, placing height and depth of the heterogeneities. The models (1 to 4) will be analysed separately in this section.

#### Model 1 - Salmsteke

In the first model a clay layer at the inner toe of the cross-section with a thickness of 2.5m is placed 1.5m below the toe. Reaching from the centre of the dike to the end of the cross-section.

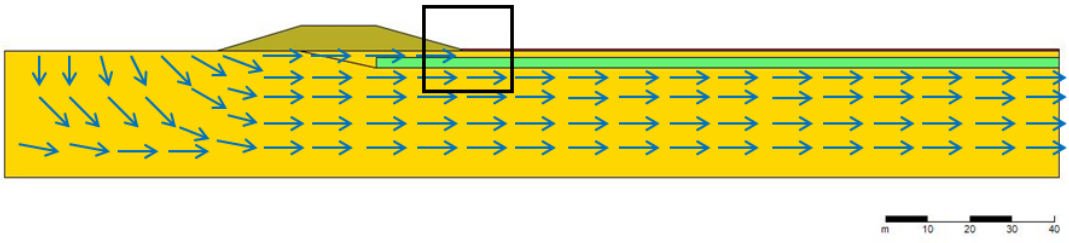


Figure 9.18: Model 1 Salmsteke, schematic flow pattern

The increase in critical head, with respect to the standard model, is from 9 to 20%. The increase can be explained by the fact that the clay layer at the inner toe is a lot less permeable (lower hydraulic conductivity)

than the surrounding sand layer. As the pipe will form just below the dike, in the sand layer. The flow velocities in this layer must be sufficient for the sand to erode.

In this case the clay layer complicates the water flow, as the hydraulic conductivity is a lot lower than the sand layer. The flow area around the exit point, where piping starts, is thereby limited to the small strip of sand above the clay layer. The process can be seen in figs. 9.18 and 9.19. Fig. 9.18 depicts the overview of the flow pattern and fig. 9.19 depicts the process described above in detail. The blue arrows depict the flow pattern. The red arrows are the flow vectors which are complicated by the clay layer due to its lower hydraulic conductivity.

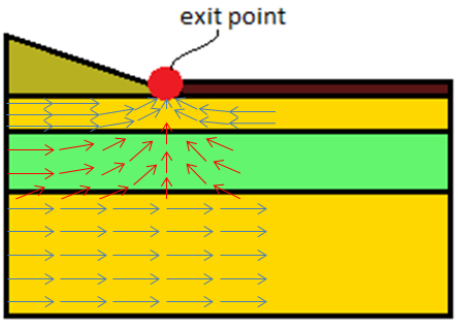


Figure 9.19: Schematic flow pattern around exit point -Model 1 Salmsteke- (detail from fig. 9.18)

The hydraulic conductivity of the clay layer defines the impact of the clay layer on the flow velocities. A lower hydraulic conductivity lead to lower flow velocities. The range in the results, from fig. 9.15, is hereby explained: A lower hydraulic conductivity leads to lower flow velocities in the layer, which leads to a less water transportation to the exit point, which leads to a higher resistance to erosion and thereby a higher critical head of the model.

**Model 2 - Salmsteke**

The second model contains a horizontal clay layer throughout the whole cross-section. This clay layer has a thickness of 1.0-2.0m and is placed at NAP-7m

The increase in critical head can be explained by the processes described in chapter 8. A resistance layer (lower hydraulic conductivity) can seal the lower part of the aquifer, the part below this layer. This reduction in flow area leads to an increase in critical head. Even if the layer is not sealed, but the added, more resistant, layer has a lower permeability than the surrounding aquifer, the water flow to the exit point is complicated and the critical head will increase.

As explained in chapter 8 the results from this chapter will be checked with the results from the case studies. The starting point is to determine which graph must be used. As the seepage length for the Salmsteke case is 58m and the hydraulic conductivity of the aquifer is 20m/day, the graph in fig. I.2 can be used and can be seen as a good approximate. The depth of the layer is NAP-7m, so the 7m line must be used. The results from the graph and the comparison with the results from the case studies can be seen in table 9.1.

Table 9.1: Comparison general and case study research, model 2

| C-value [$days$] (D/K) | Crit. head inc. fig. I.2 [%] | Crit. head inc. case study [%] | Difference [%] |
|---|---|---|---|
| 500 | 40 | 47 | 7 |
| 6.67 | 29 | 32 | 3 |
| 1000 | 40 | 47 | 7 |
| 13.33 | 40 | 41 | 1 |

The depicted increase in critical head is the increase with respect to the standard model. In the table can be seen that the differences are very small between the general research and the result from the case study research. The general research slightly underestimates the increase, but this is, most likely, due to the difference in seepage length. It can, with these findings, be concluded that the general research, for this case is a good estimate.

**Model 3 - Salmsteke**

In the third model a peat layer was added at a depth of NAP-9m. The layer has a thickness of 0.5-1.0m.

For the third model, the same holds as the second model. The increase in critical head can be explained by the fact that a horizontal layer throughout the cross-section can seal the lower part of the aquifer. This decreases the flow area and thereby increases the critical head. However, peat layers do not have a sufficient low hydraulic conductivity to seal the lower aquifer part, but the hydraulic conductivity is a lower that the hydraulic conductivity of the aquifer. This results in more resistance against water flow through the layer, which leads to less water flow to the exit point, which leads to an increase in critical head.

For this model also holds that the results from the general subsoil research can be applied. The increase in critical heads from the general research and from the case study will be compared to see what the difference is and if thereby the results from the general research can be applied. The comparison can be seen in table 9.2. The bottom of the layer is placed at a depth of NAP-9m, so the 8m line must be used.

Table 9.2: Comparison general and case study research, model 3 - Salmsteke

| C-value [$days$] (D/K) | Crit. head inc. fig. I.2 [%] | Crit. head inc. case study [%] | Difference [%] |
|---|---|---|---|
| 0.5 | 7 | 6 | 1 |
| 0.1 | 0 | 3 | 3 |
| 1.0 | 7 | 9 | 2 |
| 0.2 | 0 | 3 | 3 |

From the comparison in table 9.2 it can be concluded that the results from the general research are, again, applicable on the case study, as the difference is very small. For all the results, except for c=0.5 days, the general research slightly underestimates the results, but this can be explained by the difference in seepage length. The higher value at c=0.5 days will, most likely be the result of the step size in the computations. However, the difference is only 1%, which is not a significant.

**Model 4 - Salmsteke**

In the fourth model a clay layer throughout the cross-section is added with the bottom at a depth of NAP-10m and a thickness of 0.5-1.0m.

The explanation for the increase in critical head can be found in the analysis of the previous two models, as the explanation is the same for this model. The only difference is the resistance to flowing and the placing height. Again, the results of this case will be compared to the general subsoil research, to see how this general research can be applied on the cases. The comparison between the two can be seen in table 9.3. As the bottom of the layer is placed at a depth of NAP-10m, the 9m line must be used in this comparison.

Table 9.3: Comparison general and case study research, model 4 - Salmsteke

| C-value [$days$] (D/K) | Crit. head inc. fig. I.2 [%] | Crit. head inc. case study [%] | Difference [%] |
|---|---|---|---|
| 250 | 33 | 35 | 3 |
| 3.33 | 16 | 17 | 1 |
| 500 | 33 | 35 | 2 |
| 6.67 | 22 | 26 | 4 |

In this case it can, similar to the other models, be seen that the difference between the results from the general research and the case study is very small, this makes the general research applicable on the case and this model. The small difference which is present is the result of the difference in seepage length between the general research and the case study.

### 9.4.2. Analysis Honswijk results

In fig. 9.17 the results can be seen. The band width of the diagram represents the results of the models is because of the variation in input of the hydraulic conductivity, placing height and depth of the heterogeneities. The models (1 to 4) will be analysed separately in this section. The models (1 to 5) will be analysed separately in this section.

**Model 1 - Honswijk**

The first model contains a clayey sand layer at the outer toe of the dike. The layer is placed directly below ground level and has a thickness of 1.5m. The layer reaches from the left boundary of the cross-section to the middle of the outer slope of the dike.

The results show a large increase in critical head of 34 to 139%. This large increase can be explained by the fact that the clayey layer prevents the water to seep into the aquifer. The clayey sand layer has a lower hydraulic conductivity than the aquifer which results in more resistance against flowing through the layer.

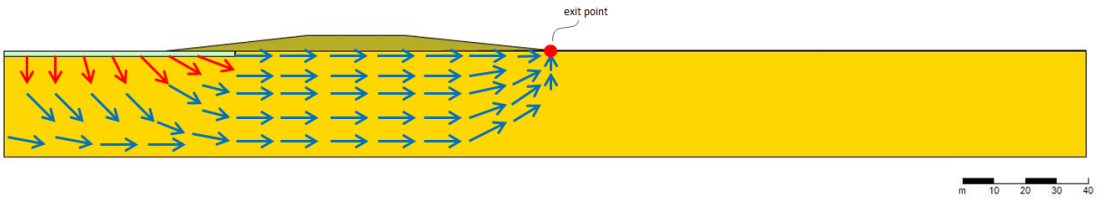


Figure 9.20: Model 1 Honswijk, schematic flow pattern

In fig. 9.20 the schematic flow pattern to the exit point can be seen. The red arrows show the flow through the clayey sand layer. This flow is resisted by the clayey sand layer and will therefore be a lot less than the flow through the surrounding sand. Therefore the pipe formation, which needs a large enough flow velocity for the particles to erode, will be complicated, resulting in a high critical head.

**Model 2 - Honswijk**

The second model contains a clayey sand layer below the exit point. It reaches from the middle of the inner slope to the right boundary. The layer is placed at ground level and has a thickness of 3.5m.

The decrease in critical head, as can be seen in fig. 9.17, can (partly) be explained, in contrary with the other results, not by looking at the hydraulic conductivity, but by looking at the particle diameter. As section 3.3.4 states, the particle diameter of clayey sand/sandy clay is half the size of the particle size of the aquifer.

In this configuration you would expect the critical head to **in**crease instead of **de**crease, because of the increase in flow resistance around the exit point, this will be explained later. However, due to the smaller particle size, less flow velocity is needed to erode the particles. As the pipe forms, partly, through the clayey sand layer, the critical head decreases because of more erosion in the clayey sand layer. To verify the above stated explanation, the computation for this model are done again, but this time with a particle size equal to the particle size of the surrounding aquifer. The results can be seen below:

Table 9.4: Results case Honswijk, model 2, including computations with other particle size

| Hyd, cond, $[m/day]$ | Critical head $[m]$ $D_{70} = 0.0001m$ | Critical head $[m]$ $D_{70} = 0.0002m$ |
|---|---|---|
| 0.1 | 5.7 (-8) | 6.7 (13) |
| 0.5 | 4.6 (-26) | 5.1 (-17) |

In the table above it can be seen that the change in particle size has effect on the critical head. However, in contrary with the expected, the results are not all positive. This can be explained by the fact that, unless the flow resistance to the exit point is increased, the total resistance against piping is decreased, due to the fact that the water around the exit point can not flow away from due to the increase in critical head around the exit point. This is illustrated by the figures below. The mechanisms causing the increase(1) and decrease(2) are depicted separately in respectively fig. 9.22aand fig. 9.22b, a schematic overview can be seen in fig. 9.21.

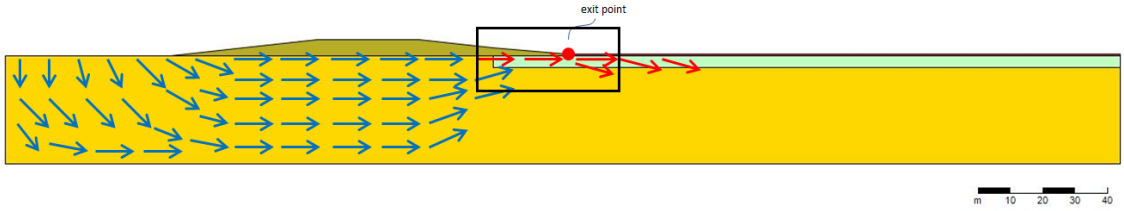


Figure 9.21: Model 2 Honswijk, schematic flow pattern


(a) Model 2 Honswijk, schematic flow pattern causing the **in**crease in critical head(1)

(b) Model 2 Honswijk, schematic flow pattern causing the **de**crease in critical head(2)

**Model 3 - Honswijk**

In the third model, a clay layer is present at the right boundary below ground level. The layer is 3.5m thick and is placed at the right boundary with a length of 75m.

The results in fig. 9.17 show that the influence of the clay layer at the right boundary is 0. This can be explained by the fact that the soil composition around the pipe has not changed in comparison with the standard model. A layer at the right boundary could affect the flow pattern in the cross-section, however, in this case the layer is not significant enough to achieve that. Therefore the influence is 0.

**Model 4 - Honswijk**

A peat layer of 2.5-3.0m thickness is added in the fourth model. It is placed at a depth of NAP-2.5m and is located from the right boundary to the inner slope of the dike.

The decrease in critical head can be explained by examining the flow in the cross-section. If a pipe is formed, water flows to the exit point. This causes an increase in water pressure around the exit point. A part of the water is drained to the surroundings, dependent on the local soil properties.

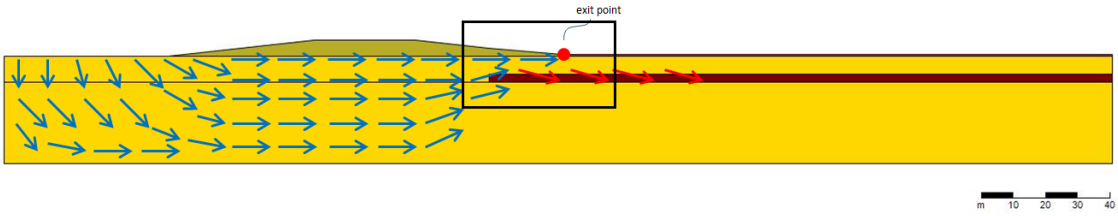


Figure 9.23: Model 4 Honswijk, schematic flow pattern

In this case the peat layer blocks this drainage to the surrounding. Without the drainage of water to the surrounding soil, the pressures around the exit point increase and the flow velocity will increase. This increase will result in more erosion and thereby a decrease in critical head.

However, at the other side, the layer, which is also positioned left of the exit point, will also prevent some water to flow to the exit point. This decrease of flow to the exit point would increase the critical head. These processes are depicted in fig. 9.23 and fig. 9.24, these figures give a schematic image of the flow in the cross-section(fig. 9.23) and in more detail around the exit point (fig. 9.24). It can, according to the results, which are a decrease in critical head, be concluded that the effect of lack of drainage to the surrounding is of more significance than the blockage of flow to the exit point. This is explainable by looking at the model. The layer reaches to just left of the exit point, which makes the blockage of water flow to exit point minimal. As the layer reaches to the right boundary, the lack of drainage can be expected to have a larger effect on the critical head.

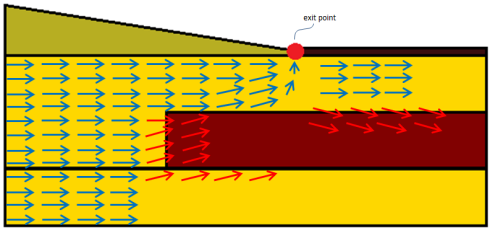


Figure 9.24: Schematic flow pattern around exit point -Model 4 Honswijk- (detail from fig. 9.23)

**Model 5 - Honswijk**

Model 5 contains a horizontal continuous clay layer at a depth of NAP -4 to -5m. The layer is 1.5-2.5m thick and crosses the whole cross-section.

In chapter 8 the process which occurs when a continuous horizontal layer is added to the cross-section, is explained. As the clay layer which is added to the cross-section has a lower hydraulic conductivity than the hydraulic conductivity of the aquifer, the aquifer part below the clay layer can not contribute entirely to the flow capacity of the cross-section. Less flowing area result in less water flow to the exit point and thereby an increase in critical head.

In chapter 8 it was explained that the results of this general research will be checked with the results from the case studies. To determine what the increase in critical head is according to the general research, the correct graph must be selected. As the hydraulic conductivity of the aquifer, in the case study, is 20m/day and the seepage length is 121.72m, the graph with K=20m/day and Lseep=m will be used. This seepage length is lower than the seepage length from the case study, so a little difference in results can be expected.

In the correct graph, the correct line must be chosen. As the layer is located at a depth of NAP -4 to -5m and the ground level is at NAP+3m, the 7 and 8m graph must be used. The comparison between the results from the case study and the results according to the general research can be seen in table 9.5.

Table 9.5: Comparison general and case study research, model 5 - Honswijk

| Depth [$NAP - m$] | C-value [$days$] (D/K) | Crit. head inc. fig. I.3 [%] | Crit. head inc. case [%] | Difference [%] |
|---|---|---|---|---|
| 4 (7m line) | 750 | 64 | 74 | 10 |
| | 10 | 40 | 45 | 5 |
| | 1250 | 62 | 71 | 9 |
| | 16.7 | 68 | 65 | 43 |
| 5 (8m line) | 750 | 56 | 63 | 7 |
| | 10 | 34 | 39 | 5 |
| | 1250 | 55 | 66 | 11 |
| | 16.7 | 58 | 52 | 6 |

In table 9.5, the difference between the case study results and the results according to the general research can be seen. It can be seen that the differences are in the order of 5-10%. This differences can be explained by the fact that the seepage lengths are not equal. A difference in seepage length has influence on the shape of the graph and the values of the general research. However, the difference are small enough to use the general research result as an estimate. Except 2 results, all the results from the general research slightly underestimate the increase in critical head, this is therefore also a safe assumption.

# 10 Conclusions

## 10.1. General soil heterogeneity research

The results from the general research, as depicted in fig. I.1 to fig. I.6, show that the three flow scenarios, which were expected, are present. Depending on the seepage length and the hydraulic conductivity the graphs have different shapes, although the trend is more or less the same.

In fig. 8.4 the three zones in de graph, corresponding to the flow scenarios are depicted. With this the conclusion can be drawn that the most resistance against piping, or highest critical head,(zone 2) is not present at the moment of largest resistance of the resistance layer, but at the moment water only passes the layer one way (only downward). This one way flow of water through a resistance layer occurs for lower hydraulic conductivities than the hydraulic conductivities for no flow through the layer. This, however, does only hold for shallow layers (depth of 5m and less), thereby also depending on the initial seepage length and the hydraulic conductivity of the aquifer. For the configurations where the second flow scenario(one way flow) does not occur, it is replaced by the third flow scenario(no flow), see fig. 8.4.

As expected do less deep resistance layers influence the critical head more and also more rapidly. This effect damps with increasing resistance layer depth. It can also be seen that the zone of increase reaches from a resistance of 1 day to a resistance of 20 days. Below 1 day, almost no increase in critical head is present, and above 20 days, flow scenario 2 or 3 occurs.

From the computations for several seepage length, it became clear that for increasing seepage length, the results become more divergent. For a small seepage length, the results per depth of the resistance layer are relatively close to each other in comparison with a larger seepage length. The increase in critical head per resistance layer depth is also higher for larger seepage lengths.

The results were computed for two hydraulic conductivities of the aquifer. It can be concluded that the trend of the results does not change with varying hydraulic conductivity of the aquifer, but the specific values of the results do change.

## 10.2. Case study specific soil heterogeneity research

### 10.2.1. Heterogeneities in the cross-section

From the literature study it was concluded that heterogeneous soils would increase the resistance against piping. Looking at fig. 9.15 and fig. 9.17 it can be concluded that the influence of specific heterogeneities in the cross-section can be positive as well as negative. The heterogeneities having a positive influence on the result complicate the flow of water through the cross-section, causing a high critical head. This increase in critical head can even be in the order of 140%.

Heterogeneities having a negative influence on the critical head or cause higher water pressures around the exit point, by complicating the drainage of water from the exit point, or ease the pipe formation because of smaller eroding particles.

For all heterogeneities hold that the placing (in height and in horizontal direction), the thickness and the soil characteristic determine the extent of their influence. One constant trend is that shallow heterogeneities have more influence than deeper heterogeneities, positive and negative, depending on the above named variations. The same trend holds for heterogeneities with very low hydraulic conductivities. The influence of a layer increases by decreasing hydraulic conductivity.

### 10.2.2. Application general research

In the analysis of the influence of the heterogeneities, the results were checked with the findings from the general research, if a layer through the whole cross-section was present. From the comparison of the results it became clear that the general research can be applied relatively easily. The prediction according to the general research were on point and had a maximum difference of 10%.

Despite the differences in initial seepage length, the results from the general research approach the results from the case study research very closely. Increasing difference in seepage length , however, increases the difference in result.

# III

# Discussion, Conclusions and Recommendations

# 11 Discussion

In the discussion, the results are discussed and evaluated. As this Thesis split in two main subjects, both subjects are discussed separately. For both research parts, the foreshore research (section 11.1) and the subsoil heterogeneity research(section 11.2), the most important findings are named and discussed. For both subjects, the limitations and shortcomings of the research are discussed.

## 11.1. Foreshore

The effect of a foreshore on the result of the piping safety analysis (critical head result) is conducted in two ways. A general part and a case study specific part . In the general part, the effects of a foreshore are determined for a variation in foreshore cover layer resistance and a variation in foreshore length. In the case study specific part realistic foreshores are modelled and analysed. Sensitivity analyses are performed on possible variations.

### General foreshore research

In the general foreshore research, standard models are varied in foreshore length and resistance. With this approach the effects of increasing foreshore length, increasing foreshore resistance and a combination of both are searched for. The effects of the variations in foreshore length and resistance are explained and discussed. As a conclusion to this discussion, a graph is presented depicting the discussed effects, see fig. 11.1.

**Effect of increasing foreshore resistance**

The resistance of the foreshore cover layer has a large influence on the hydraulic conductivity. Less water can penetrate the aquifer through the foreshore cover layer by increasing resistance, this results in lower water pressures in the aquifer, which leads to more resistance to piping. Values of increasing resistance reach from the lower boundary, which is determined by the situation without foreshore, to the higher boundary, which approaches the result from the Sellmeijer formula in which the whole foreshore is included.

The increase in critical head is not linear, but has a typical S-shape (on logarithmic scale). This shape also states that the degree of increase is largest in the middle range of the resistances. The exact range is dependent on the foreshore length, but, in the computations done, it starts around a foreshore resistance value of 2.5days. Below the 2.5days value, the increase in critical head is equal for different foreshore lengths. This can be explained by the fact that the foreshore gives a resistance to vertical water flow, but below a value of 2.5days, this resistance is so small, that water still can flow through the foreshore. For resistance values larger than 2.5days, the results start to diverge until a value for which no further increase of the critical head can be seen. This resistance value is larger for increasing foreshore lengths.

**Effect of increasing foreshore length**

Increasing foreshore length leads, to an increase in critical head. As this seems logical, its not always the case. Until a foreshore cover layer resistance value of 2.5days, the influence of the foreshore length is similar for all foreshore lengths. As water can just flow through the foreshore for this value. For resistances higher than 2.5days, the length of the foreshore has an increasing effect by increasing resistance. This means that the differences between the results for different foreshore lengths becomes larger for larger resistances. The increase in critical head progresses, for each foreshore length, to a specific value. This specific value approaches the

critical head results from the Sellmeijer formula in which the whole foreshore length is included. This "limit value" becomes higher for larger foreshore length, as well as the resistance at which this value is reached. In other words: for smaller foreshore lengths, the "limit value" is reached in an earlier stadium.

**Effect of changing initial seepage length**

Changing the initial conditions for the model, in this case the seepage length, affects the results. As the initial critical head is already higher for longer seepage length, the effect of including a foreshore is smaller than for shorter initial seepage lengths. Changing the initial seepage length has effect on the values, but has no influence on the shape of the graph. This states that the findings, discussed in the previous subsections, also hold for the results if other seepage lengths are used.

**Summary**

In the graph below, the discussed effects of changing components can be seen. As the variation in resistance is one of the axis, no specific line for this effect in included. Three lines can be seen in the graph:

1. Begin situation for showing the effects: Line 1, foreshore length= 100m, initial seepage length is 50m;
2. Foreshore length variation: Line 2, foreshore length= 200m, initial seepage length is 50m;
3. Initial seepage length variation: Line 3, foreshore length= 100m, initial seepage length is 100m;

The arrows indicate the actual effect of the variations.

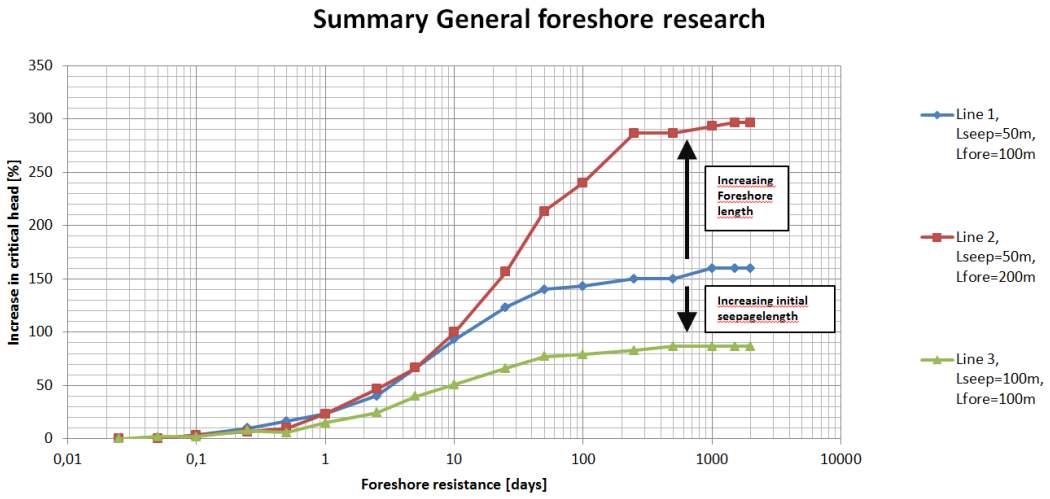


Figure 11.1: Summary discussion general foreshore research

In the graph above, three lines, explained in the summation above, can be seen. The blue line (Line 1) can be seen as the 0-situation in this comparison. When only the foreshore length is increased, Line 2 occurs from Line 1. The difference between Line 1 and Line 2 indicates the change in influence on the critical head when the foreshore length is increased. Increasing only the initial seepage length, Line 3 occurs from Line 1. The difference between Line 1 and Line 3 indicates the change in influence on the critical head when the initial seepage length is increased.

**Limitations**

In approaching the research several assumptions are done, limiting the research and are, possible, subjects for further research.

In the standard model, the hydraulic conductivity of the aquifer was assumed(20 m/day). Changing this assumption would affect the results. As already has been seen, changing the initial conditions results in different results. The influence of changing the hydraulic conductivity of the aquifer has not been included in this research. The same holds for more initial seepage lengths. As this research was limited to two initial seepage lengths, the effect of the initial seepage length is based on two findings.

In the set-up of the standard model, homogeneous conditions for both the subsoil and the foreshore were assumed in composition and thickness. Influence of heterogeneous compositions of the subsoil on the effect of a foreshore are thereby excluded, but could be of importance. This heterogeneity was also excluded from the foreshore. As in reality the foreshore would not be a continuous layer, having the same properties through its whole reach, this could also affect the results. Next to heterogeneity in soil property sense, the heterogeneity in geometrical characteristics of the foreshore is not included. The effect of thinner/thicker parts in the foreshore could be of interest and would, most likely, also affect the general conclusions. The effect of a varying height foreshore can also contribute to the application of the general foreshore research to practical cases.

### Case specific foreshore research

In the case study foreshore research, local foreshore geometries were analysed and variations were applied. The hydraulic conductivity of the foreshore, the presence of holes in the foreshore and the properties of these holes were varied to see how they influence the result. This influence was in comparison with the standard, case specific, foreshore model. This includes a foreshore in which holes are present. These holes are determined using the AHN. The difference in critical head result between a foreshore in which holes are present or not is depicted in the figure below. In this figure also the results of the standard models, in which no foreshore is present, is shown.

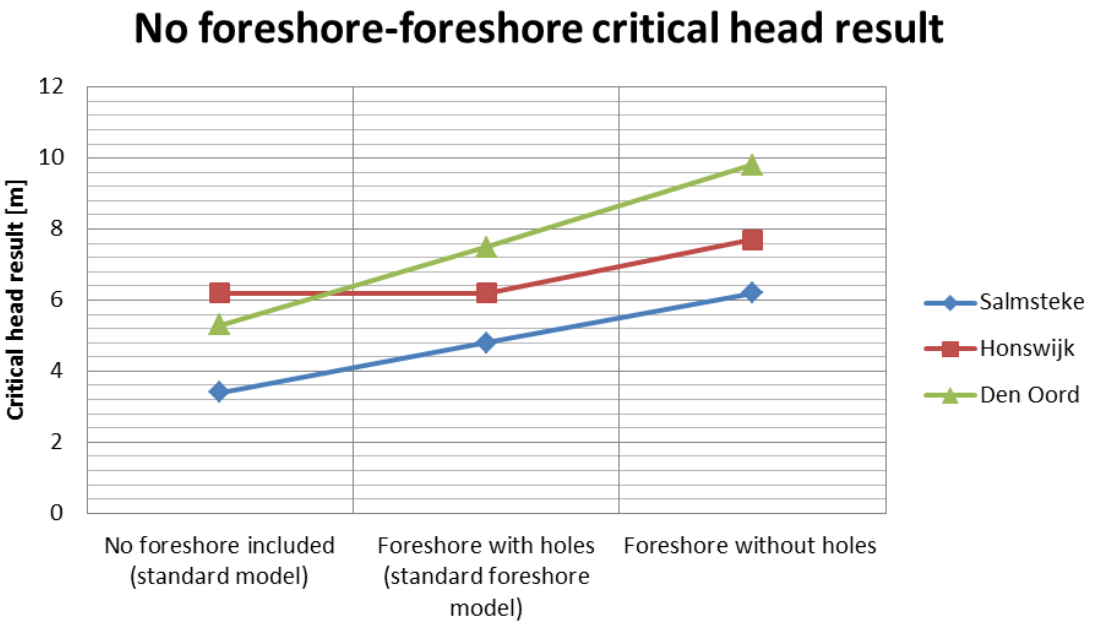


Figure 11.2: Results of the standard model, standard foreshore model and a model with a full foreshore(without holes) for all three cases

The progression of the lines for each case is the result of the comparison of the critical head result of the models. This includes the standard model, with the seepage length following from the safety analysis, the standard foreshore models, with seepage length corresponding to the holes determined from the AHN and a full foreshore model in which no holes are present. In the following table, the seepage lengths of the standard models and seepage lengths as the result of the holes in the standard foreshore model can be seen.

Table 11.1: Seepage lengths of the different models, as an explanation of fig. 11.2

| Case: | Salmsteke | Honswijk | Den Oord |
|---|---|---|---|
| Init. Seep. Length | 58.09m | 121.72m | 100.82m |
| Seep. Length Holes | 80m-150m | 105m-125m | 135m |
| Seep. Length River | 300m | 360m | 545m |

For the cases of Salmsteke and Den Oord a more or less linear progression of the lines in fig. 11.2 can be

seen. This is due to the increase of seepage length between the standard model, standard foreshore model and the model with a full foreshore. For the case of Honswijk something else occurs. As the seepage length from the standard model (121.72m) does not differ a lot from the seepage lengths as a result of the holes (105-125m) there is no increase in critical head result between the standard model and the standard foreshore model.

**Standard foreshore models**

The geometry of the standard foreshore models for the cases was determined based on the AHN. As the AHN-3 data is reasonably up-to-date, this data can be assumed as correct. The choice of layer separation is debatable, as the depth of the foreshore cover layer was limited to a constant depth, determined using the AHN. In reality this depth would not be constant and even be deeper or less deep. This would affect the resistance of the foreshore and thereby the results.

**Hydraulic conductivity of the foreshore**

The hydraulic conductivity of the foreshore cover layer greatly influences the critical head result. As the information about the actual hydraulic conductivity of the foreshore cover layer was absent, the assumption of 0.1m/day was done. Variation of this assumption lead to large differences in critical head. A higher hydraulic conductivity decreases the resistance in the foreshore, where a lower hydraulic conductivity increases the resistance. The extent of the influence of a changing hydraulic conductivity of the foreshore cover layer is governed by the geometrical characteristics of the foreshore. The cover layer thickness and the position of the holes on the foreshore determine this extent.

**Variations on the foreshore**

In the standard foreshore model, holes were identified based on the AHN. The properties of these holes were varied, as the exact properties can not be determined from the AHN. The influence of the properties of a hole is mainly due to the fact whether the hole reaches to the aquifer or not. Even for a small layer between the aquifer and the outer water in a hole, it holds that a pipe will form from another point at which the outer water and the aquifer are in direct contact. If there is contact between the outer water and the aquifer, the area of contact is of less significant influence, as an increase in contact area of 50x only causes a decrease in critical head of 8%, where a small layer of silt of 0.05m in a hole causes an increase of more than 20%. In analysing a foreshore it is therefore better to focus on the fact if a hole reaches to the aquifer than to focus on the area of aquifer exposed to the outer water. As mentioned in the previous subsection, the results are based on a hydraulic conductivity of the foreshore cover layer of 0.1m/day. A change in hydraulic conductivity of the foreshore cover layer could influence the effect of several variations, however it is expected that the trend is the same for different hydraulic conductivities.

**Application general foreshore research on the cases**

Applying the results of the general research on the cases brought up some difficulties. The cause of these were the differences in initial seepage length and the fact that a foreshore from a case is not horizontal with a continuous thickness. To overcome these differences, some correction factors were used. These correction factors were the result of trial-and-error calculations in which the case study results were approached. Using the results from the general research and adapting these results with the correction factors, the case study results were closely approached. It is however the question if this is just coincidence or if it is widely applicable.

**Limitations**

As all the variations of the foreshore are done with the assumption that the hydraulic conductivity of the foreshore cover layer is 0.1m/day, the effect of a change in hydraulic conductivity on the other conclusions is not accounted for. The effect of a different assumption of hydraulic conductivity of the foreshore cover layer is therefore uncertain, it can however be expected that the results, for different hydraulic conductivities, follow the same trend as the current results do.

From the AHN the foreshore geometry was determined. To model this, a horizontal separation line between the foreshore cover layer and the aquifer must be chosen. This was also done by use of the AHN. This assumption is rough and based on a geometry, where the separation could better be determined from soil samples,

to see until what depth the foreshore cover layer reaches. Next to this, the horizontal separation line is also incorrect. In reality this separation will not be completely horizontal. The influence of these differences with the reality is not searched for in this thesis.

In this research the variations of the foreshore were done one by one to check their influence. It is however not determined what the effect of a combination of these variations would be.

In the choice for the standard model, homogeneous compositions of the foreshore and the aquifer were assumed. In reality this will not be the case. This change will change the results, the extent is however uncertain and is not searched for in this thesis.

## 11.2. Soil heterogeneity research

The research to the effects of soil heterogeneities on the critical head result is conducted in two ways: A general research and a case specific research. In the general research the influence of a continuous layer throughout the whole cross-section is determined by changing the depth of this layer and its resistance. In the case specific research, local heterogeneities are identified based on local data and the effect of a specific heterogeneity is determined.

### General soil heterogeneity research

In the general heterogeneity research, a continuous horizontal layer (resistance layer) throughout the whole cross-section is added to a standard model. This layer is then varied with respect to its resistance and depth. In this research, variations on initial situations are done and their effects will also be discussed.

#### Effect of increasing resistance

Increasing resistance has a very significant effect on the critical head result. As with increasing resistance less water can penetrate through the layer into the lower aquifer, the results are affected. The progression of the results is not linear, but has a typical shape (on logarithmic scale). As expected, an increase in critical head by increasing resistance is present. This increase continues to a value which can be approached by the Sellmeijer formula if only the top part of the aquifer, the part above the resistance layer, is accounted for. However, for some depths of the resistance layer, the increase in critical head for very high resistance values is not the largest. A flow scenario, for lower resistances of the resistance layer, can occur where water can seep through the resistance layer into the lower aquifer, but can not flow back into the higher aquifer, causing the largest increase in critical head. This flow scenario occurs more frequently for lower depths of the resistance layer. The left and right boundary of the graphs can be approached by use of the Sellmeijer formula. The left boundary is for the case where the whole aquifer works as flow area, accounting the whole thickness of the aquifer in the Sellmeijer formula. The right boundary is determined by the case where only the upper part of the aquifer(above the resistance layer) is accounted for in the Sellmeijer formula. In all the graphs it can be seen that the section in which the largest increase in critical head is between 1 and 20 days. This is the transition area between full flow through the resistance layer and no flow through the layer.

#### Effect of increasing depth

Increasing depth of the resistance layer decreases the influence on the critical head. This is due to the effect that the difference in critical head between the two boundaries(left and right) is smaller for deeper resistance layers, as the top aquifer thickness is larger for deeper resistance layers. The probability of occurrence of the mechanism were water is drained into the lower layer, causing higher increases than the the right boundary, is larger for less deep layers, as the resistance is higher in the cross-section.

#### Effect of changing initial conditions

A change in initial conditions, the initial seepage length and the hydraulic conductivity of the aquifer, causes some differences in results. The values for certain resistances differ, but the shape of the graphs, for different initial conditions, is relatively similar. Increasing the initial seepage length results in increasing influence on the critical head. The ratio between the seepage length and the aquifer thickness becomes larger, causing an amplification of the influence on the critical head. Increasing hydraulic conductivity of the aquifer decreases the influence on the critical head, because water flow is more easier through the aquifer, the effect of a resistance layer is less.

**Summary**
In the graph below, the effect of the changing components is visualized. In this graph, changes in values and shapes can be seen. In this graph 4 lines can be detected:

1. Begin situation: Line 1, $K_{aq}$=20m/day, Lseep=50m, Depth=3m;
2. Depth variation: Line 2: $K_{aq}$=20m/day, Lseep=50m, Depth=5m;
3. Seepage length variation: Line 3: $K_{aq}$=20m/day, Lseep=100m, Depth=3m;
4. Hyd. Cond. aquifer variation: Line 4: $K_{aq}$=40m/day, Lseep=50m, Depth=3m;

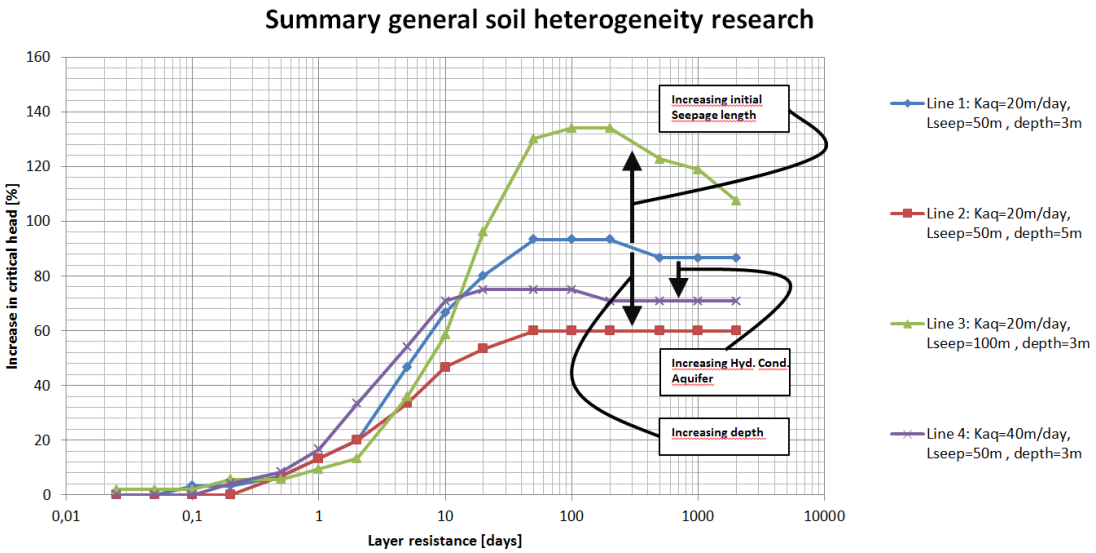


Figure 11.3: Summary discussion general soil heterogeneity research

In the figure above, the lines represent the situations explained by the summation above. The blue line (Line 1) has to be seen as a starting point in this comparison. Increasing the depth of the resistance layer, the influence on the critical head becomes less, resulting in Line 2. The difference between Line 1 and Line 2 indicates the difference in influence on the critical head if the depth of the resistance layer is increased. If the initial seepage length is increased, the influence on the critical head also increases. Line 1 shifts therefore up in the graph, resulting in Line 3. The difference between Line 1 and Line 3 is the effect of increasing initial seepage length on the influence on the critical head. If the hydraulic conductivity of the aquifer is increased, the influence on the critical head is decreased, see Line 4. The difference between Line 1 and Line 4 is the effect of increasing hydraulic conductivity of the aquifer on the influence on the critical head.

**Limitations**
Computations are done for several initial seepage lengths and hydraulic conductivities of the aquifer. The influence of the change in initial conditions was discussed, however, not enough computations are done to give an answer to how the results are exactly influenced by a change in initial conditions.

The influence of a horizontal continuous resistance layer was determined. In reality, layers are not completely horizontal and continuous. The effect of the resistance layer being not horizontal and discontinuous are therefore not included in this thesis. However in reality, a layer in the subsoil is, most likely, not completely horizontal with changing thickness.

This research only covers the influence of a continuous resistance layer. Heterogeneities in this layer can influence the effect on the critical head, as well as holes in this layer. Next to this, heterogeneities in the aquifer around this resistance layer could also affect the degree of influence of the resistance layer.

## Case specific heterogeneity research
In the case specific research, cross-sections were developed in which the heterogeneities were identified. Because of uncertainty two values of the hydraulic conductivity were used for the heterogeneities, these values

follow from the literature study.

The cross-sections were created based on local samples and completed with the GeoTop model, if necessary. Although this model was handled with care, the uncertainty in this model is very large, hereby the question arises if the heterogeneities determined with the GeoTop model are present in practice. It gives however still a good impression in how a certain heterogeneity influences the critical head result.

**Effect of the heterogeneities**
Heterogeneities in the subsoil influence the critical head results. The extend of this influence is however very dependent on the properties of the heterogeneity. Heterogeneities preventing the water from seeping into the aquifer have a large positive influence on the critical head results. Where heterogeneities around the exit point can have positive, as well as negative influences on the critical head, depending on their hydraulic conductivity and particle diameter. Heterogeneities reaching through the whole cross-section, which are less permeable than the aquifer, do always have a positive effect on the critical head, the extend of this influence is determined by the placing height and hydraulic conductivity of this heterogeneity. For almost all heterogeneities hold that the influence is in a range, dependent on the range of hydraulic conductivities, depths and thickness of the heterogeneities . It was proven to be possible that in the range of hydraulic conductivity the changing point from a positive to negative effect is present. The one heterogeneity far from the pipe formation, had no influence on the critical head result. However, it can not be said that this holds for all heterogeneities out of the path of the pipe, as they still can influence the flowing conditions in a cross-section.

**Application general research**
Applying the general research results on the cases prove to be easy and accurate. Some slight differences were present, but they can be explained by the difference in initial seepage length. It became however clear that for increasing difference in initial seepage length, the differences in results also increase. The general research results can however only be applied on heterogeneities crossing the whole cross-section. It is also unclear how accurate the results are when a layer is not horizontal with a continuous thickness.

**Limitations**
The approach in creating a cross-section with heterogeneities comes with some difficulties and uncertainties. The uncertainty of the GeoTop model was already addressed, but has to be named. After the samples were made, by use of local samples completed with GeoTop, it was chosen to put these samples, in the form of boreholes, in D-Geo Flow and let D-Geo Flow create a cross-section by use of linear interpolation between the input boreholes. This causes the problem that between the boreholes the layers, assigned in the boreholes, were assumed to continue. However, in reality, the heterogeneities can be interrupted, creating gaps in the heterogeneity. By Stoop(2018)[13], it was determined that gaps in a heterogeneities the cross-section can be of large influence. With this remark, the results from the case specific heterogeneity research can not be assumed to represent the reality in detail, but the results give a good image of how a certain heterogeneity can influence the result of the critical head.

The effect of the heterogeneities is determined by modelling the heterogeneities in the cross-section one-by-one. In this way the effect of the heterogeneities was determined separately per heterogeneity. The result for a heterogeneous cross-section, in which all the heterogeneities are incorporated is not computed. As the heterogeneities could reduce or enlarge each others' effects, the result is different.

The heterogeneities which were added to the cross-section were assumed to be a constant soil body. With this it is meant that there are no heterogeneous properties throughout the soil body. Effects of heterogeneous properties throughout one soil body are, with this assumption, not included in this thesis.

# 12 Conclusions

## 12.1. Introduction

In this thesis, a study is done to analyse how a foreshore and heterogeneities in the subsoil influence the result of the piping safety analysis. This study is done by use of a model, D-Geo Flow. Insights in how a foreshore or heterogeneities influence the safety analysis result, can improve the piping safety analysis. In this chapter the final conclusions, based on the study in this thesis, are presented. As final conclusion an answer is given to the main research question:

*"What is the effect of the foreshore and soil heterogeneities on the result of the piping safety analysis?"*.

After answering this question, it can be concluded if the research objective of this thesis is met. The research objective hold:

*"Improve the piping safety analysis by including the effects of the foreshore and soil heterogeneities."*

## 12.2. Conclusions Foreshore (part I)

The main objective for the foreshore research was to give answer to the question what the effects of a foreshore are on the result of the piping safety analysis and how this can improve the piping safety analysis. A two way approach was used to answer this: A general approach and a case specific approach.

In the safety analysis of piping, a foreshore, if present, is included in the seepage length. Holes on the foreshore can reduce this seepage length, as well as the hydraulic conductivity of the foreshore cover layer, for which a representative seepage length is determined. This representative seepage length is then used in the Sellmeijer formula. From this thesis, it can be concluded that the approach of reducing the seepage length when a permeable foreshore cover layer is present is the right approach, as the hydraulic conductivity of the foreshore cover layer highly influences the critical head result. The extent of this influence is dependent on the foreshore length, thickness of the foreshore cover layer, hydraulic conductivity of the foreshore and the presence or location of holes on the foreshore.

The properties a hole on the foreshore can greatly affect the critical head result. The largest influence can be found in the presence of some resistance in a hole. If the hole does not reach the aquifer, but some resistance in presence in this hole, the aquifer is "sealed" at the location of this hole, so almost no seepage will occur through this hole into the aquifer. This resulted, in the cases used, to increases in critical head up to 30%. The influence of hole width, especially the part reaching to the aquifer is of less influence. An increase of 50x the width of a hole reaching to the aquifer results is a decrease in critical head of around 8%.

In the choice of seepage length and the handling of the holes in the foreshore, the holes need to be assessed closely. Choosing a less long seepage length because of the presence of a hole on the foreshore could underestimate the resistance to piping, as a small resistance in a hole leads to the same situation as the hole would not be present. This finding leads to the insight that a cross-section could be more resistance against piping than thought beforehand.

## 12.3. Conclusions Soil heterogeneities (part II)

The main objective for the soil heterogeneity research is to see how a heterogeneous soil effects the result of the piping safety analysis. The research is done in a general and a case specific part.

In the safety analysis, the subsoil is assumed to be homogeneous with certain characteristics. From this research it can be concluded that the assumptions underestimate the actual resistance against piping. Heterogeneities in the subsoil influence the critical head result in a positive and negative way, however, the positive influences are larger and overshadow the negative effects. As only two out of nine identified heterogeneities proved to decrease the critical head result with a maximum of -26%, where the positive heterogeneities increase the critical head with a maximum 139%. It can be concluded that based on the findings in this thesis, a heterogeneous cross-section is more resistant to piping than a homogeneous cross-section.

A layer with a lower hydraulic conductivity than the aquifer(resistance layer) crossing the whole cross-section always increases the critical head in comparison with a situation without such a layer. This extent of increase is determined by the resistance against vertical flowing of this layer. Higher resistances lead to higher critical heads. Dependent on the geometry of the cross-section, however, a flow scenario can occur for which the critical head is not at its highest at the highest resistance. This flow scenario, the "one-way flow", occurs for resistances for the resistance layer between 20 and 500days. The occurence of this scenario increases for decreasing resistance layer depth.

---

The answer to the main research question can now be formulated:

The effect of the foreshore and soil heterogeneities on the result of the piping safety analysis is locally specific. The approach used in the safety analysis in incorporating the foreshore should focus more on the properties of holes on the foreshore, as they influence the result very significantly. The effect of soil heterogeneities on the result of the piping safety analysis is per heterogeneity different, but a heterogeneous subsoil has a higher resistance against piping than the currently used homogeneous subsoil.

The objective: *"Improve the accuracy of the piping safety analysis by including the effects of the foreshore and soil heterogeneities"*, is, by answering the research question, met. As more knowledge about the effects of the foreshore and soil heterogeneity can be used in the decisions which have to be made in the piping safety analysis.

# 13

# Recommendations and further research

## 13.1. Introduction

In this chapter, recommendations are given based on the findings in this thesis. The recommendations are both for the most important implementations of the findings in this thesis on the safety analysis, as for the further research which would improve the knowledge of piping and the piping safety analysis.

## 13.2. Implementing the results in the safety analysis

In the safety analysis of piping the choice of the seepage length, including the foreshore, is determined based on the permeability conditions of the foreshore and the presence of holes on the foreshore. This research made clear that the approach of reducing the seepage length if a permeable foreshore is present is the right way. The method and extent of reducing was not in the scope of this thesis. The way holes on the foreshore are incorporated in the analysis is not correct. The implementation of the findings concerning holes on the foreshore would be to assess a hole on the foreshore in more detail to determine if this hole reaches to the aquifer or not.

The influence of a continuous, horizontal layer throughout the whole cross-section was examined in a general heterogeneity research part. The application of this research proved that the results from this general research can be applied relatively easy on practical situations. If, at a certain location, it is known such a layer is present, the results from this research can estimate the influence of such a layer on the critical head in an easy and quick way.

## 13.3. Further research

Piping is a very complex problem to understand and a lot of research has already been done. However, in this thesis, several aspects of the piping problem arose for which the knowledge is insufficient to really understand the processes of piping. Therefore several aspects for further research are named.

### Foreshore

The general foreshore research revealed that the characteristics on the foreshore cause difficulties in assuming which representative values have to be used. A more in depth research in choosing these values could, probably, eventually lead to a stepwise choice pattern resulting in a accurate prediction of the critical head when a foreshore is present.

Another foreshore related topic for further research is the comparison of the general foreshore research from this thesis with the current approach in determining a representative seepage length in case of a more permeable foreshore cover layer. If these results will prove to be similar, the current approach is the right way. If differences are found, a better approach could be determined.

### One-way sealing

The general soil heterogeneity research resulted in generic results, directly applicable on several components of the case. This research also revealed that the maximum increase in critical head does not occur at impermeability of a layer, but when the layer is nearly impermeable, so water only progresses through the layer in

one way(downward). One ways sealing of the aquifer could be a good solution to prevent piping, if construction is possible. A research to the application of this finding is suggested.

### Soil characteristics

In this thesis, several soil characteristics where used, based on literature. This literature study proved that soil characteristics are hard to determine and that wide ranges of these characteristics are given. More research into the soil characteristics and soil characteristic predictions could lead to a big improvement in the piping safety analysis.

### D-Geo Flow

The research in this thesis was conducted in D-Geo Flow. D-Geo Flow, a graphical interface model, is, for now, only validated for simple soil-compositions. This can also be seen in the validation of the standard model in this thesis, see section 4.2. The question is however if the results, generated from D-Geo Flow for more complex situations are also valid. This is therefore a good subject for further research. With this recommendation, also a downside arises. Generating real life results of complex soil compositions is hard, expensive and time-consuming. For that reason the recommendation for further research is in two ways: To continue the validation of D-Geo Flow for other compositions and to search for ways how to generate reliable, real life results for complex compositions. A hopeful outcome of this thesis was that in the limit of some variations, the Sellmeijer formula was approached, this indicates, but not proves, the correctness of the model, if Sellmeijer is assumed as correct.

### Soil composition

The soil heterogeneity research revealed a shortcoming in knowledge in how to predict the subsoil composition. The data which is available is limited and interpretations in soil layer progression through the cross-section have to be made to come up with a schematic representation of the subsoil. A topic for further research would be to search for ways in how to interpret and transfer the available data to create a representative cross-section. This would greatly increase the accuracy of the piping safety analysis. As this is a big and difficult subject, a good start is to determine in more depth what kind of heterogeneities determine the resistance against piping in a cross-section.

### Foreshore and heterogeneities

In this research, two topics were analysed: The foreshore and the heterogeneities in the subsoil. To increase the knowledge in how heterogeneities in a cross-section (which also includes the foreshore) influence the result of the piping safety analysis, the two topics have to be combined in a coupled research. It is, for now, still unclear whether variations in the subsoil influence the effect of a foreshore ans vice-versa. This could however, be of great importance in the choices and results of the safety analysis.

### Anisotropy

This research emerged as a follow-up on the research by Stoop(2018)[13]. In his research he searched for the effect of anisotropy on the result of the piping safety analysis. In this thesis, the anisotropy was left out of consideration. It is therefore recommended to firstly determine the amount of anisotropy for several soil types and secondly to see how anisotropy influences the results which were presented in this thesis. This would close the gap between the model and reality and thereby increase the accuracy of the piping safety analysis.

# Glossary

| Term | Description |
|---|---|
| Anisotropy | The inequality between horizontal and vertical flow of water through the soil |
| Aquifer | The permeable layer below the dike through which groundwater can flow, consists of sand or gravel soil types, in this layer pipe formation occurs |
| Blanket | An impermeable layer at ground level, covers the layers underneath |
| Critical head (result) | The head which a cross-section, at maximum, can resist. It is the value for which the pipe formation reaches its last equilibrium. |
| Foreshore | A piece of elevated land between the river flowing bed and the dike. It is located out of the dike protection zone and can therefore be flooded during high water conditions |
| Heave | The process in which the pressures caused by groundwater flow exceeds the effective stress of the soil particles, causing fluidization and washing out of the particles. Follows the mechanism of uplift before pipe formation occurs. |
| Heterogeneity | An inhomogeneous component in the subsoil. |
| Holocene formation | Type of formation deposited in the Holocene era, the last 11000 years. Deposit is very heterogeneous. |
| Hydraulic conductivity | Determines the ease of water flow though a soil. High values indicate easy flow, where low values indicate complicated flow. |
| Piping | Pipe formation process in which sand particles are eroded from the aquifer, causing a pipe below the dike to form. This erosion is caused by a hydraulic gradient across the dike body. Follows the processes of heave and uplift. |
| Piping safety analysis | Can be in the form of assessment and design. The way a cross-section of a dike is tested to check its resistance to piping. |
| Resistance layer | Horizontal heterogeneity reaching through the whole cross-section. This layer has a lower hydraulic conductivity than its surroundings |
| Samples | Site tests containing information about the soil. Can be in different forms as boreholes or CPT-probings. |
| Silting up | Mechanisms were, by flooding of a foreshore, particles are deposited on the foreshore. |
| Uplift | Mechanisms in which the pressures in the aquifer cause the blanket to crack. Pressures are induces by the difference in head across a dike. Precedes heave and piping. |

# List of Symbols

| Symbol | Description | Unit |
|---|---|---|
| $c$ | Resistance | $days$ |
| $d_f$ | Thickness of the foreshore cover layer | $m$ |
| $d_{70}$ | Grain diameter for which 70% passes the particular sieve | $m$ |
| $d_{70_m}$ | Mean grain diameter (from small scale tests($2.08 * 10^{-4}$) | $m$ |
| $h$ | Hydraulic head | $m$ |
| $h_{exit}$ | Hydraulic head at exit point | $m$ |
| $i$ | Heave gradient | – |
| $k_{h_{aq}}$ | Horizontal hydraulic conductivity of the aquifer | $m/day$ |
| $k_{v_f}$ | Vertical hydraulic conductivity of the foreshore cover layer | $m/day$ |
| $n$ | Porosity | – |
| $r_c$ | Reduction factor for exit head loss | – |
| $r_{exit}$ | Damping or response factor at exit point | – |
| | | |
| $C_l$ | Resistance of the resistance layer | $days$ |
| $C_{seep}$ | Correction coefficient seepage length difference | – |
| $D_{aq}$ | Thickness of the aquifer | $m$ |
| $D_{blanket}$ | Thickness of the blanket | $m$ |
| $D_{foreshore}$ | Thickness foreshore cover layer | $m$ |
| $D_l$ | Thickness of the resistance layer | $m$ |
| $F_p$ | Pipe progression stability factor | – |
| $H_{cr_{c_{av}}}$ | Critical head for average resistance of foreshore | $m$ |
| $H_{cr_{c_{min}}}$ | Critical head for minimal resistance of foreshore | $m$ |
| $H_{cr_{new}}$ | Critical head result, after correction | $m$ |
| $H_{cr_{rep}}$ | Representative critical head | $m$ |
| $K$ | Hydraulic conductivity | $m/day$ |
| $K_{foreshore}$ | Hydraulic conductivity foreshore cover layer | $m/day$ |
| $K_l$ | Hydraulic conductivity of the resistance layer | $m/day$ |
| $K_x$ | Horizontal hydraulic conductivity | $m/day$ |
| $K_y$ | Vertical hydraulic conductivity | $m/day$ |
| $L_{init_{cas}}$ | Initial seepage length from case | $m$ |
| $L_{init_{gen}}$ | Initial seepage length from general foreshore research | $m$ |
| $L(_l)$ | (Seepage) Length | $m$ |
| $L_{seep_{fic}}$ | Fictive seepage length | $m$ |
| $RD$ | Relative density | – |
| $RD_m$ | Mean relative density (from small scale tests(0.725)) | – |
| | | |
| $\alpha$ | Compressibility | $M^2/N$ |
| $\gamma'_p$ | Unit weight particles | $kN/m^3$ |
| $\gamma_{sat}$ | Unit weight saturated soil | $kN/m^3$ |
| $\gamma_{w(ater)}$ | Unit weight water | $kN/m^3$ |
| $\eta$ | White's constant | – |
| $\kappa$ | Intrinsic permeability | $m^2$ |
| $\lambda_l$ | Representative foreshore length | $m$ |
| $\Delta H_c$ | Critical hydraulic head difference | $m$ |
| $\Delta\phi$ | Head difference | $m$ |
| $\Delta\phi_{c,u}$ | Critical head difference across the dike | $m$ |
| $\Theta$ | Bedding angle | deg |

# List of Figures


1.1 Water depth in the Netherlands in case of flooding . . . 1
1.2 failure mechanisms . . . 2

2.1 The approach depicted in a scheme . . . 5

3.1 Sand boil . . . 7
3.2 Piping process . . . 8
3.3 Determine the representative seepage length, foreshore . . . 11
3.4 Ringing of a sand boil . . . 12
3.5 Anisotropy and Heterogeneity . . . 13
3.6 Parent material in the Netherlands . . . 14
3.7 Holocene Formations . . . 14
3.8 Sampling of the different areas . . . 15

4.1 The river Lek . . . 19
4.2 Location of the case studies along the Lek . . . 19
4.3 Standard model boundary conditions . . . 21
4.4 Standard model in D-Geo Flow for the Salmsteke case, overview . . . 22
4.5 Standard model in D-Geo Flo for the Salmsteke case, exit configuration . . . 22

5.1 Schematic cross-section of the varied foreshore length, not on scale, river located on the left . . . 27
5.2 Results general foreshore research . . . 29
5.3 Results general foreshore research(2) . . . 30

6.1 Height profile along the Lek . . . 31
6.2 Cross-sectional height profile of Salmsteke, river is located at the right . . . 32
6.3 Cross-sectional height profile of Honswijk, river is located at the right . . . 32
6.4 Cross-sectional height profile of Den Oord, river is located at the right . . . 32
6.5 Cross-section of Salmsteke, pointing out the holes in the foreshore. . . . 33
6.6 Standard foreshore model for Salmsteke . . . 34
6.7 Standard foreshore model detail for Salmsteke . . . 34
6.8 Cross-section of Honswijk, pointing out the holes in the foreshore . . . 34
6.9 Standard foreshore model for Honswijk . . . 34
6.10 Standard foreshore model detail for Honswijk . . . 35
6.11 Cross-section of Den Oord, pointing out the holes in the foreshore . . . 35
6.12 Standard foreshore model for Den Oord . . . 35
6.13 Standard foreshore model detail for Den Oord . . . 35
6.14 Schematic figure of the width variation of the holes . . . 37
6.15 Foreshore variations . . . 37
6.16 Influence on the critical head result of the variation of the hydraulic conductivity of the foreshore cover layer . . . 38
6.17 Influence on critical head results of the variation of the hole width . . . 40
6.18 Influence on critical head results of the variation of the hole depth . . . 41
6.19 Influence on critical head results of the variation of the silt deposit thickness . . . 42
6.20 Cross-section of Salmsteke with the holes and the river pointed out . . . 43
6.21 Cross-section of Honswijk with the holes and the river pointed out . . . 44

7.1 Foreshore variations including the "no hole computations" . . . 48

8.1 Overview of the parameters in an example model . . . 55

8.2 Three flow scenarios . . . 56
8.3 Results for L=50m, K=20m/day . . . 57
8.4 The 3 mechanisms showed as 3 zones for L=50m, K=20m/day . . . 59

9.1 Cross section Salmsteke case, deposit layers . . . 62
9.2 Location of the samples for the Salmsteke case . . . 62
9.3 Cross section Salmsteke case, soil type layers according to GeoTop . . . 63
9.4 Cross section from D-Geo Flow, from boreholes and GeoTop, case Salmsteke . . . 63
9.5 Workable cross-section from D-Geo Flow, simplified from fig. 9.4 case Salmsteke . . . 64
9.6 Cross section Honswijk case, deposit layers . . . 64
9.7 Location of the samples for the Honswijk case . . . 65
9.8 Cross section Honswijk case, soil type layers according to GeoTop . . . 65
9.9 Cross section from D-Geo Flow, from boreholes and GeoTop, case Honswijk . . . 66
9.10 Workable cross-section from D-Geo Flow, simplified from fig. 9.4 case Honswijk . . . 66
9.11 Cross section Den Oord case, deposit layers . . . 67
9.12 Location of the samples for the Den Oord case . . . 67
9.13 Cross section Den Oord case, soil type layers according to GeoTop . . . 68
9.15 Summary heterogeneity research Salmsteke . . . 70
9.17 Summary heterogeneity research Honswijk . . . 71
9.18 Model 1 Salmsteke, schematic flow pattern . . . 71
9.19 Schematic flow pattern around exit point -Model 1 Salmsteke- (detail from fig. 9.18) . . . 72
9.20 Model 1 Honswijk, schematic flow pattern . . . 74
9.21 Model 2 Honswijk, schematic flow pattern . . . 75
9.23 Model 4 Honswijk, schematic flow pattern . . . 75
9.24 Schematic flow pattern around exit point -Model 4 Honswijk- (detail from fig. 9.23) . . . 76

11.1 Summary discussion general foreshore research . . . 82
11.2 Results of the standard model, standard foreshore model and a model with a full foreshore(without holes) for all three cases . . . 83
11.3 Summary discussion general soil heterogeneity research . . . 86

B.1 Sampling of the different areas . . . 111

D.1 D-Geo Flow interace . . . 121
D.2 Example of a borehole in D-Geo Flow . . . 122

E.1 Hydraulic conductivity variation of the foreshore . . . 126
E.2 Graphical result of the width variation, case Salmsteke . . . 127
E.3 Graphical result of the width variation, case Honswijk . . . 128
E.4 Graphical result of the width variation, case Den Oord . . . 129
E.5 Graphical result of the depth variation, case Salmsteke . . . 130
E.6 Graphical result of the depth variation, case Honswijk . . . 131
E.7 Graphical result of the depth variation, case Den Oord . . . 132
E.8 Graphical result of the silt thickness variation, case Salmsteke . . . 133
E.9 Graphical result of the silt thickness variation, case Honswijk . . . 134
E.10 Graphical result of the silt thickness variation, case Den Oord . . . 135

F.1 Representative seepage lengths . . . 139

G.1 Location of the samples for the Salmsteke case . . . 141
G.5 Samples Salmsteke:S15 102 AL . . . 143
G.6 Samples Salmsteke:S15 102 BERM . . . 144
G.7 Location of the samples for the Salmsteke case . . . 145
G.10 Sample B39A1073 . . . 146
G.11 Location of the samples for the Den Oord case . . . 147
G.14 Sample B39A1274 . . . 148

H.1 Coverage GeoTop model . . . . . 149

I.1 Result: Seepage length=25m, Hydraulic conductivity aquifer = 20m/day . . . . . 154
I.2 Result: Seepage length=50m, Hydraulic conductivity aquifer = 20m/day . . . . . 155
I.3 Result: Seepage length=100m, Hydraulic conductivity aquifer = 20m/day . . . . . 156
I.4 Result: Seepage length=25m, Hydraulic conductivity aquifer = 40m/day . . . . . 157
I.5 Result: Seepage length=50m, Hydraulic conductivity aquifer = 40m/day . . . . . 158
I.6 Result: Seepage length=100m, Hydraulic conductivity aquifer = 40m/day . . . . . 159

J.1 D-Geo Flow model, Salmsteke model 1 . . . . . 161
J.2 D-Geo Flow model, Salmsteke model 2 . . . . . 161
J.3 D-Geo Flow model, Salmsteke model 3 . . . . . 162
J.4 D-Geo Flow model, Salmsteke model 4 . . . . . 162
J.5 D-Geo Flow model, Honswijk model 1 . . . . . 163
J.6 D-Geo Flow model, Honswijk model 2 . . . . . 163
J.7 D-Geo Flow model, Honswijk model 3 . . . . . 163
J.8 D-Geo Flow model, Honswijk model 4 . . . . . 164
J.9 D-Geo Flow model, Honswijk model 5 . . . . . 164

# List of Tables


3.1 Summary soil characteristics . . . 16
3.2 Characteristics ranges in D-Geo Flow . . . 16
3.3 Summary definitive soil characteristics . . . 17

4.1 Input characteristics of the safety analysis and the result (Crit. Head) of the safety analysis . . . 20
4.2 Standard model Boundary Conditions . . . 21
4.3 Difference Safety Analysis-Standard Model and results from Sellmeijer . . . 22

5.1 Verification of influence of varying combinations of the foreshore thickness and hydraulic conductivity on the critical head result . . . 28
5.2 Lower and upper boundaries from the foreshore model computations (see fig. 5.1) . . . 28
5.3 Comparison "expected"(Sellmeijer) and "computed"(D-Geo Flow) Lower and upper boundaries 29

6.1 Critical head results of the standard foreshore models(with holes) and the results from the standard model(no foreshore) . . . 36
6.2 Standard foreshore model critical head results . . . 38
6.3 Critical head results of the cases when no holes on the foreshore are would be present . . . 43

7.1 Critical head results of the cases when no holes on the foreshore are would be present . . . 48

8.1 Verification . . . 56
8.2 Limit states for the different heights of the resistance layer . . . 57

9.1 Comparison general and case study research, model 2 . . . 72
9.2 Comparison general and case study research, model 3 - Salmsteke . . . 73
9.3 Comparison general and case study research, model 4 - Salmsteke . . . 73
9.4 Results case Honswijk, model 2, including computations with other particle size . . . 74
9.5 Comparison general and case study research, model 5 - Honswijk . . . 76

11.1 Seepage lengths of the different models, as an explanation of fig. 11.2 . . . 83

A.1 Creep ratios for different soil types by Bligh(1910) and Lane(1935) . . . 108

C.1 Hydraulic conductivities(K) in $[m/day]$ . . . 117
C.2 Anisotropy coefficient($C_A$) . . . 118
C.3 Particle diameter . . . 118
C.4 Porosity . . . 118
C.5 Compressibility . . . 119

E.1 Results of the hydraulic conductivity variations of the foreshore, case Salmsteke . . . 125
E.2 Results of the hydraulic conductivity variations of the foreshore, case Honswijk . . . 125
E.3 Results of the hydraulic conductivity variations of the foreshore, case Den Oord . . . 125
E.4 Results with bottom width variations of the entry points on the foreshore, case Salmsteke . . . 127
E.5 Results with bottom width variations of the entry points on the foreshore, case Honswijk . . . 128
E.6 Results with bottom width variations of the entry point on the foreshore, case Den Oord . . . 129
E.7 Results of the depth variations of the entry points on the foreshore, case Salmsteke . . . 130
E.8 Results of the depth variations of the entry points on the foreshore, case Honswijk . . . 131
E.9 Results of the depth variations of the entry points on the foreshore, case Den Oord . . . 132
E.10 Results of the silting up variations of entry points on the foreshore, case Salmsteke . . . 133
E.11 Results of the silting up variations of entry points on the foreshore, case Honswijk . . . 134

E.12 Results of the silting up variations of entry points on the foreshore, case Den Oord . . . . . 135

F.1 Results generic foreshore research(1), 50m initial seepage length . . . . . 137
F.2 Results generic foreshore research(2), 50m initial seepage length . . . . . 137
F.3 Results generic foreshore research(1), 100m initial seepage length . . . . . 137
F.4 Results generic foreshore research(2), 100m initial seepage length . . . . . 138

H.1 Estimate data . . . . . 151
H.2 Conditioning result . . . . . 151

I.1 Results continuous layer- Lseep=25m - Kaq=20m/day . . . . . 153
I.2 Results continuous layer- Lseep=50m - Kaq=20m/day . . . . . 155
I.3 Results continuous layer- Lseep=100m - Kaq=20m/day . . . . . 156
I.4 Results continuous layer- Lseep=25m - Kaq=40m/day . . . . . 157
I.5 Results continuous layer- Lseep=50m - Kaq=40m/day . . . . . 158
I.6 Results continuous layer- Lseep=100m - Kaq=40m/day . . . . . 159

J.1 Results case Salmsteke, model 1 . . . . . 161
J.2 Results case Salmsteke, model 2 . . . . . 161
J.3 Results case Salmsteke, model 3 . . . . . 162
J.4 Results case Salmsteke, model 4 . . . . . 162
J.5 Results case Honswijk, model 1 . . . . . 163
J.6 Results case Honswijk, model 2 . . . . . 163
J.7 Results case Honswijk, model 3 . . . . . 163
J.8 Results case Honswijk, model 4 . . . . . 164
J.9 Results case Honswijk, model 5 . . . . . 164

# Bibliography


[1] M. Kok, R. Jongejan, M. Nieuwjaar, and I. Tanczos, "Grondslagen voor hoogwater- bescherming," 2016.

[2] V. Nederland, "Nederland in kaart," no. November, 2011.

[3] Technische Adviescommissie voor de Waterkeringen, "Grondslagen voor waterkeren," pp. 1–167, 1998.

[4] V. V. Beek, A. Bezuijen, and H. Sellmeijer, *Backward Erosion Piping*. No. April 2013, 2013.

[5] W. Kanning, *The Weakest Link*, vol. 97. 2009.

[6] K. Vandenboer, a. Bezuijen, and V. M. Van Beek, "3D character of backward erosion piping: Small-scale experiments," *Scour and Erosion*, vol. 1, pp. 81 – 86, 2015.

[7] V. M. V. Beek, "Evaluation of Dutch backward erosion piping models and a future perspective Evaluation of Dutch backward erosion piping models and a future," pp. 97–113, 2017.

[8] ICOLD, "Internal Erosion of Existing Dams, Levees and Dikes, and their Foundations," *ICOLD Bulletin*, vol. 1, no. 164, p. 342, 2015.

[9] U. Förster, G. van den Ham, E. Calle, and G. Kruse, "Zandmeevoerende Wellen," p. 362, 2012.

[10] J. Vrijling, M. Kok, E. Calle, W. Epema, M. Van der Meer, P. Van den Berg, T. Schweckendiek, and V. J.K., "Piping. Realiteit of Rekenfout?," pp. 1–91, 2010.

[11] V. van Beek, Q. Yao, and M. Van, "Backward Erosion Piping Model Verification Using Cases in China and the Netherlands," *Seventh International Conference on Case Histories in Geotechnical Engineering*, no. 3, pp. 1–7, 2013.

[12] V. Van Beek, a. Bezuijen, J. Sellmeijer, and F. Barends, "Initiation of backward erosion piping in uniform sands," *Géotechnique*, vol. 64, no. 12, pp. 927–941, 2014.

[13] N. M. Stoop, "The effects of anisotropy and heterogeneity in the piping sensitive layer," 2018.

[14] J. Sellmeyer, "On the mechanism of piping under impervious structures," p. 116, 1988.

[15] V. Van Beek, H. Knoeff, and T. Schweckendiek, "Piping: over 100 years of experience," *A Feeling for Soil and Water - A Tribute to Prof. Frans Barends*, pp. 143–158, 2011.

[16] F. Silvis, "Verificatie Piping Model: Proeven in de Deltagoot - Evaluatierapport," 1991.

[17] H. Knoeff, H. Sellmeijer, J. Lopez, and S. Luijendijk, "SBW Piping - Hervalidatie piping," 2009.

[18] J. Huizinga-Heringa, "Regeling veiligheid primaire waterkeringen," *Staatscourant*, no. 11 september 2007, nr. 175, 2007.

[19] Rijkswaterstaat, "Schematiseringshandleiding piping," no. november 2016, 2017.

[20] T. A. voor de Waterkeringen, "Water tegen de dijk 1993," 1993.

[21] TAW Technische Adviescommissie voor de Waterkeringen, "Druk op de dijken 1995. De toestand van de rivierdijken tijdens het hoogwater van januari-februari 1995.," pp. 1–76, 1995.

[22] L. Ikelle and L. Amundsen, *Introduction to Petroleum Seismology*. No. v. 12 in Introduction to Petroleum Seismology, Society of Exploration Geophysicists, 2005.

[23] H.P. Ritzema, "Drainage principles and applications," 1994.

[24] W. Mairaing and S. Lapkrengkrai, "Ratio of vertical to horizontal permeabilities of compacted soils,"

[25] D. Bakker, D. Bakker, and D. Bakker, "Concise description of the soils in the Netherlands," pp. 23–62, 2006.

[26] F. S. Busschers and H. J. T. Weerts, "Beschrijving lithostratigrafische eenheid: Kreftenheye Formatie," *Nederlands Instituut voor Toegepaste Geowetenschappen TNO*, no. 1975, pp. 1–8, 2003.

[27] J. Schokker, F. D. D. Lang, H. J. T. Weerts, C. D. Otter, and S. Passchier, "Formatie van Boxtel Beschrijving lithostratigrafische eenheid," *Nederlans Instituut voor Toegepaste Geowetenschappen TNO*, pp. 1–9, 2005.

[28] P. van der Hulst, "Piping in the Maasvallei: A possibility or far-fetched scenario?," 2017.

[29] J. Schokker, F. D. D. Lang, C. D. Otter, S. Passchier, B. Noordzee, and F. V. Boxtel, "Beschrijving lithostratigrafische eenheid," pp. 1–9, 2005.

[30] J. Schokker, F. D. D. Lang, C. D. Otter, S. Passchier, B. Noordzee, and F. V. Boxtel, "Beschrijving lithostratigrafische eenheid," no. 1975, pp. 1–9, 2005.

[31] H. Weerts, "Beschrijving lithostratigrafische eenheid Formatie van Naaldwijk," pp. 1–7, 2003.

[32] J. Schokker, F. D. D. Lang, C. D. Otter, S. Passchier, B. Noordzee, and F. V. Boxtel, "Beschrijving lithostratigrafische eenheid," pp. 1–9, 2005.

[33] TNO, "Dinoloket."

[34] Deltares, "D-Geo Flow," 2017.

[35] Wikipedia, "Lek river."

[36] B. A. Robbins and V. M. van Beek, "Backward Erosion Piping : A Historical Review and Discussion of Influential Factors," *ASDSO Dam Safety*, no. September 2015, pp. 1–20, 2015.

[37] d. A. Wiersma and d. G. Kruse, "Schatting van de doorlatendheid van zandpaketten onder de Lekdijk tussen Nieuwegein en Schoonhoven, dijktraject 15-1," tech. rep., Deltares, 2018.

[38] AHN, "Actueel Nederlands Hoogtebestand."

[39] W. J. D. Lange, J. C. Hunink, and J. C. Hoogewoud, "Geohydrologische analyse van stroming uit met slib gevulde zandwinputten," 2010.

[40] KIVI, "Reader geotechniek,"

[41] United States Army Corps of Engineers, "Design and Construction of Levees," no. March 1978, p. 164, 2000.

[42] L. Smedema and D. Rycroft, *Land drainage:planning and design of agricultural drainage systems*. 1983.

[43] J. Bear, *Dynamics of fluids in poreus media*. 1972.

[44] NEN-EN-ISO, "Geotechnisch onderzoek en beproeving - Identificatie en classificatie van de grond - Deel 1:Identificatie en beschrijving," tech. rep., 2016.

[45] W. Krumbein and E. Aberdeen, "The sediments of Barataria Bay," *Journal of sedimentary research*, 1937.

[46] C. Yu, J. Cheng, L. Jones, Y. Wang, E. Faillace, C. Loureiro, and Y. Chia, "Data collection handbook to support modeling the impacts of radioactive material in soil," no. July 2014, 1993.

[47] P. Domenico and M. Miffilin, "Water from low permeability sediments and land subsidence," tech. rep., 1965.

[48] Deltares, "D-Geo Flow."

[49] Deltares, "D-Geo Flow manual,"

[50] J. Stafleu, D. Maljers, F. Busschers, J. Gunnink, J. Schokker, R. Dambrink, H. Hummelman, and M. Schijf, "GeoTop construction (in Dutch)," *TNO reports*, p. 216, 2013.

[51] TNO, "Berekenen van de meest waarschijnlijke lithoklasse in GeoTOP," vol. 1, pp. 1–5, 2014.

[52] T. N. O. Geologische and D. Nederland, "Modelonzekerheid in GeoTOP," pp. 1–9, 2014.

# IV

# Appendices

# A

# Piping research through history

## Clibborn and Beresford (1902)

Colonel J. Clibborn was perhaps the first to describe the process of piping, although this term was not used. His interest originated from a number of weir failures in Egypt and India [36]. Clibborn and Beresford described a relation between the head across the structure ($H$), a coefficient describing the geometry and soil parameters($E$) and the seepage length($L$) [14]:

$$L = E \cdot H \tag{A.1}$$

Their formula was used for the design of diversion weirs constructed in Egypt and India [36].

## Bligh (1910)

The first real description of piping was done by British engineer for the Royal Navy, W.G. Bligh. During his time in India, numerous weirs failed due to piping. As a design rule, he came up with an empirical rule known as the creep theory. His empirical rule describes the relation between the maximum allowable head across a structure($H_{cr}$) and the seepage length($L$). The relation between these parameters was described by the percolation coefficient or creep ratio($C_{creep}$):

$$C_{creep} = \frac{L}{H_{cr}} \tag{A.2}$$

He defined the creep ratio for various soil types, shown in table A.1. As the formula by Bligh provided a safe critical head to prevent piping, it has been a base for the design of dams, weirs and dikes for a long time [13] [15]. The advantage of Bligh's approach is the simplicity, due to the small number of input parameters.

## Terzaghi (1922)

Terzaghi presented in 1922 a concept of a vertical critical gradient, which occurs when the upward seepage forces exceed the downward gravitational forces . If this critical gradient is reached, the sand fluidizes and boils. This process, already described in section 3.1.1, is referred to as *heave* [36]. The critical heave gradient was described by Terzaghi in the following relation [4]:

$$i_c = \frac{(\gamma_s - \gamma_w)}{\gamma_w} \cdot (1 - n) \tag{A.3}$$

In which $n$ is the porosity, $\gamma_s$ is the unit weight of the saturated soil and $\gamma_w$ is the unit weight of water. The formula by Terzaghi describes the *heave* criterion, so the initiation of the pipe(s), this does not imply that pipe(s) will form.

In the Dutch assessment method for piping, it is assumed that the vertical exit gradient must exceed 0.5 for sand boils to form [13], when this occurs, assessment for piping is needed. The criterion for *heave* is [9]:

$$i_o = \frac{(\phi_0 - h_p)}{D} \leq i_c \tag{A.4}$$

In which $\phi_0$ is the hydraulic head at the bottom of the top layer, where the exit gradient is maximum, $h_p$ is the inner water level(free water level or ground level) and $D$ is the aquifer thickness [9] .

## Lane (1935)

When piping occurs in a vertical way, the formula of Lane(1935) can be used. Lane revised the creep ratio concept by Bligh to more accurately account for the increased resistance to flow provided by cut-offs [36],[13]. He based this revision through a review of 278 dams, he adjusted the creep ratio from Bligh to a ratio known as the weighted creep ratio. Lane (1935) suggested the following relation [36]:

$$\Delta H_c = \frac{\frac{1}{3}L_h + L_v}{C_{w,creep}} \tag{A.5}$$

In which $\Delta H_c$ is the critical hydraulic head across the structure, $L_h$ and $L_v$ are the horizontal and vertical seepage lengths and $C_{w,creep}$ is the weighted creep ratio. While the creep ratios from Lane (1935) are a significant improvement over the ratios from Bligh(1910), the largest shortcomings of Bligh's approach are not overcome by Lane, because the safety factor against piping is unknown and no site-specific conditions can be accounted for [36]. The weighted creep ratios can be seen in table A.1 next to the creep ratios from Bligh.

Table A.1: Creep ratios for different soil types by Bligh(1910) and Lane(1935) [9]

| Soil types | Median grain size [$\mu m$][1] | $C_{creep}$ (Bligh) | $C_{w,creep}$ (Lane) |
|---|---|---|---|
| Very fine sand, silt | <105 | | 8.5 |
| Very fine sand | 105-150 | 18 | |
| Fine sand(mica) | | 18 | 7 |
| Moderate fine sand(quartz) | 150-210 | 15 | 7 |
| Medium sand | 210-300 | | 6 |
| Coarse sand | 300-2000 | 12 | 5 |
| Fine gravel | 2000-5600 | 9 | 4 |
| Medium gravel | 5600-16000 | | 3.5 |
| Coarse gravel | >16000 | 4 | 3 |

[1]Indications conform NEN 5104 (Sep, 1989)

## USACE (1956)

The United States Army Corps of Engineers, with Bennet(1946), developed analytical solutions for assessing levee-underseepage [36]. This approach is known as the *Blanket Theory* in the United States. In this it is assumed that all seepage through the blanket (cover layer) is vertical and through the foundation(aquifer) is horizontal. The *Blanket Theory* is very accurate for situations where the permeability of the blanket is significantly lower than the permeability of the aquifer (factor >10) [36]. The United states adopted this approach as their primary guideline in their manual "Design and Construction of levees" [41]. The governing criterion, used in the United States, for designing against piping is the exit gradient. The design guidelines can be seen in [41].

## Schmertmann(2000)

Schmertmann developed an a method with empirical factor derived from several experiments. His empirically based method incorporated numerous factors based on theory, such as the influence of pipe orientation and anisotropy. The method is based on point gradients, the local gradients upstream of the advancing pipe [36]. These local gradients are compared to the local critical gradients to determine the factor of safety. These critical gradients are derived from laboratory tests [36]. Schmertmann acknowledged the influence of the uniformity coefficient of the soil [12]. The disadvantage of Schmertmann's method is the difficulty of using it,

although it is, perhaps, the most comprehensive model for assessing piping.

## Hoffmans(2014)

Hoffmans describes an analytical model based on Ohm's law. The flow underneath the blanket is determined by the resistance and the potential differences of the soil. The flow through the aquifer is schematised by different flows: groundwater flow on the upper side, vertical flow towards the pipes, pipe flow on the entry points, pipe flow on the inner side and groundwater flow on the inner side. The groundwater flow is modelled by Darcy's law and is laminar. The pipe flow, described by Hagen-Poiseuille flow is also laminar [8].

The model distinguishes the critical head for *heave* and the critical head for *initiation*. Shields is used, after adjusting it for laminar flow, for the motion of the particles. Critical gradients of Shields and Darcy are used to calculate the critical hydraulic gradient [8].

Just like Sellmeijer's model does Hoffmans' model use a isotropic homogeneous aquifer as a schematization. But Hoffmans assumes two layers in the aquifer, one layer affecting the hydraulic head and the other layer not. The thickness of the layer influencing the hydraulic head is approximated with a relation between the discharge through the layer, the hydraulic conductivity and the gradient. The formulas used for the model by Hoffmans can be seen in [7, 8].

# B

# Appendix: Samples subsoil study

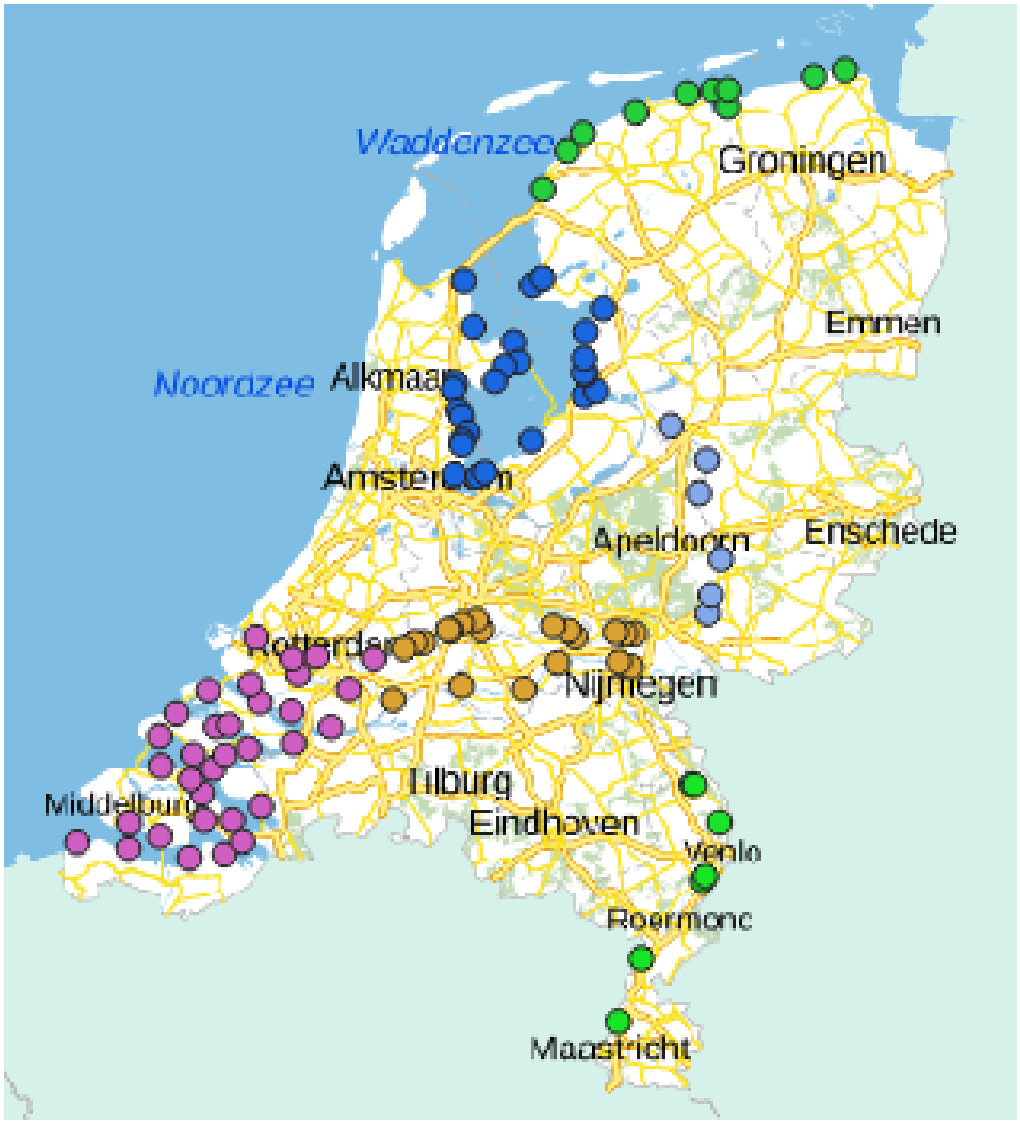


Figure B.1: Sampling of the different areas

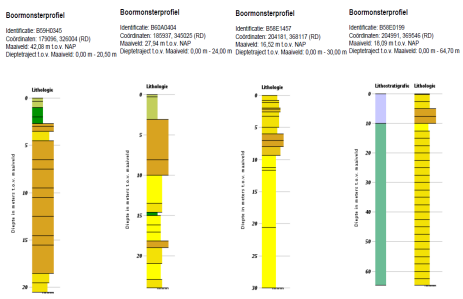

(a) Samples Meuse valley(1)

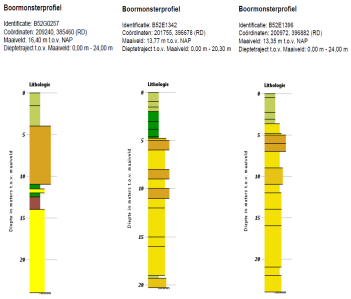

(b) Samples Meuse valley(2)

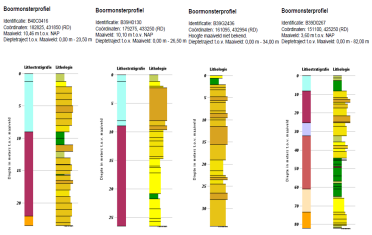

(a) Samples River Lands(1)

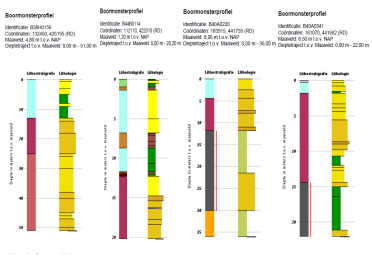

(b) Samples River Lands(2)

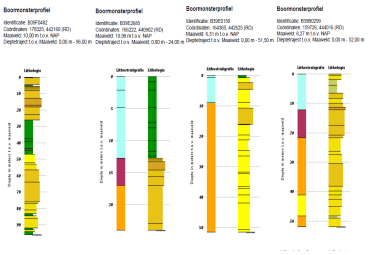

(a) Samples River Lands(3)

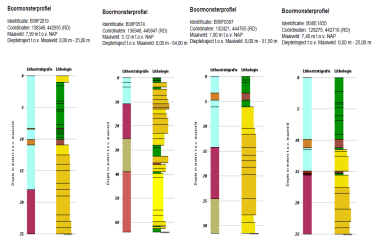

(b) Samples River Lands(4)

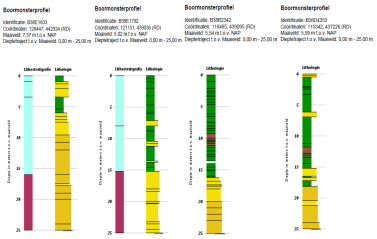

(a) Samples River Lands(5)

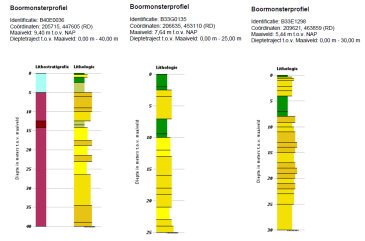

(b) Samples IJssel river(1)

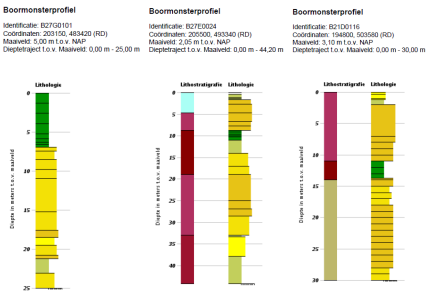

(a) Samples IJssel river(2)

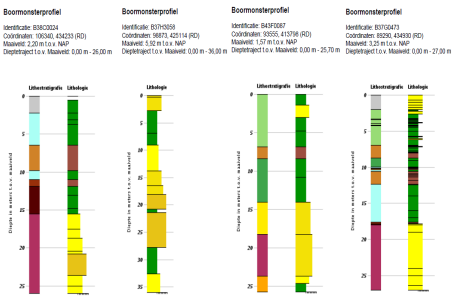

(b) Sampels Delta area(1)

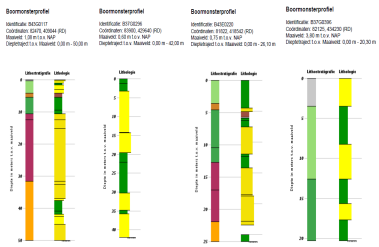

(a) Sampels Delta area(2)

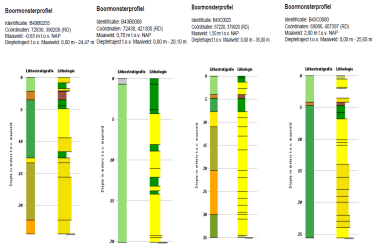

(b) Sampels Delta area(3)

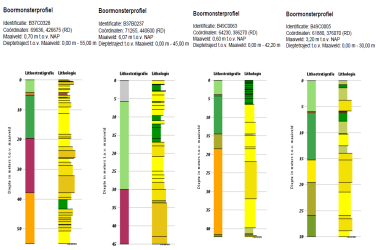

(a) Sampels Delta area(4)

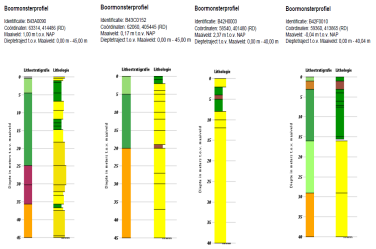

(b) Sampels Delta area(5)

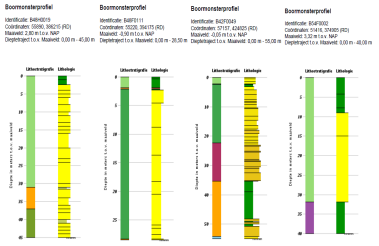

(a) Sampels Delta area(6)

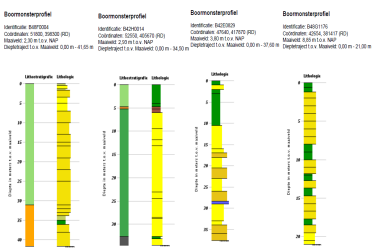

(b) Sampels Delta area(7)

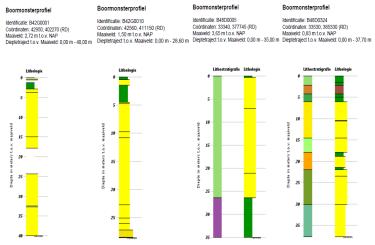

(a) Sampels Delta area(8)

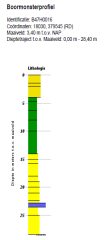

(b) Sampels Delta area(9)

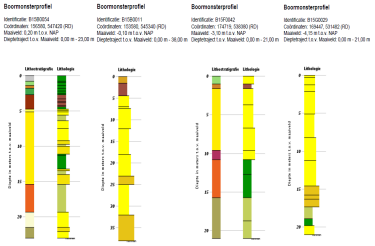

(a) Samples IJsselmeer area(1)

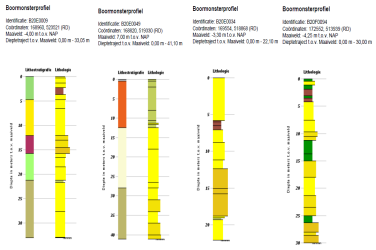

(b) Samples IJsselmeer area(2)

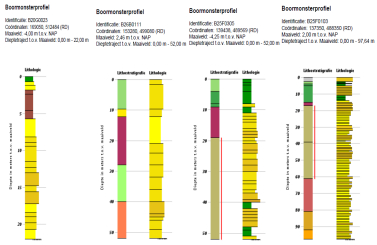

(a) Samples IJsselmeer area(3)

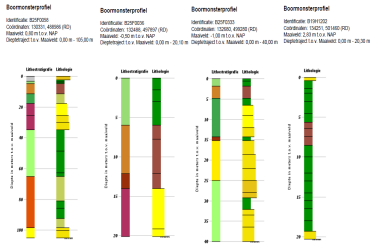

(b) Samples IJsselmeer area(4)

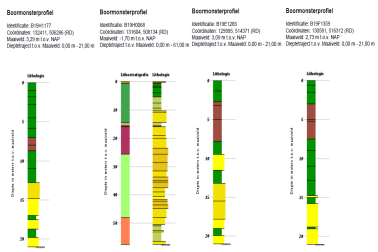

(a) Samples IJsselmeer area(5)

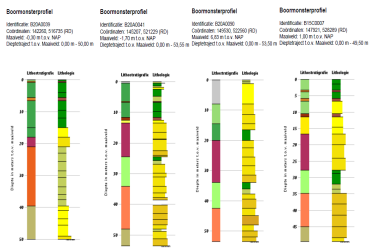

(b) Samples IJsselmeer area(6)

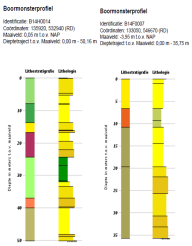

(a) Samples IJsselmeer area(7)

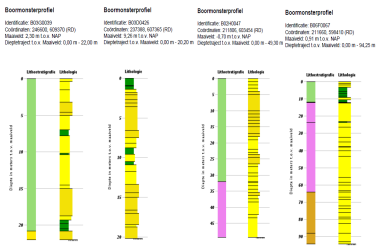

(b) Samples Waddenzee area(1)

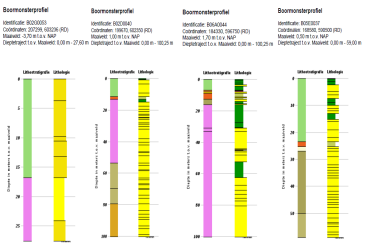

(a) Samples Waddenzee area(2)

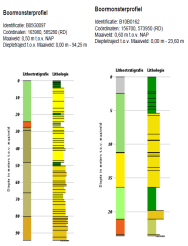

(b) Samples Waddenzee area(3)

# C

# Soil characteristics

## Hydraulic conductivity

As described above, only the horizontal hydraulic conductivity is discussed in this part. The hydraulic conductivity is the ease by which water flows through a soil. As the flow of water through a soil type is dependent on the open spaces in the soil and the connection of these spaces, each soil type has a different hydraulic conductivity. Smedema and Rycroft(1983)[42] state that the same soil types have different values of the hydrauluic conductivity due to the variability in soils and came up with a generalized table, describing the hydraulic conductivities of soil types. As in this Thesis, the soil classification by *Dinoloket* [33] is used, the table by Smedema and Rycroft is adjusted to this classification.

Förster(2017) [19] describes the hydraulic conductivity of the permeable sand and gravel layers, depending on their origin. The values are implemented on the classification as stated above by the *Dinoloket*. The values described are representative for the assessment in the Netherlands.

Bear(1972)[43] also described the hydraulic conductivity. The values were modified to the classification.

Table C.1: Hydraulic conductivities(K) in $[m/day]$

| Soil types | K-value [42] | K-value [19] | K-value [43] |
|---|---|---|---|
| Gravel | 30-50 | 58.8-84.7 | 86.4-864 |
| Coarse sand | 10-30 | 24.2-58.8 | 8.64-86.4 |
| Medium sand | 1-5 | 8.1-13.0 | 4.32-8.64 |
| Fine sand | 1-3 | 0.9-4.4 | 0.864-4.32 |
| Clayey sand or sandy clay | 0.2-2 | - | |
| Clay | 0.002-0.2 | - | 0.000864 - 0.0864 |
| Peat | - | - | 0.864-8.64 |

## Anisotropy coefficient

The anisotropy coefficient is the directional inequality in hydraulic conductivity and is defined as $C_A = \frac{K_x}{K_y}$ in which $K_x$ is the horizontal and $K_y$ the vertical hydraulic conductivity. Anisotropy is described in section 3.2.2. The value of the anisotropy coefficient is not very well known and is dependent on the soil type. Forster(2017) [19] states that the coefficient can value from 2 to more than 10, for respectively sand and clay, where other literature state that the coefficient can vary from 1 to 40 [24]. According to the literature it can be concluded that the hydraulic conductivity is dependent on the soil type and that for coarse soils the hydraulic conductivity is smaller than for fine soils and with this it is assumed, for now, that the coefficient has a linear dependency to the soil types. With this assumption, the following values for the different soils are chosen:

Table C.2: Anisotropy coefficient($C_A$)

| Soil types | Anistropy coefficient [19] |
|---|---|
| Gravel | 0 |
| Coarse sand | 2 |
| Medium sand | 4 |
| Fine sand | 6 |
| Clayey sand or sandy clay | 8 |
| Clay | 10 |
| Peat | - |

## Particle diameter

The particle diameter used in the models and the piping assessment is the $D_{70}$ *grain size*. The $D_{70}$ is the grain size for which 70% of the mass percentage passes the sieve with a mesh of $D$. The particle diameter has a direct influence on the distribution of spaces in the soil and therefore on the flow of water through the soil. As all the soil parameters, the grain size also has a range, due to the variability of the soil, from this range the $D_{70}$ can be concluded. In ISO 14688-1 [44] the grain sizes of sands are given. Krumbein(1937) [45] defined a classification scale based on the grain size, the grain size distribution is adapted to the classification from*Dinoloket*

Table C.3: Particle diameter

| Soil types | Particle diameter [44] [$m$] | Particle diameter [45] [$m$] |
|---|---|---|
| Gravel | - | $2.0 * 10^{-3}$ - $3.2 * 10^{-2}$ |
| Coarse sand | $6.3 * 10^{-4}$ - $2.0 * 10^{-3}$ | $5.0 * 10^{-4}$ - $1.0 * 10^{-3}$ |
| Medium sand | $2.0 * 10^{-4}$ - $6.3 * 10^{-4}$ | $2.5 * 10^{-4}$ - $5.0 * 10^{-4}$ |
| Fine sand | $6.3 * 10^{-5}$ - $2.0 * 10^{-4}$ | $1.25 * 10^{-4}$ - $2.5 * 10^{-4}$ |
| Clayey sand or sandy clay | - | - |
| Clay | $\leq 2.0 * 10^{-5}$ | $9.8 * 10^{-7}$ - $3.9 * 10^{-6}$ |
| Peat | - | - |

## Porosity

The porosity of the soil is the amount of open spaces in the soi. These "open" spaces can be filled with a liquid or air. Yu(1993) [46] defined the range for the porosity for the different soil types.

Table C.4: Porosity

| Soil types | Porosity [−] [46] |
|---|---|
| Gravel | 0.25-0.36 |
| Coarse sand | 0.31-0.46 |
| Medium sand | - |
| Fine sand | 0.25-0.53 |
| Clayey sand or sandy clay | - |
| Clay | 0.34-0.57 |
| Peat | - |

## Compressibility

Compressibility is the amount of loss in volume. It is expressed in $[m^2/N]$. From the ranges the compression is given in, the lowest value is chosen for the models. The compression values for the different soil types are [47]:

Table C.5: Compressibility

| Soil types | Compressibility [$m^2/N$] [47] |
|---|---|
| Gravel | $1.0 * 10^{-8}$ - $5.2 * 10^{-8}$ |
| Coarse sand | $1.0 * 10^{-7}$ - $1.0 * 10^{-8}$ |
| Medium sand | $1.0 * 10^{-7}$ - $1.0 * 10^{-8}$ |
| Fine sand | $1.0 * 10^{-7}$ - $1.0 * 10^{-8}$ |
| Clayey sand or sandy clay | - |
| Clay | $2.0 * 10^{-6}$ - $1.3 * 10^{-7}$ |
| Peat | - |

# D

# D-Geo Flow

## D.1. Introduction ([48])

To see how several aspects influence the result of the critical head, D-Geo Flow is used. In D-Geo Flow cross-sections can be modelled and calculation can be done. D-Geo Flow is a graphical interface. In fig. D.1 the user interface can be seen.

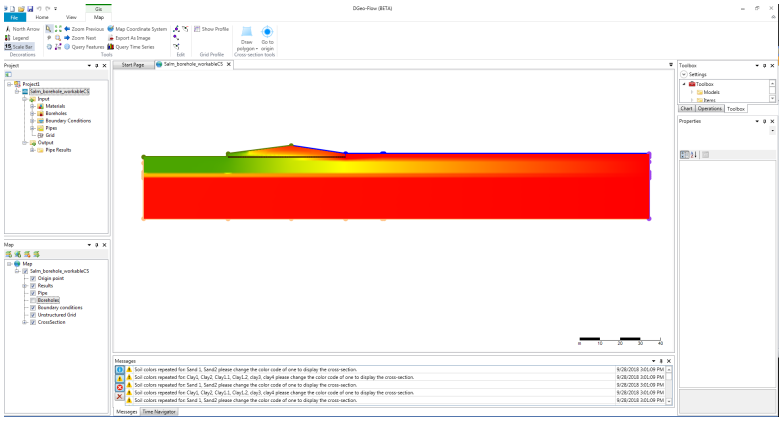

Figure D.1: D-Geo Flow interace

It is the graphical interface for the computing platform DGFlow. In DGflow the finite element method is used to compute the results. In D-Geo Flow a piping module is present to predict whether piping can occur or not, given a certain water level. This module is based on the model by Sellmeijer, in which the force balance of the grains in the top of the erosion channel is assessed. In D-Geo Flow the subsoil can be modelled and 2D transient groundwater flow calculations can be performed. In this calculations time-dependence, compressibility and changes in the phreatic line are incorporated. In the following sections D-Geo Flow is explained in more depth and the downsides of the program are named. For the scientific background of the DGFlow platform, the D-Geo Flow manual[49] is recommended.

## D.2. Working with D-Geo Flow

As explained is D-Geo Flow a graphical user interface. This means that , if it's done in the right way, you see what you are doing. How to work with D-Geo Flow will explained in the steps that have to be taken to calculated with D-Geo Flow.

Materials
In D-Geo Flow the materials that will be used have to be put in manually. Two types of materials can be distinguished: Soils and Water.

**Soils**
Per soil type, several soil parameters must be put in. Also a soil type name and color have to be chosen. These parameters will later determine the flow pattern and erosion. The soil parameters which have to be put in D-Geo Flow are:

- Porosity ($n$) [$-$]

- Compressibility ($\alpha$) $[m^2/N]$
- Grain particle density ($\rho_s$) $[kN/m^3]$
- Particle diameter ($D_{70}$) $[n]$
- White's constant ($\eta$) $[-]$
- Bedding angle ($\Theta$) $[deg]$
- Hydraulic conductivity ($K_{x,y}$) $[m/day]$

Per soil types most of the parameters differ. However, for some parameters it is recommended by Förster[9] to use set values. The parameters with the follwing values are recommended:

- White's constant ($\eta$) = 0.25
- Bedding angle ($\Theta$) = 37 deg
- Grain particle density ($\rho_s$) = $2.65 * 10^3$ $kN/m^3$

**Water**
The input values for water are already given by D-Geo Flow. These are the values for fresh water. Water used in the models can be assumed as fresh water, so these properties do not have to be changed.

Boreholes
To create a cross-section, D-Geo Flow uses linear interpolation between boreholes. These boreholes have to be put into D-Geo Flow. The boreholes consist of information about the soil at that specific location in the cross-section. The boreholes consist therefore the following information:

- A name: Boreholes can be named, D-Geo Flow automatically gives numbers to the boreholes, but they can be adjusted;
- X-location: location in the 2D cross-section (see fig. D.1);
- Top level: the ground level height at that location;
- Soil layering: per soil layer a upper boundary, a lower boundary and soil layer have to be assigned.

An example of a borehole with different layers can be seen in fig. D.2. When several boreholes are created, D-Geo Flow interpolated the soil layers between these boreholes to create a cross-section. The cross-section can only be changed by changing the boreholes.

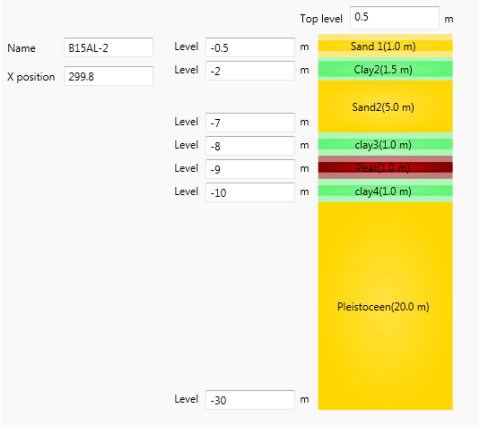

Figure D.2: Example of a borehole in D-Geo Flow

Boundary conditions
For D-Geo Flow to calculate, all boundaries of the model need to have a boundary condition. In D-Geo Flow 5 types of boundary conditions can be assigned:

1. Head boundary: A constant head, has to be assigned to the boundaries which are in contact with a uniform head in time and space;
2. Flux boundary: A boundary at which water is crossing the boundary in or out of the model;
3. Seepage boundary: A boundary through which water can seep into the outer atmosphere;
4. Submerging boundary: A variable head, has to be assigned to the boundaries which are in contact with water level which are time-variable;
5. No-flow boundary: Assigned to locations where no flow crosses the boundary.

Each of these boundaries have their specific characteristics. More information about the characteristics of these boundaries can be seen in Stoop(2018)[13].

Pipe
When the cross-section is, almost, done, a pipe can be assigned. In D-Geo Flow a pipe must be added manually and must be, at both sides, in contact with the outer atmosphere. This means entry and exit points must already be added in the model, by use of the boreholes. In D-Geo flow the pipe must be horizontal.

Grid
The last step in making the model is generating the grid. In the grid menu, two values must be chosen: The default mesh coarseness and the Pipe coarseness. The mesh coarseness is the size of one side the an element in the grid. A low values states that small elements are generated. The pipe coarseness is the dividing factor of the elements along the pipe. This means that the size of an element is divided by the pipe coarseness value and therefore more elements will be present along the pipe to improve the accuracy of the calculations along the pipe.

A low value of the Default mesh coarseness leads to smaller elements and therefore an increase in calculation duration. The same counts for a high value of the pipe coarseness.

## D.3. Limitations of D-Geo Flow

With the use of D-Geo Flow, some limitations occur, as the software is relatively new, no solutions can yet be implemented in the software. In this section the limitations will be summed up.

- Changing the cross-section in an easy way. In D-Geo Flow, the cross-sections are created by use of interpolation between boreholes. If a cross-section has to be changed all the boreholes have to be changed in order to do so. This is a time-consuming and impractical way in changing the cross-section;
- The development of the pipe, or in D-Geo Flow the modelling of the pipe, can only be horizontal in D-Geo Flow. This horizontal pipe also has to be placed directly beneath the dike body. This is, partly, due to the fact that D-Geo Flow can not calculate vertical erosion. This makes the prediction of the pipe progression unreliable if, in practice, the pipe proves to progress in an un-horizontal way;
- Complex cross-sections are difficult to model. If a complex cross-section is modelled, the D-Geo Flow software can gives some errors. This is due to the fact that D-Geo Flow, for long thin elements, can not create a grid with the given grid properties. In fact, no triangles can be generated, but elements with more than three sides are then generated. These errors are unclear in where the problem occurs or how to solve the problem. This can cause a time-consuming search for the problem;
- If a grid for a complex cross-section can be generated, D-Geo Flow can take forever to give a result. This makes it hard to model complex, extensive cross-sections;
- As D-Geo Flow is a user interface, it seems to be easy in use, However, because of the simple interface, implementation of models with a complex composition is very time-consuming;
- The preparation steps to create a model are very clear. However, the calculation is a black box. It is unclear to see what and how the software is doing its calculations;
- The calculation time prediction is not very accurate. If calculations are performed, a screen pops up in which the progression of the calculation can be seen in time and in percentages. These percentages are correct, but the time prediction is not correct;
- 3D-flow calculations are not possible. This makes a spatial variation along the dike impossible to put in the model and can lead to misleading results.

# E

# Appendix: Results foreshore sensitivity analysis

## E.1. Hydraulic conductivity of the foreshore

Salmsteke

Table E.1: Results of the hydraulic conductivity variations of the foreshore, case Salmsteke

| Hyd. Cond. Foreshore: | K = 0.001 m/day | K= 0.01m/day | K = 0.1 m/day | K =1.0 m/day | K =10 m/day |
|---|---|---|---|---|---|
| Critical head result [$m$]: | 5.5 | 5.4 | 4.8 | 3.8 | 3.4 |

Honswijk

Table E.2: Results of the hydraulic conductivity variations of the foreshore, case Honswijk

| Hyd. Cond. Foreshore: | K = 0.001 m/day | K= 0.01m/day | K = 0.1 m/day | K =1.0 m/day | K =10 m/day |
|---|---|---|---|---|---|
| Critical head result [$m$]: | 6.4 | 6.3 | 5.9 | 4.8 | 4.1 |

Den Oord

Table E.3: Results of the hydraulic conductivity variations of the foreshore, case Den Oord

| Hyd. Cond. Foreshore: | K = 0.001 m/day | K= 0.01m/day | K = 0.1 m/day | K =1.0 m/day | K =10 m/day |
|---|---|---|---|---|---|
| Critical head result [$m$]: | 8.7 | 8.5 | 7.5 | 6.8 | 6.6 |

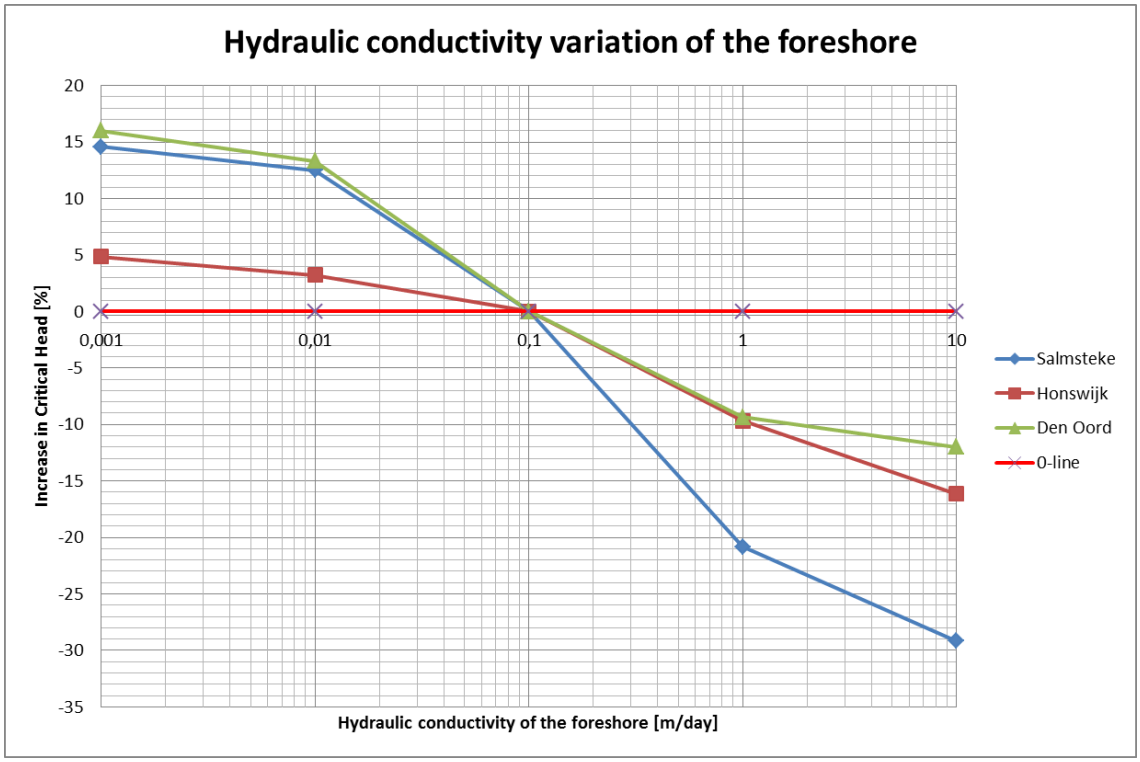


Figure E.1: Hydraulic conductivity variation of the foreshore

## E.2. Width of the entry points

Salmsteke

Table E.4: Results with bottom width variations of the entry points on the foreshore, case Salmsteke

| Bottom width pool 1: → Bottom width pool 2: ↓ | W=0.1m | W=0.5m | W=1.0m | W=5.0m |
|---|---|---|---|---|
| W=0.1m | 4.8 | 4.7 | 4.7 | 4.4 |
| W=0.5m | 4.9 | 4.7 | 4.6 | 4.4 |
| W=1.0m | 4.9 | 4.7 | 4.6 | 4.5 |
| W=5.0m | 4.8 | 4.8 | 4.5 | 4.4 |

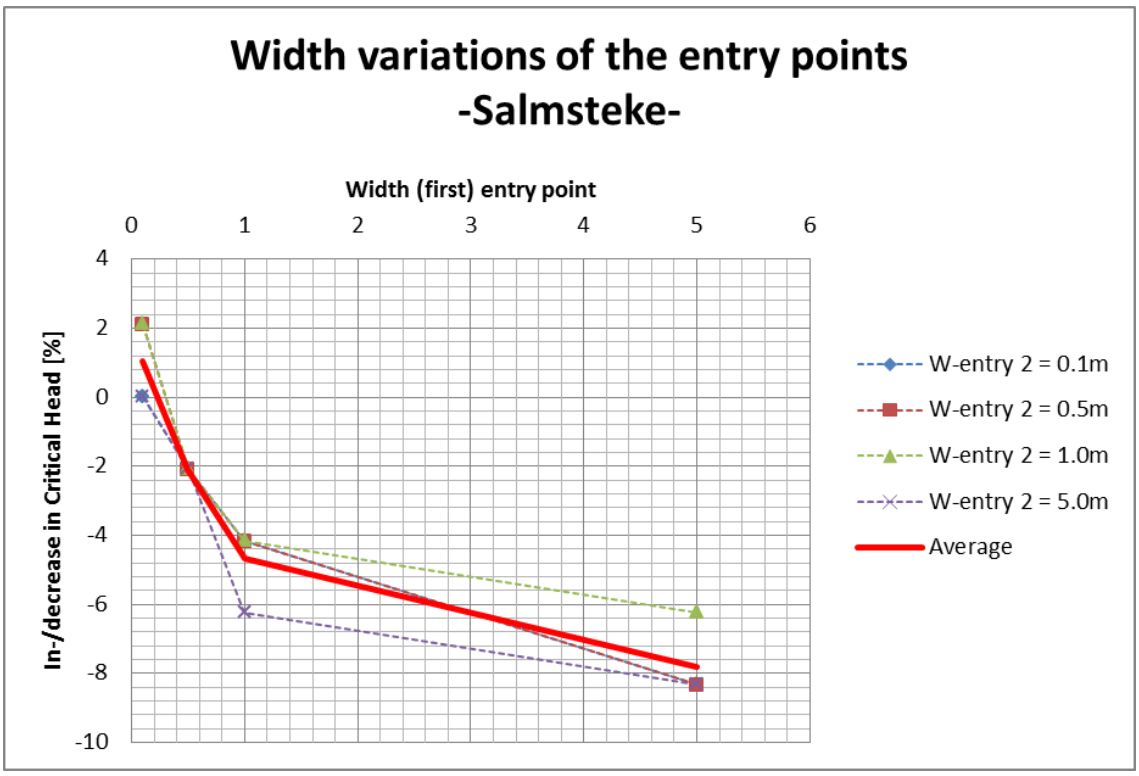


Figure E.2: Graphical result of the width variation, case Salmsteke

Honswijk

Table E.5: Results with bottom width variations of the entry points on the foreshore, case Honswijk

| Bottom width pool 1: → Bottom width pool 2: ↓ | W=0.1m | W=0.5m | W=1.0m | W=5.0m |
|---|---|---|---|---|
| W=0.1m | 6.3 | 6.1 | 6.0 | 5.9 |
| W=0.5m | 6.2 | 5.9 | 6.0 | 5.8 |
| W=1.0m | 6.1 | 6.1 | 6.0 | 5.8 |
| W=5.0m | 6.1 | 6.1 | 6.0 | 5.8 |

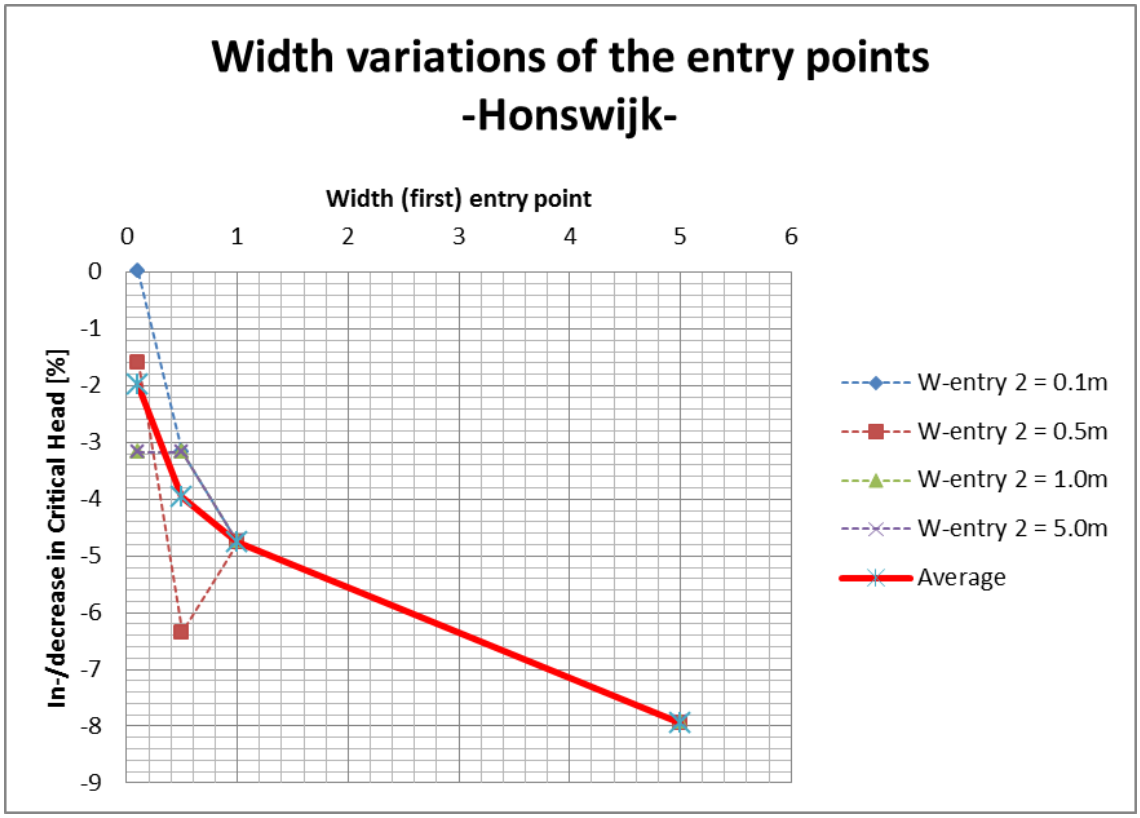


Figure E.3: Graphical result of the width variation, case Honswijk

Den Oord

Table E.6: Results with bottom width variations of the entry point on the foreshore, case Den Oord

| Bottom width pool: | W=0.1m | W=0.5m | W=1.0m | W=5.0m |
|---|---|---|---|---|
| Critical head result [m]: | 7.5 | 7.4 | 7.3 | 6.9 |

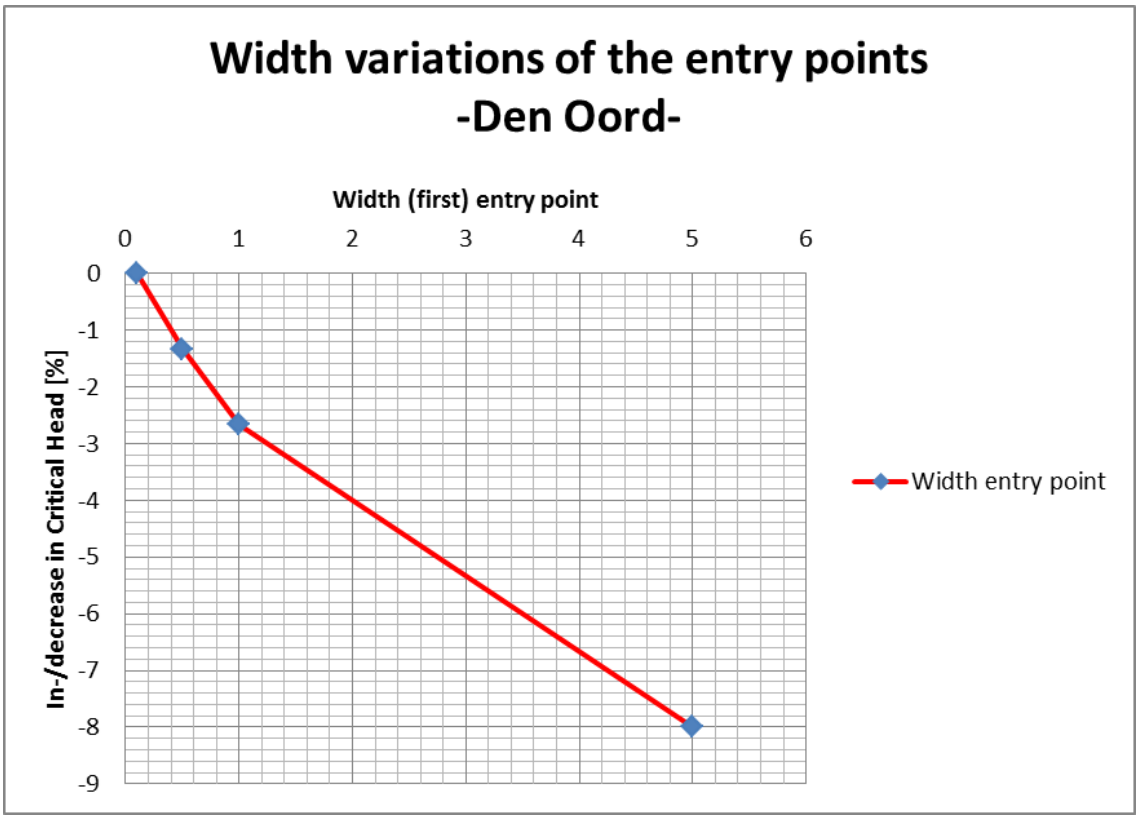


Figure E.4: Graphical result of the width variation, case Den Oord

## E.3. Depth of the entry points

### Salmsteke

Table E.7: Results of the depth variations of the entry points on the foreshore, case Salmsteke

| Depth percentage filled ent.point 1: → Depth percentage filled ent.point 2: ↓ | 0% (0m) | 10% (0.05m) | 25% (0.125m) | 50% (0.25m) | 75% (0.375m) |
|---|---|---|---|---|---|
| 0% (0m) | 4.8 | 5.8 | 5.8 | 5.8 | 5.8 |
| 10% (0.05m) | 5.0 | 6.0 | 6.0 | 6.1 | 6.1 |
| 25% (0.125m) | 5.0 | 6.1 | 6.1 | 6.1 | 6.1 |
| 50% (0.25m) | 5.0 | 6.2 | 6.1 | 6.1 | 6.2 |
| 75% (0.375m) | 5.0 | 6.1 | 6.1 | 6.2 | 6.2 |

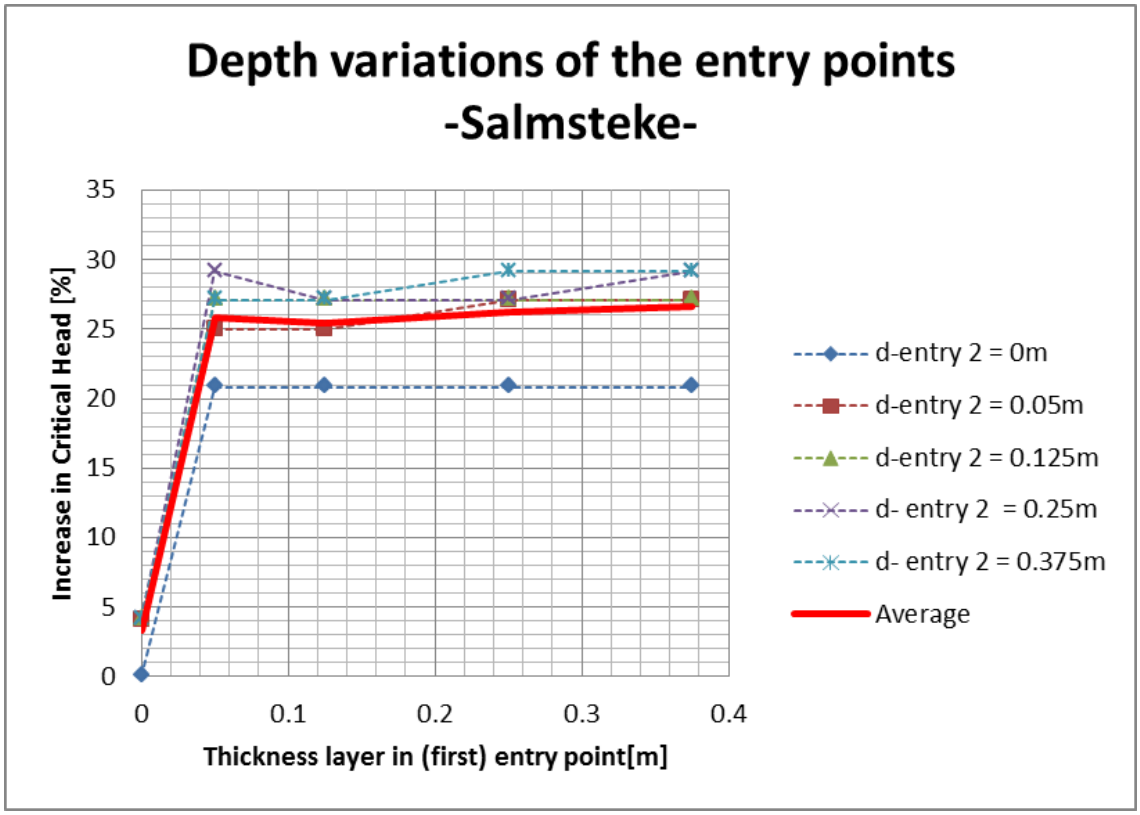


Figure E.5: Graphical result of the depth variation, case Salmsteke

### Honswijk

Table E.8: Results of the depth variations of the entry points on the foreshore, case Honswijk

| Depth percentage filled ent.point 1: → Depth percentage filled ent.point 2: ↓ | 0% (0m) | 10% (0.05m) | 25% (0.125m) | 50% (0.25m) | 75% (0.375m) |
|---|---|---|---|---|---|
| 0% (0m) | 6.2 | 6.9 | 7.0 | 6.9 | 6.9 |
| 10% (0.05m) | 6.4 | 7.7 | 7.7 | 7.7 | 7.7 |
| 25% (0.125m) | 6.5 | 7.7 | 7.7 | 7.8 | 7.8 |
| 50% (0.25m) | 6.5 | 7.5 | 7.7 | 7.6 | 8.1 |
| 75% (0.375m) | 6.5 | 7.7 | 7.8 | 7.6 | 7.8 |

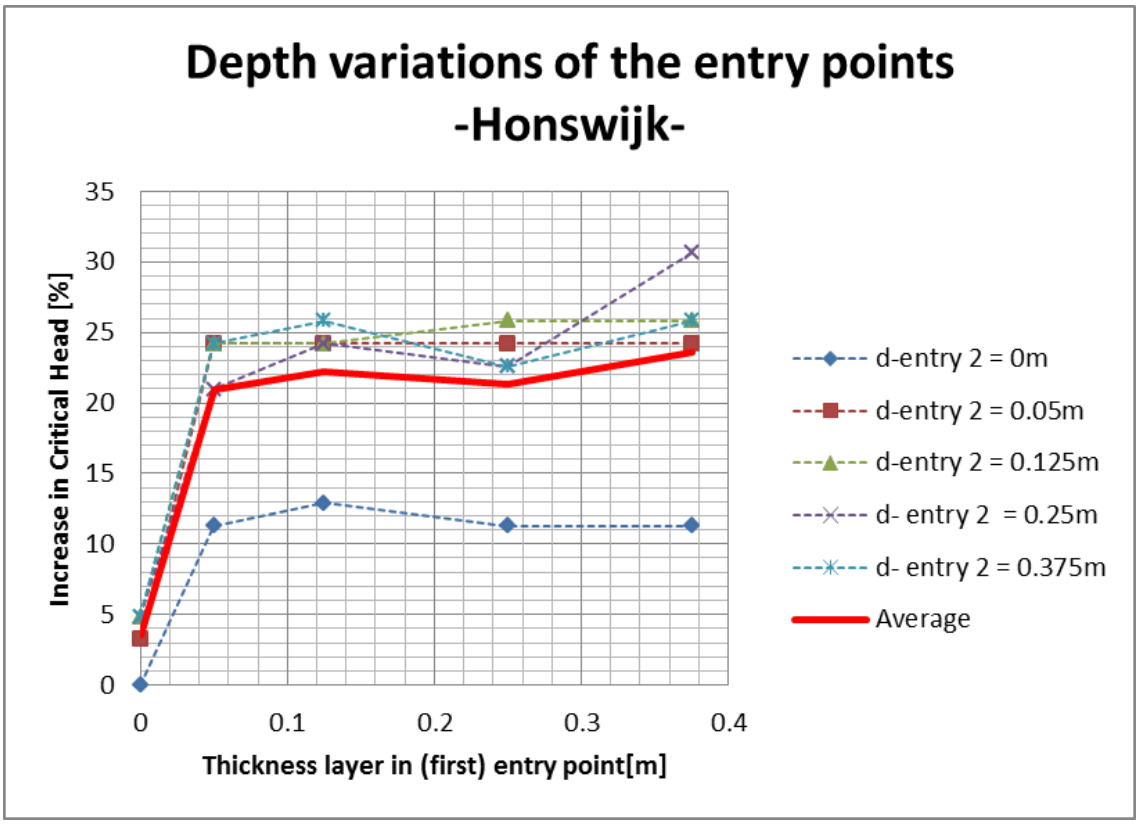


Figure E.6: Graphical result of the depth variation, case Honswijk

### Den Oord

Table E.9: Results of the depth variations of the entry points on the foreshore, case Den Oord

| Depth percentage filled ent.point: | 0% (0m) | 10% (0.05m) | 25% (0.125m) | 50% (0.25m) | 75% (0.375m) |
|---|---|---|---|---|---|
| Critical head result [$m$]: | 7.5 | 9.8 | 9.8 | 9.8 | 9.8 |

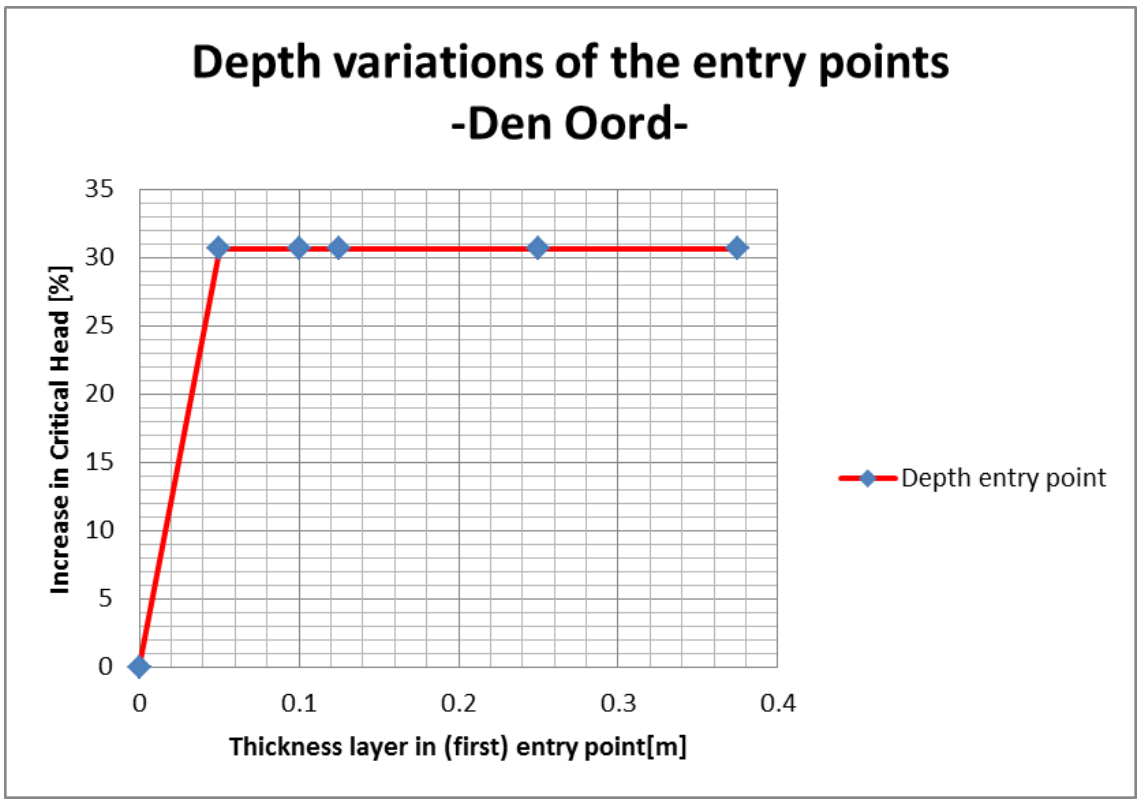


Figure E.7: Graphical result of the depth variation, case Den Oord

## E.4. Silting up of the entry points

### Salmsteke

Table E.10: Results of the silting up variations of entry points on the foreshore, case Salmsteke

| Thickness silt layer ent.point 1: → Thickness silt layer ent.point 2: ↓ | H=0m) | H=0.05m | H=0.10m | H=0.15m | H=0.20m |
|---|---|---|---|---|---|
| H=0m | 4.8 | 5.8 | 5.7 | 5.7 | 5.7 |
| H=0.05m | 5.0 | 6.2 | 6.2 | 6.2 | 6.2 |
| H=0.10m | 5.0 | 6.2 | 6.2 | 6.2 | 6.1 |
| H=0.15m) | 5.0 | 6.2 | 6.1 | 6.1 | 6.2 |
| H=0.20m | 5.0 | 6.2 | 6.2 | 6.2 | 6.2 |

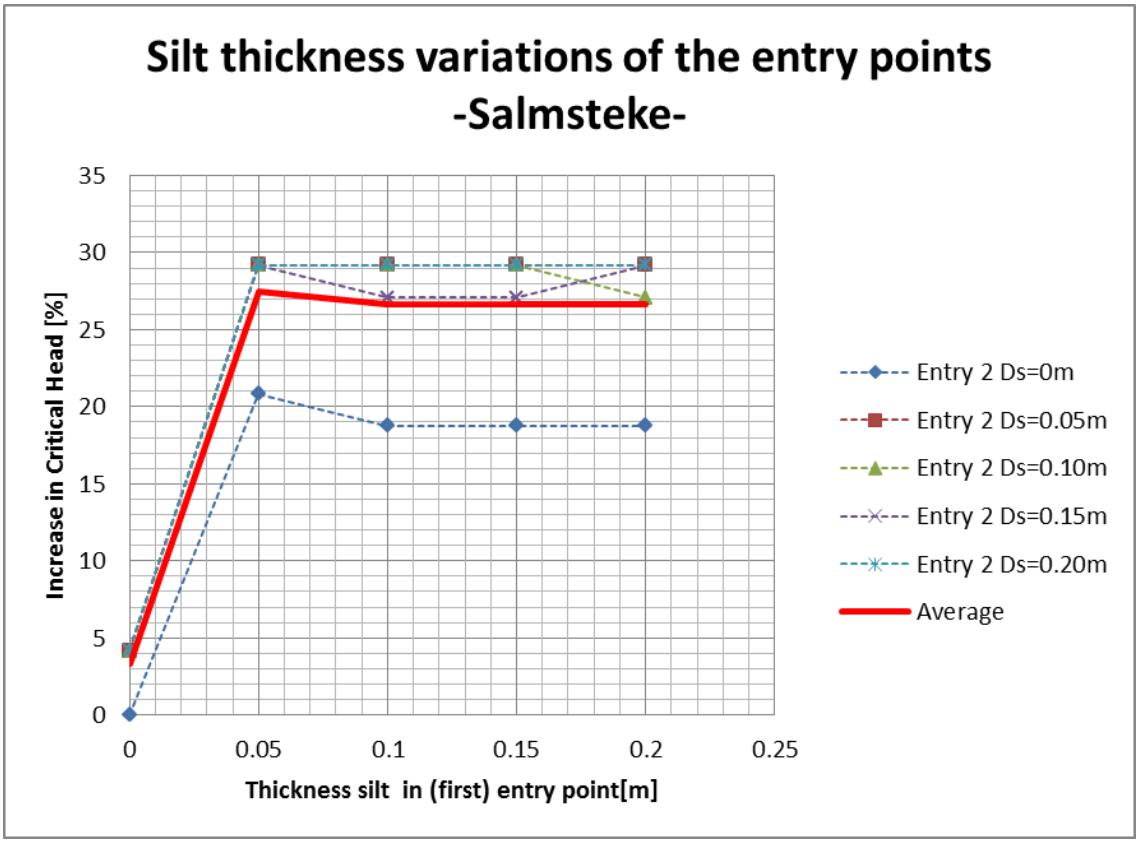


Figure E.8: Graphical result of the silt thickness variation, case Salmsteke

**Honswijk**

Table E.11: Results of the silting up variations of entry points on the foreshore, case Honswijk

| Thickness silt layer ent.point 1: → Thickness silt layer ent.point 2: ↓ | H=0m) | H=0.05m | H=0.10m | H=0.15m | H=0.20m |
|---|---|---|---|---|---|
| H=0m | 6.2 | 6.9 | 6.9 | 6.9 | 6.9 |
| H=0.05m | 6.4 | 7.9 | 7.8 | 7.8 | 7.8 |
| H=0.10m | 6.4 | 7.8 | 7.8 | 7.9 | 7.9 |
| H=0.15m) | 6.4 | 7.8 | 7.8 | 7.9 | 7.9 |
| H=0.20m | 6.4 | 7.8 | 7.8 | 7.9 | 7.9 |

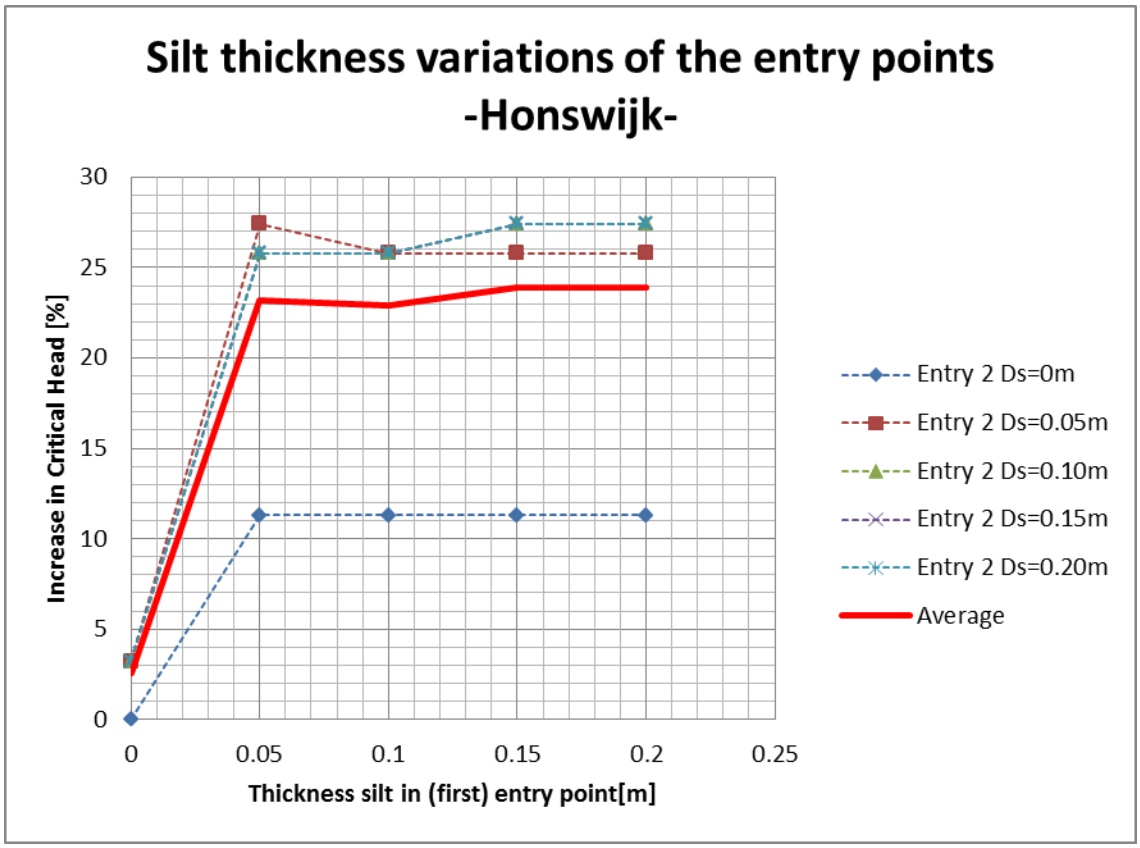


Figure E.9: Graphical result of the silt thickness variation, case Honswijk

**Den Oord**

Table E.12: Results of the silting up variations of entry points on the foreshore, case Den Oord

| Thickness silt layer: | H=0m | H=0.05m | H=0.10m | H=0.15m | H=0.20m |
|---|---|---|---|---|---|
| Critical head result [$m$]: | 7.5 | 9.8 | 9.8 | 9.8 | 9.8 |

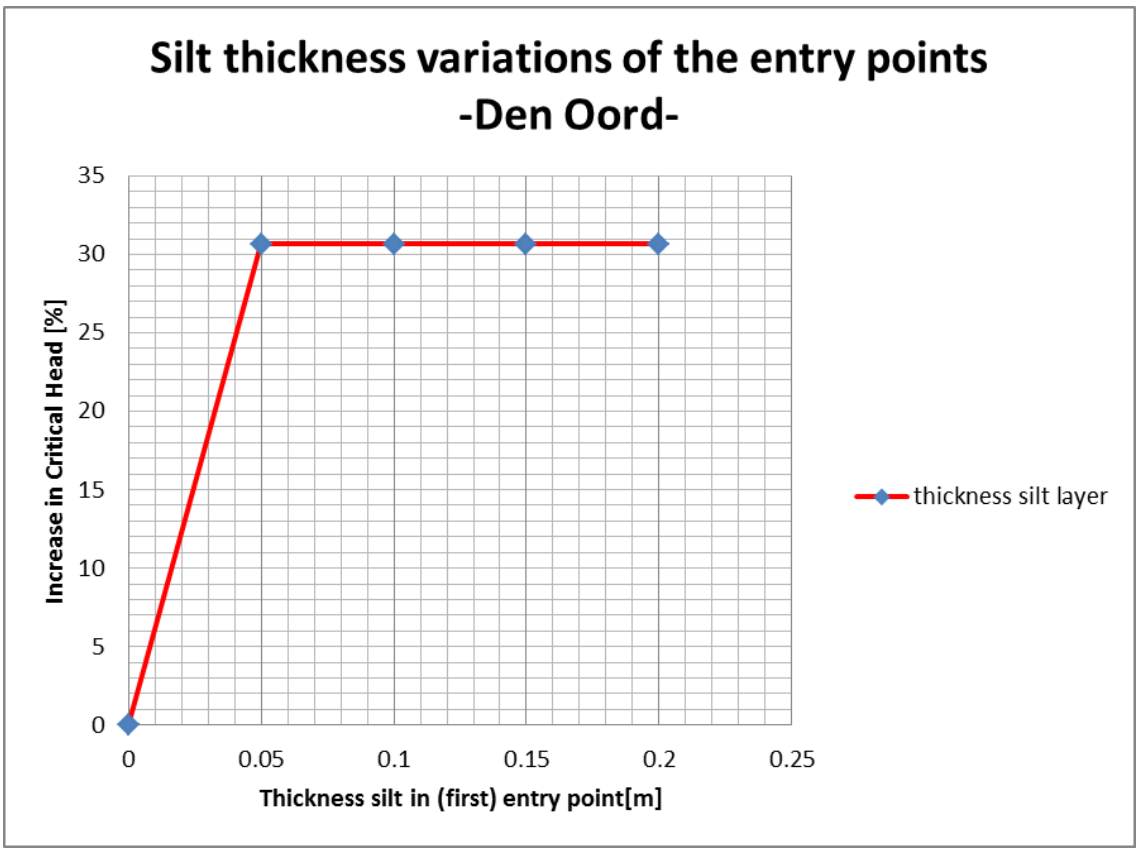


Figure E.10: Graphical result of the silt thickness variation, case Den Oord

# Appendix: Generic Foreshore results

## F.1. Initial seepage length = 50m

Table F.1: Results generic foreshore research(1), 50m initial seepage length

| C-value foreshore [$days$]: | 2000 | 1500 | 1000 | 500 | 250 | 100 | 50 | 25 | 10 | 5 |
|---|---|---|---|---|---|---|---|---|---|---|
| L-foreshore | $H_{cr}$ [$m$] | | | | | | | | | |
| 50 | 5.3 | 5.3 | 5.3 | 5.35 | 5.3 | 5.3 | 5.2 | 5 | 4.9 | 4.6 |
| 100 | 7.8 | 7.8 | 7.8 | 7.5 | 7.5 | 7.3 | 7.2 | 6.7 | 5.8 | 5 |
| 150 | 10 | 10 | 9.6 | 9.5 | 9.3 | 8.8 | 8.2 | 7.3 | 5.9 | 5 |
| 200 | 11.9 | 11.9 | 11.8 | 11.6 | 11.6 | 10.2 | 9.4 | 7.7 | 6 | 5 |
| 250 | 14.1 | 14.1 | 14 | 14 | 13.4 | 11.7 | 9.7 | 8 | 6.1 | 5 |

Table F.2: Results generic foreshore research(2), 50m initial seepage length

| C-value foreshore [$days$]: | 2.5 | 1 | 0.5 | 0.25 | 0.1 | 0.05 | 0.025 |
|---|---|---|---|---|---|---|---|
| L-foreshore | $H_{cr}$ [$m$] | | | | | | |
| 50 | 4.2 | 3.7 | 3.5 | 3.3 | 3.1 | 3 | 3 |
| 100 | 4.2 | 3.7 | 3.5 | 3.3 | 3.1 | 3 | 3 |
| 150 | 4.3 | 3.7 | 3.3 | 3.2 | 3.1 | 3 | 3 |
| 200 | 4.4 | 3.7 | 3.3 | 3.2 | 3.1 | 3 | 3 |
| 250 | 4.4 | 3.7 | 3.3 | 3.2 | 3.1 | 3 | 3 |

## F.2. Initial seepage length = 100m

Table F.3: Results generic foreshore research(1), 100m initial seepage length

| C-value foreshore [$days$]: | 2000 | 1500 | 1000 | 500 | 250 | 100 | 50 | 25 | 10 | 5 |
|---|---|---|---|---|---|---|---|---|---|---|
| L-foreshore | $H_{cr}$ [$m$] | | | | | | | | | |
| 50 | 7.7 | 7.7 | 7.7 | 7.7 | 7.7 | 7.7 | 7.5 | 7.5 | 7.2 | 7.0 |
| 100 | 9.9 | 9.9 | 9.9 | 9.9 | 9.7 | 9.5 | 9.4 | 8.8 | 8.0 | 7.4 |
| 150 | 10 | 10 | 9.6 | 9.5 | 9.3 | 8.8 | 8.2 | 7.3 | 5.9 | 5 |
| 200 | 11.9 | 11.9 | 11.8 | 11.6 | 11.6 | 10.2 | 9.4 | 7.7 | 6 | 5 |
| 250 | 14.1 | 14.1 | 14 | 14 | 13.4 | 11.7 | 9.7 | 8 | 6.1 | 5 |

Table F.4: Results generic foreshore research(2), 100m initial seepage length

| C-value foreshore [$days$]: | 2.5 | 1 | 0.5 | 0.25 | 0.1 | 0.05 | 0.025 |
|---|---|---|---|---|---|---|---|
| L-foreshore | $H_{cr}$ [$m$] | | | | | | |
| 50 | 6.5 | 6.1 | 5.7 | 5.7 | 5.4 | 5.4 | 5.3 |
| 100 | 6.6 | 6.1 | 5.6 | 5.7 | 5.4 | 5.4 | 5.3 |
| 150 | 4.3 | 3.7 | 3.3 | 3.2 | 3.1 | 3 | 3 |
| 200 | 4.4 | 3.7 | 3.3 | 3.2 | 3.1 | 3 | 3 |
| 250 | 4.4 | 3.7 | 3.3 | 3.2 | 3.1 | 3 | 3 |

## F.3. Representative seepage lengths

A good way to see how the foreshore can be used in the safety analysis is to express the results of the generic safety analysis in a representative seepage length, as this can be used in the Sellmeijer formula. To achieve this, the results from the generic research are translated, by rewriting the Sellmeijer formula, to a representative seepage length. This is done for both the case with the initial seepage length of 50m and for the case with the initial seepage length of 100m. The results can be seen in figs. F.1a and F.1b.

Figure F.1: Representative seepage lengths

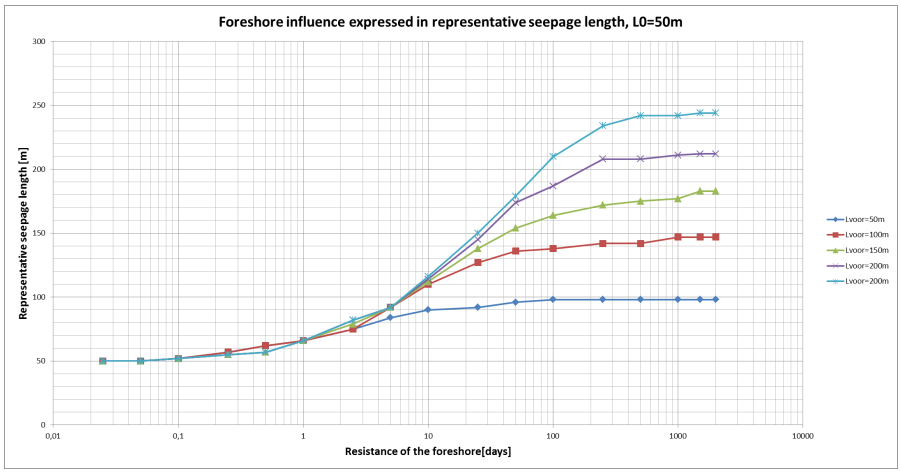


(a) Results expressed in representative seepage lengths, initial seepage length of 50m

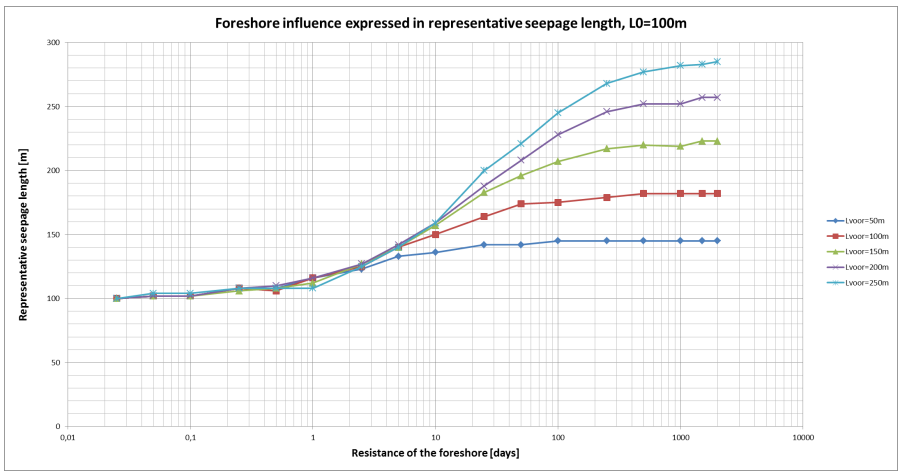


(b) Results expressed in representative seepage lengths, initial seepage length of 100m

Some comments can be placed by the above depicted graphs. As a maximum foreshore resistance, 2000 days was chosen, in the graphs can be noticed that even for this large resistance a minimal seepage through the foreshore occurs, as the representative seepage length is lower than the pipe length in the model(initial length + foreshore length). The difference between these two gets larger by increasing the foreshore length, this is however logical as more area leads to more seepage. It can also be seen that there's a difference between the results of the two initial seepage length. As the difference with a longer initial seepage length is larger, it can be concluded that some seepage occurs through the dike. This difference is however not significant.

# G

# Appendix:Case samples

## G.1. Salmsteke

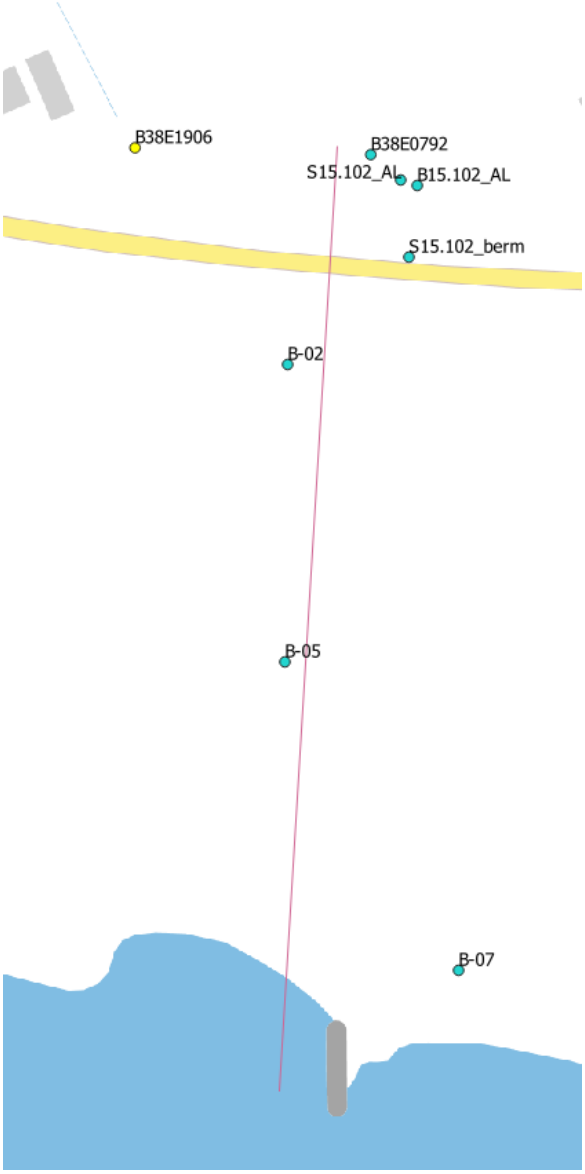


Figure G.1: Location of the samples for the Salmsteke case

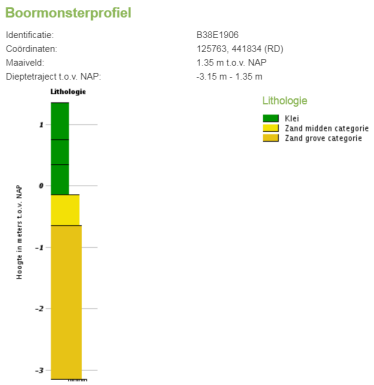


(a) Sample B38E1906

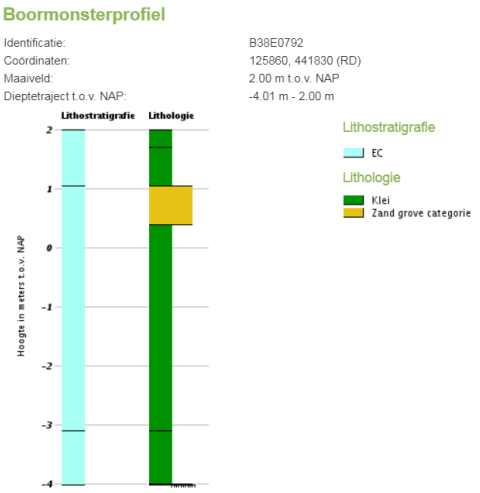


(b) Sample B38E0792

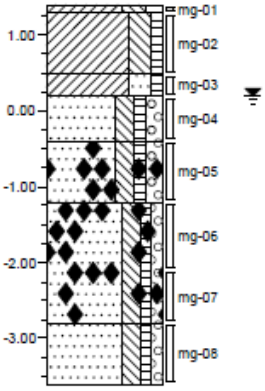


(a) Sample B02

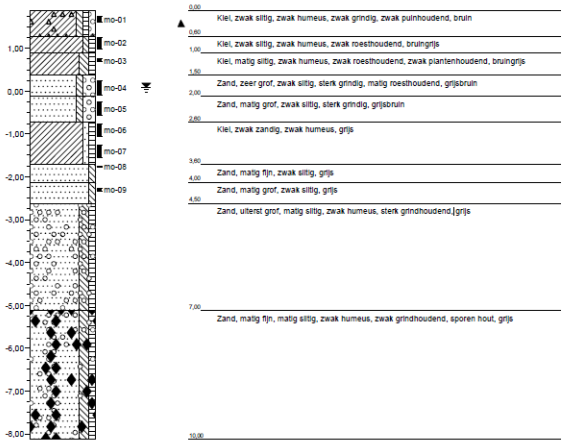


(b) Sample B-15.102-AL

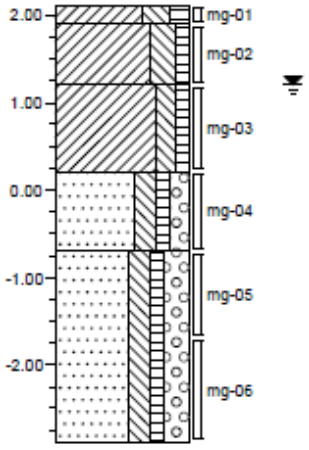


(a) Sample B05

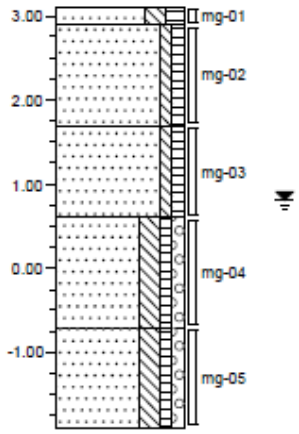


(b) Sample B07

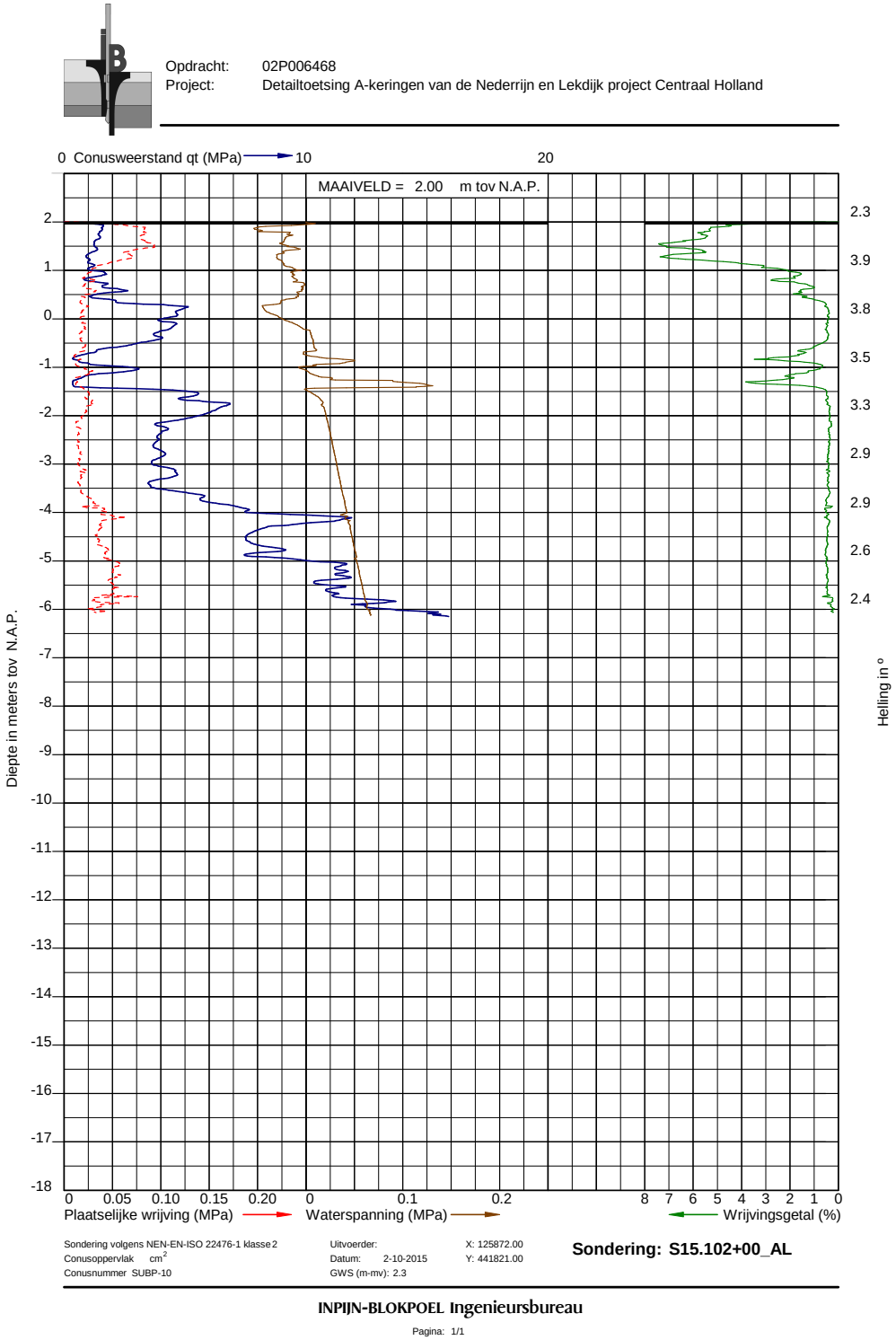


Figure G.5: Samples Salmsteke:S15 102 AL

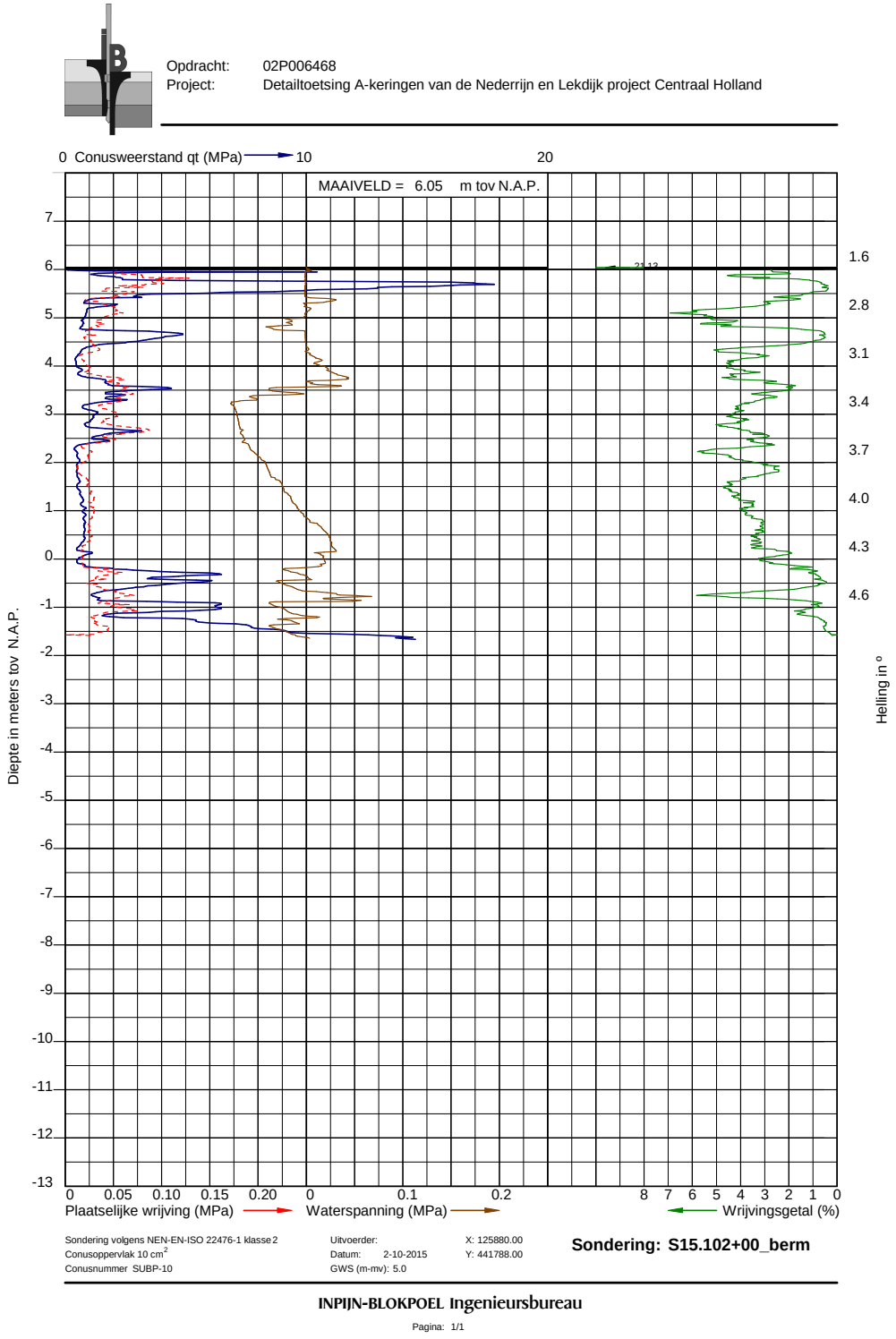


Figure G.6: Samples Salmsteke:S15 102 BERM

## G.2. Honswijk

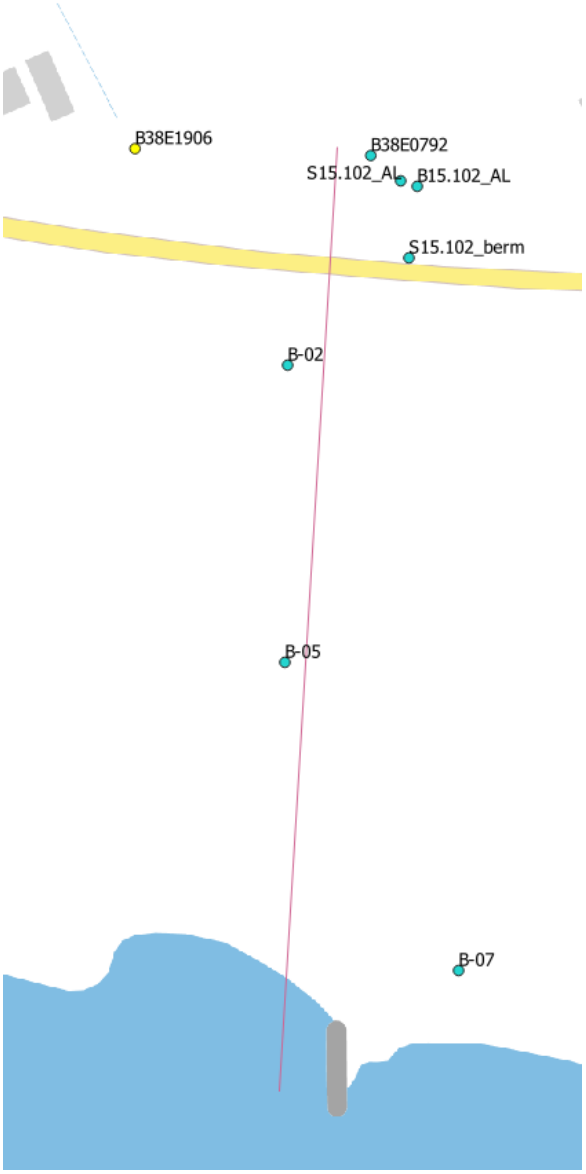


Figure G.7: Location of the samples for the Salmsteke case

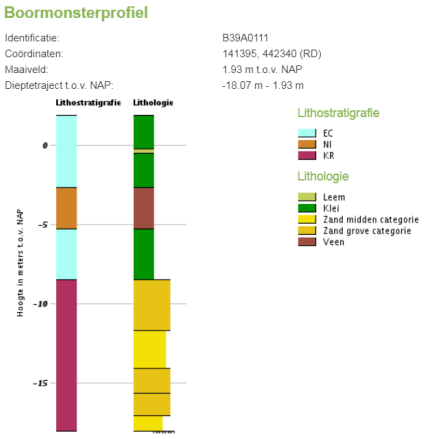


(a) Sample B39A0111

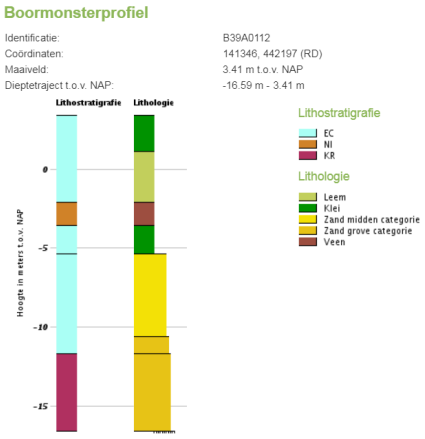


(b) Sample B39A0112

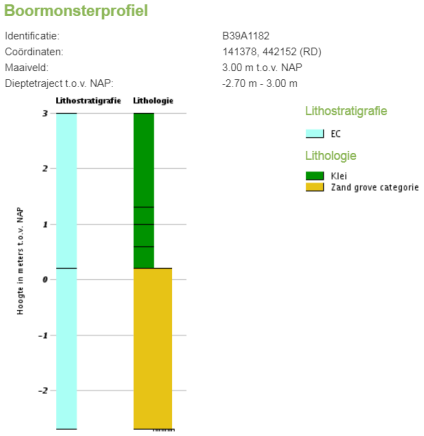


(a) Sample B39A1182

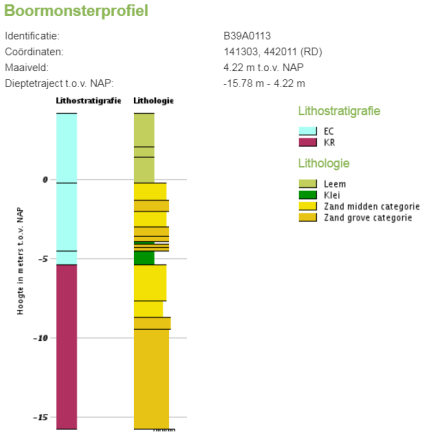


(b) Sample B39A0113

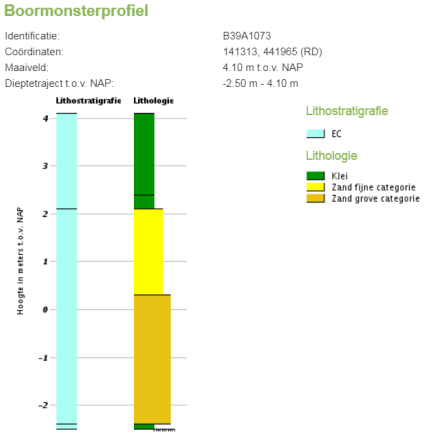


Figure G.10: Sample B39A1073

## G.3. Den Oord

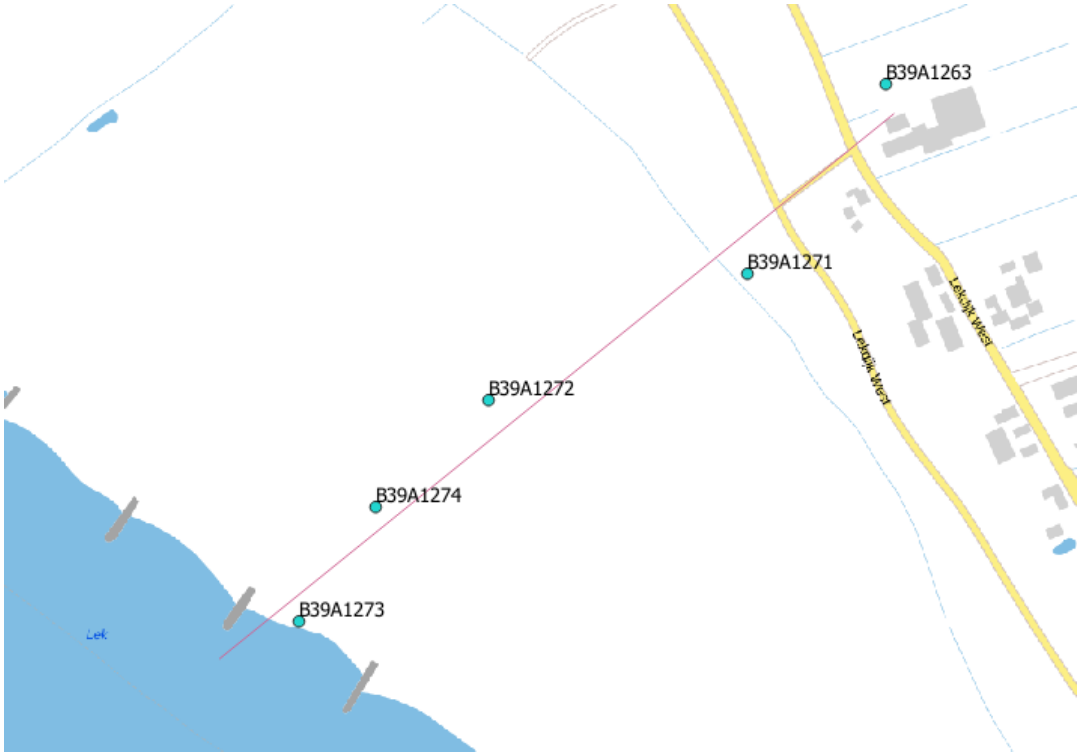


Figure G.11: Location of the samples for the Den Oord case

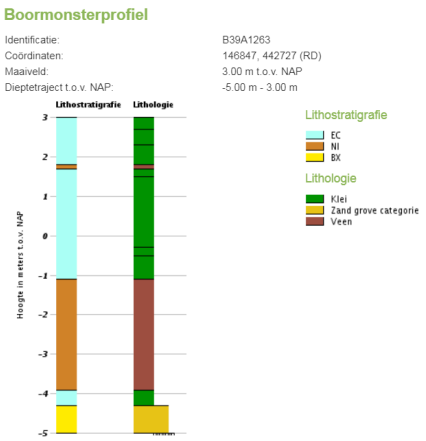


(a) Sample B39A1263

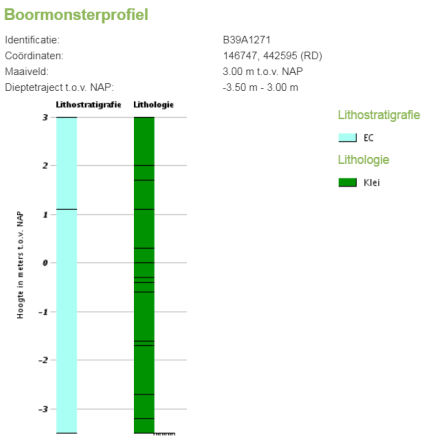


(b) Sample B39A1271

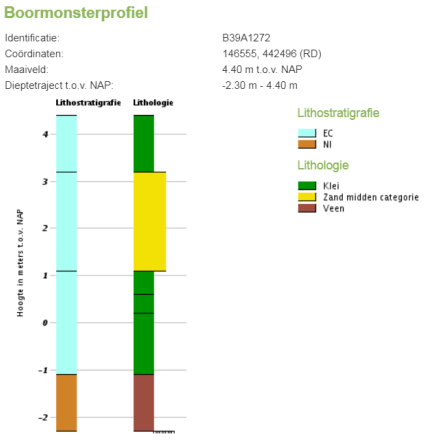


(a) Sample B39A1272

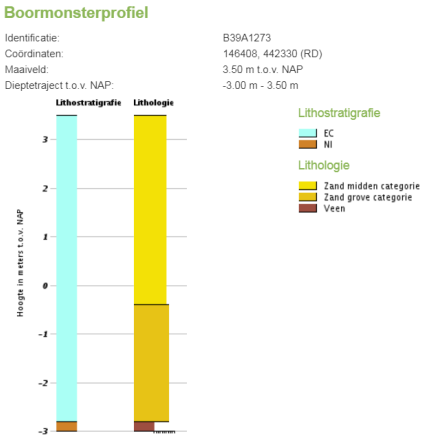


(b) Sample B39A1273

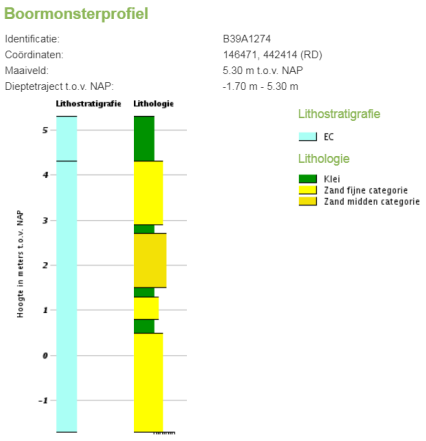


Figure G.14: Sample B39A1274

# Appendix: GeoTop model

## H.1. Introduction

The dutch subsoil is mapped by the Geological service of TNO, a knowledge institute in the Netherlands. Mapping the soil is done by use of several computer models, one of these models is the GeoTop model. The GeoTop model is a 3D-model in which the subsoil to a depth of around 30-50m is mapped. In the GeoTop model, information about the soil types (lithoclasses) with some physical and chemical characteristics can be found.

## H.2. Description of the model

The GeoTop models gives the information about the soil in a 3D image which is divided in voxels. The voxels in the model are 100x100x0.5m (width x length x height). The base of the model is the information from the samples (core-drillings, boreholes, etc.) which can be found at Dinoloket([33]), this information is supplemented with sample data from external sources.

Next to the samples which are used for the model, digital maps, for instance geological maps, are also used to make the model as complete as possible. As the soil is not measured in detail at all locations, the available data is translated to a complete model by use of interpolation techniques, this will be explained later. The GeoTop model does not cover the whole area of the Netherlands. An overview of the mapped areas can be seen in fig. H.1. In this figure different areas can be seen, these *modelareas* are the areas which are mapped at once based on the available data.

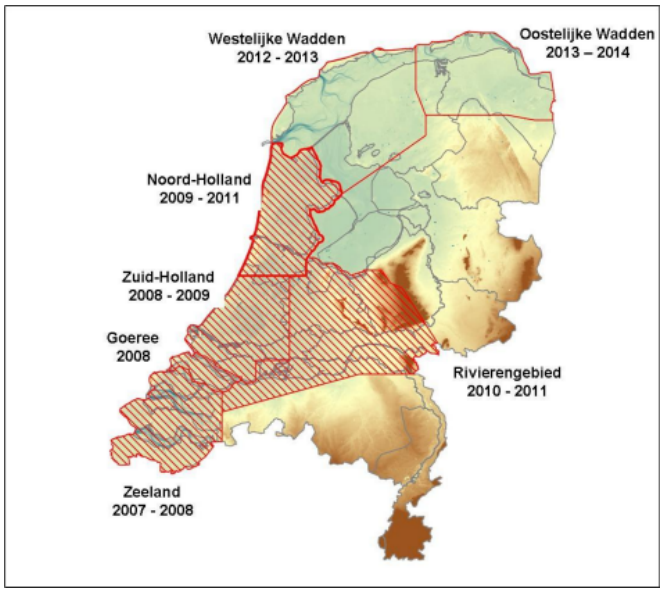


Figure H.1: Coverage GeoTop model[50]

As described above, the GeoTop model is a made out of voxels which contain a certain information about the soil. The voxelmodel can be described as an area which is divided in "boxes" of the same size in length, width and height. These boxes, or from now on voxels, have certain soil characteristics. In one voxel these characteristics are uniform. For this Thesis, the soil type characteristics are of the highest interest. How the soil type, or lithoclass, is determined per voxel will be explained in the next section.

## H.3. Determining the soil types(lithoclasses) [51]

Because the soil type is, at most places, determined by an interpolation method, the soil type is displayed as a "most probable soil type". In the GeoTop model, 9 classes are used:

1. Organic material (peat);
2. Clay;
3. Clayey sand or sandy clay;
4. Fine sand;
5. Medium coarse sand;
6. Coarse sand;
7. Gravel;
8. Shells.

To determine the soil type, the subsoil is divided per geological unit, these geological units can be seen as the different deposits in the subsoil. Per geological unit, each soil class has a probability of occurrence(**estimate**). Also a global ratio of occurrences is needed. In the following step the probability of occurrence for each class is conditioned to the global ratio(**target**). Conditioning can best be explained by an example.

**Example: assigning soil classes**
**Initial data**

Table H.1: Estimate data

| Voxel no. | Soil class 1 | Soil class 2 | Soil class 3 |
|---|---|---|---|
| 1 | 0.3 | 0.4 | 0.3 |
| 2 | 0.2 | 0.7 | 0.1 |
| 3 | 0.6 | 0.1 | 0.3 |
| 4 | 0.5 | 0.1 | 0.4 |

Target data:

- Soil class 1 : 0.3;
- Soil class 2 : 0.6;
- Soil class 3 : 0.1

Target voxels:

- Soil class 1 : $0.3 * 4 = 1.2$;
- Soil class 2 : $0.6 * 4 = 2.4$;
- Soil class 3 : $0.1 * 4 = 0.4$.

**Step 1**:
Highest target voxel: Soil class 2.
Highest estimate for soil class 2: Voxel 2 → Voxel 2 gets soil class 2.
1 out of 2.4 voxels filled, next highest target voxel is used.

**Step 2**:
Highest target voxel: Soil class 1.
Highest estimate for soil class 1: Voxel 3 → Voxel 3 gets soil class 1.
1 out of 1.2 voxels filled, next highest target voxel is used.

**Step 3**:
Highest target voxel: Soil class 3.
Highest estimate for soil class 3: Voxel 4 → Voxel 4 gets soil class 3.
1 out of 0.4 voxels filled, next highest target voxel is used.

**Step 4**:
Highest target voxel: Soil class 2.
Last voxel: Voxel 1 → Voxel 1 gets soil class 2.
2 out of 2.4 voxels filled. All voxels are now filed.

Table H.2: Conditioning result

| Voxel no. | Soil class: |
|---|---|
| 1 | 2 |
| 2 | 2 |
| 3 | 1 |
| 4 | 3 |

## H.4. Model uncertainties([52])

In the GeoTop model, two clear uncertainties can be identified:

1. Uncertainty in geological unit;
2. Uncertainty in soil class.

In the set-up of the GeoTop model, the most important source are the samples from Dinoloket([33]). Most of the samples do not cover the whole 30-50m in depth of the GeoTop model, this means that when going in depth, less and less samples remain. This states that for the deeper voxels the soil class or geological unit must be determined based on less data and more and more based on estimations. These estimations are made based on stochastic interpolation techniques. In the stochastic interpolation techniques the probabilities of occurrence of the several soil classes is determined based on around 100 calculations per voxel.

In this Thesis the heterogeneities in the Holocene layer are used. The Holocene deposit, in comparison with, for instance, the Pleistocene deposit, is a very variable deposit. More variations in the deposit can lead to a more inaccurate estimation, as more possibilities per voxel can occur.

# Appendix: Results generic subsoil research

## I.1. Hydraulic conductivity aquifer = 20m/day

Seepage length =25m

Table I.1: Results continuous layer- Lseep=25m - Kaq=20m/day

| Layer depth m: | | | 10 | 9 | 8 | 7 | 6 | 5 | 4 | 3 | 2 |
|---|---|---|---|---|---|---|---|---|---|---|---|
| C-value layer | K-value layer | | | | | | | | | | |
| 2000 | 0.00025 | | 17.6 | 17.6 | 23.5 | 23.5 | 29.4 | 35.3 | 47.1 | 58.8 | 82.4 |
| 1000 | 0.0005 | | 17.6 | 17.6 | 23.5 | 23.5 | 29.4 | 35.3 | 47.1 | 58.8 | 82.4 |
| 500 | 0.001 | | 17.6 | 17.6 | 23.5 | 23.5 | 29.4 | 35.3 | 47.1 | 58.8 | 82.4 |
| 200 | 0.0025 | | 17.6 | 17.6 | 23.5 | 23.5 | 29.4 | 35.3 | 47.1 | 58.8 | 82.4 |
| 100 | 0.005 | | 17.6 | 17.6 | 23.5 | 23.5 | 29.4 | 35.3 | 47.1 | 58.8 | 82.4 |
| 50 | 0.01 | | 17.6 | 17.6 | 23.5 | 23.5 | 29.4 | 35.3 | 47.1 | 58.8 | 82.4 |
| 20 | 0.025 | | 17.6 | 17.6 | 17.6 | 23.5 | 29.4 | 35.3 | 47.1 | 58.8 | 82.4 |
| 10 | 0.05 | | 11.8 | 17.6 | 17.6 | 23.5 | 29.4 | 29.4 | 41.2 | 52.9 | 64.7 |
| 5 | 0.1 | | 11.8 | 11.8 | 17.6 | 17.6 | 23.5 | 29.4 | 53.3 | 41.2 | 58.8 |
| 2 | 0.25 | | 5.9 | 5.9 | 11.8 | 11.8 | 11.8 | 17.6 | 23.5 | 29.4 | 35.3 |
| 1 | 0.5 | | 5.9 | 5.9 | 5.9 | 5.9 | 11.8 | 11.8 | 11.8 | 17.6 | 23.5 |
| 0.5 | 1.0 | | 5.9 | 5.9 | 5.9 | 5.9 | 5.9 | 5.9 | 11.8 | 11.8 | 11.8 |
| 0.2 | 2.5 | | 0.0 | 0.0 | 0.0 | 0.0 | 5.9 | 5.9 | 5.9 | 5.9 | 5.9 |
| 0.1 | 5 | | 0.0 | 0.0 | 0.0 | 0.0 | 0.0 | 0.0 | 0.0 | 0.0 | 5.9 |
| 0.05 | 10 | | 0.0 | 0.0 | 0.0 | 0.0 | 0.0 | 0.0 | 0.0 | 0.0 | 0.0 |
| 0.025 | 20 | | 0.0 | 0.0 | 0.0 | 0.0 | 0.0 | 0.0 | 0.0 | 0.0 | 0.0 |

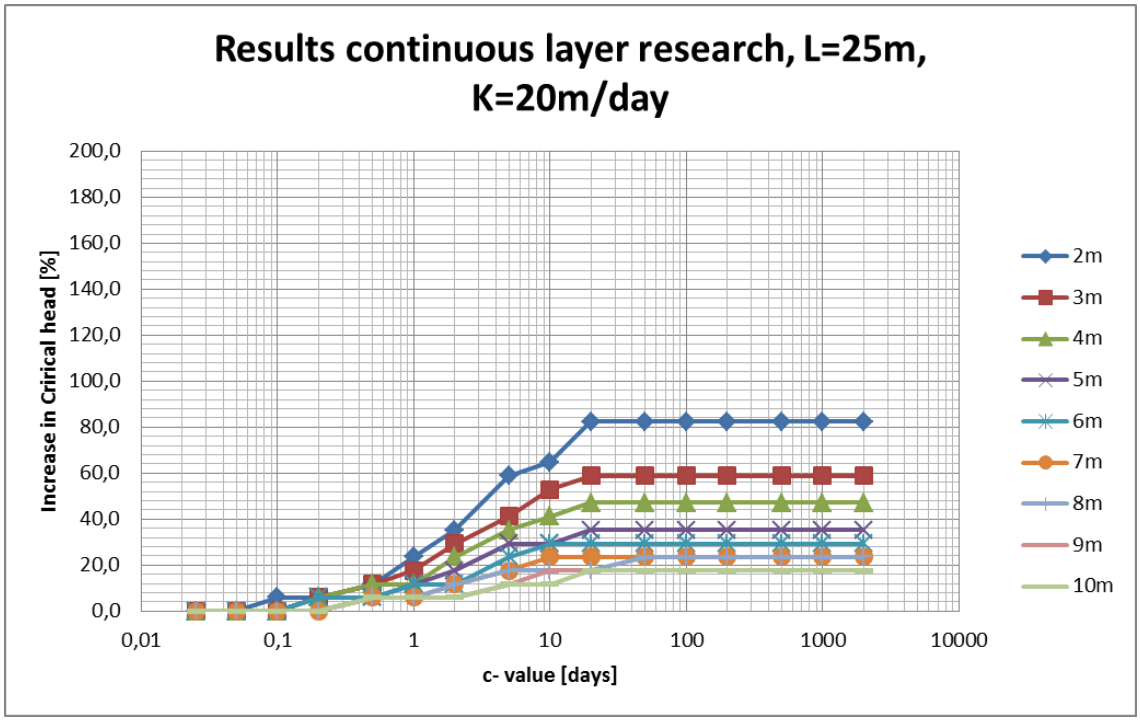


Figure I.1: Result: Seepage length=25m, Hydraulic conductivity aquifer = 20m/day

Seepage length =50m

Table I.2: Results continuous layer- Lseep=50m - Kaq=20m/day

| Layer depth m: | | | 10 | 9 | 8 | 7 | 6 | 5 | 4 | 3 | 2 |
|---|---|---|---|---|---|---|---|---|---|---|---|
| C-value layer | K-value layer | | | | | | | | | | |
| 2000 | 0.00025 | | 26.7 | 26.7 | 33.3 | 40 | 46.7 | 60 | 66.7 | 86.7 | 106.7 |
| 1000 | 0.0005 | | 26.7 | 26.7 | 33.3 | 40 | 46.7 | 60 | 66.7 | 86.7 | 106.7 |
| 500 | 0.001 | | 26.7 | 33.3 | 33.3 | 40 | 46.7 | 60 | 66.7 | 86.7 | 106.7 |
| 200 | 0.0025 | | 26.7 | 33.3 | 33.3 | 40 | 46.7 | 60 | 73.3 | 93.3 | 113.3 |
| 100 | 0.005 | | 26.7 | 33.3 | 33.3 | 40 | 46.7 | 60 | 73.3 | 93.3 | 113.3 |
| 50 | 0.01 | | 26.7 | 33.3 | 33.3 | 40 | 46.7 | 60 | 73.3 | 93.3 | 113.3 |
| 20 | 0.025 | | 26.7 | 33.3 | 33.3 | 40 | 46.7 | 53.3 | 66.7 | 80 | 106.7 |
| 10 | 0.05 | | 20.0 | 26.7 | 26.7 | 33.3 | 40 | 46.7 | 56.7 | 66.7 | 80 |
| 5 | 0.1 | | 13.3 | 20.0 | 20.0 | 26.7 | 26.7 | 33.3 | 40 | 46.7 | 53.3 |
| 2 | 0.25 | | 6.7 | 13.3 | 13.3 | 13.3 | 13.3 | 20.0 | 20.0 | 20.0 | 26.7 |
| 1 | 0.5 | | 3.3 | 6.7 | 6.7 | 6.7 | 6.7 | 13.3 | 13.3 | 13.3 | 13.3 |
| 0.5 | 1.0 | | 3.3 | 6.7 | 6.7 | 6.7 | 6.7 | 6.7 | 6.7 | 6.7 | 6.7 |
| 0.2 | 2.5 | | 0.0 | 0.0 | 0.0 | 0.0 | 0.0 | 0.0 | 3.3 | 3.3 | 6.7 |
| 0.1 | 5 | | 0.0 | 0.0 | 0.0 | 0.0 | 0.0 | 0.0 | 3.3 | 3.3 | 3.3 |
| 0.05 | 10 | | 0.0 | 0.0 | 0.0 | 0.0 | 0.0 | 0.0 | 0.0 | 0.0 | 0.0 |
| 0.025 | 20 | | 0.0 | 0.0 | 0.0 | 0.0 | 0.0 | 0.0 | 0.0 | 0.0 | 0.0 |

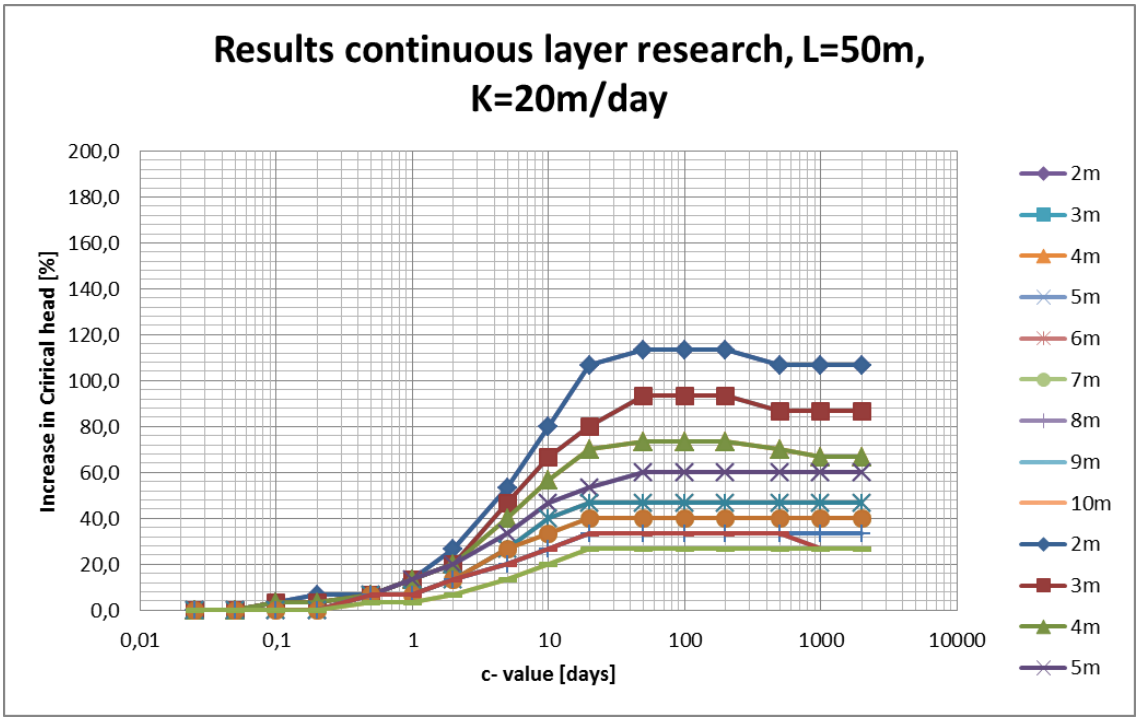


Figure I.2: Result: Seepage length=50m, Hydraulic conductivity aquifer = 20m/day

Seepage length =100m

Table I.3: Results continuous layer- Lseep=100m - Kaq=20m/day

| Layer depth m: | | 10 | 9 | 8 | 7 | 6 | 5 | 4 | 3 | 2 |
|---|---|---|---|---|---|---|---|---|---|---|
| C-value layer | K-value layer | | | | | | | | | |
| 2000 | 0.00025 | 43.4 | 50.9 | 54.7 | 62.3 | 73.6 | 77.4 | 96.2 | 107.5 | 137.7 |
| 1000 | 0.0005 | 47.2 | 50.9 | 54.7 | 62.3 | 73.6 | 81.1 | 100 | 118.9 | 141.5 |
| 500 | 0.001 | 47.2 | 50.9 | 58.5 | 66.0 | 73.6 | 84.9 | 103.8 | 122.6 | 149.1 |
| 200 | 0.0025 | 47.2 | 50.9 | 58.5 | 66.0 | 77.4 | 88.7 | 107.5 | 134.0 | 183.0 |
| 100 | 0.005 | 47.2 | 50.9 | 58.5 | 69.8 | 81.1 | 88.7 | 107.5 | 134.0 | 175.5 |
| 50 | 0.01 | 47.2 | 50.9 | 58.5 | 66.0 | 77.4 | 88.7 | 107.5 | 130.2 | 167.9 |
| 20 | 0.025 | 39.6 | 43.4 | 47.2 | 54.7 | 62.3 | 69.8 | 81.1 | 96.2 | 107.5 |
| 10 | 0.05 | 32.1 | 32.1 | 35.8 | 39.6 | 43.4 | 50.9 | 54.7 | 58.5 | 69.8 |
| 5 | 0.1 | 20.8 | 24.5 | 28.3 | 32.1 | 28.3 | 28.3 | 32.1 | 35.8 | 39.6 |
| 2 | 0.25 | 13.2 | 13.2 | 13.2 | 13.2 | 13.2 | 13.2 | 13.2 | 13.2 | 17.0 |
| 1 | 0.5 | 9.4 | 9.4 | 9.4 | 9.4 | 9.4 | 9.4 | 9.4 | 9.4 | 9.4 |
| 0.5 | 1.0 | 5.7 | 5.7 | 5.7 | 5.7 | 5.7 | 5.7 | 5.7 | 5.7 | 5.7 |
| 0.2 | 2.5 | 5.7 | 5.7 | 5.7 | 5.7 | 5.7 | 5.7 | 5.7 | 5.7 | 1.9 |
| 0.1 | 5 | 5.7 | 5.7 | 5.7 | 5.7 | 5.7 | 5.7 | 5.7 | 1.9 | 1.9 |
| 0.05 | 10 | 5.7 | 1.9 | 1.9 | 1.9 | 1.9 | 1.9 | 1.9 | 1.9 | 1.9 |
| 0.025 | 20 | 1.9 | 1.9 | 1.9 | 1.9 | 1.9 | 1.9 | 1.9 | 1.9 | 1.9 |

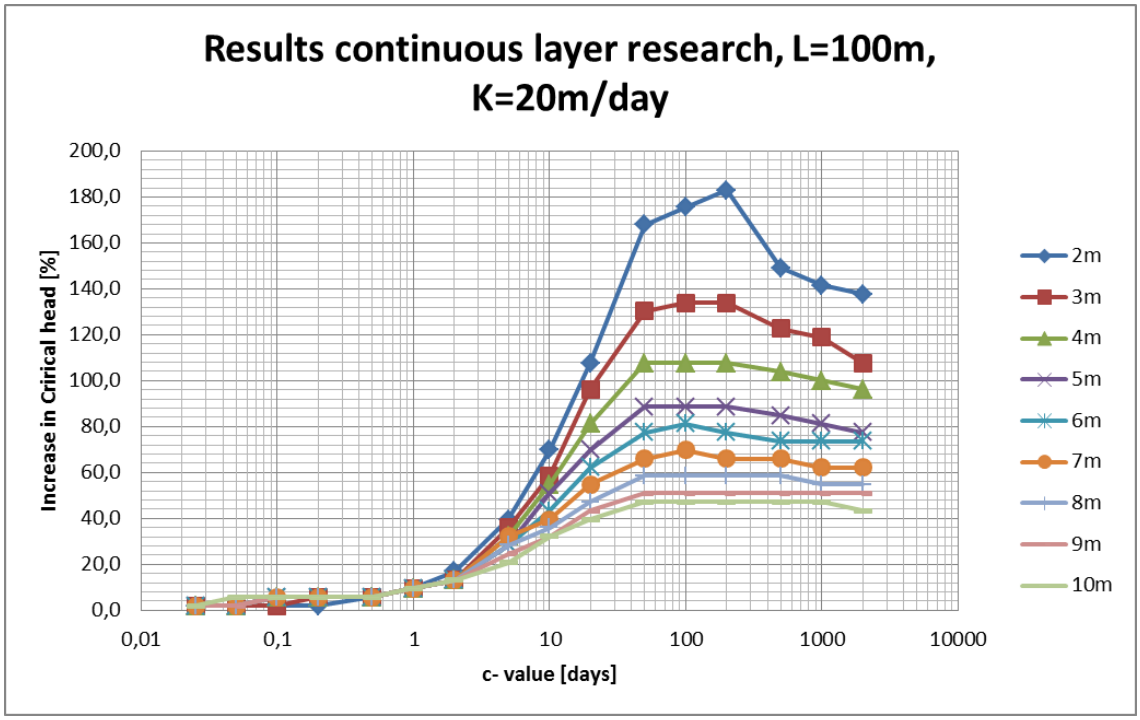


Figure I.3: Result: Seepage length=100m, Hydraulic conductivity aquifer = 20m/day

# I.2. Hydraulic conductivity aquifer = 40m/day

Seepage length =25m

Table I.4: Results continuous layer- Lseep=25m - Kaq=40m/day

| Layer depth m: | | | 10 | 9 | 8 | 7 | 6 | 5 | 4 | 3 | 2 |
|---|---|---|---|---|---|---|---|---|---|---|---|
| C-value layer | K-value layer | | | | | | | | | | |
| 2000 | 0.00025 | | 23.1 | 23.1 | 23.1 | 30.8 | 30.8 | 38.5 | 38.5 | 61.5 | 69.2 |
| 1000 | 0.0005 | | 23.1 | 23.1 | 23.1 | 30.8 | 30.8 | 38.5 | 38.5 | 61.5 | 69.2 |
| 500 | 0.001 | | 23.1 | 23.1 | 23.1 | 30.8 | 30.8 | 38.5 | 38.5 | 61.5 | 69.2 |
| 200 | 0.0025 | | 23.1 | 23.1 | 23.1 | 30.8 | 30.8 | 38.5 | 38.5 | 61.5 | 92.3 |
| 100 | 0.005 | | 23.1 | 23.1 | 23.1 | 30.8 | 30.8 | 38.5 | 38.5 | 69.2 | 92.3 |
| 50 | 0.01 | | 23.1 | 23.1 | 23.1 | 30.8 | 30.8 | 38.5 | 38.5 | 69.2 | 92.3 |
| 20 | 0.025 | | 23.1 | 23.1 | 23.1 | 30.8 | 30.8 | 38.5 | 38.5 | 69.2 | 92.3 |
| 10 | 0.05 | | 15.4 | 23.1 | 23.1 | 30.8 | 30.8 | 38.5 | 38.5 | 61.5 | 84.6 |
| 5 | 0.1 | | 15.4 | 15.4 | 23.1 | 23.1 | 30.8 | 38.5 | 38.5 | 61.5 | 69.2 |
| 2 | 0.25 | | 15.4 | 15.4 | 15.4 | 23.1 | 23.1 | 30.8 | 30.8 | 46.2 | 53.8 |
| 1 | 0.5 | | 7.7 | 15.4 | 15.4 | 15.4 | 15.4 | 23.1 | 23.1 | 30.8 | 38.5 |
| 0.5 | 1.0 | | 7.7 | 7.7 | 7.7 | 15.4 | 15.4 | 15.4 | 15.4 | 23.1 | 23.1 |
| 0.2 | 2.5 | | 7.7 | 7.7 | 7.7 | 7.7 | 7.7 | 7.7 | 7.7 | 15.4 | 15.4 |
| 0.1 | 5 | | 7.7 | 7.7 | 7.7 | 7.7 | 7.7 | 7.7 | 7.7 | 7.7 | 7.7 |
| 0.05 | 10 | | 7.7 | 0.0 | 7.7 | 7.7 | 7.7 | 7.7 | 7.7 | 7.7 | 7.7 |
| 0.025 | 20 | | 0.0 | 0.0 | 0.0 | 0.0 | 0.0 | 0.0 | 0.0 | 7.7 | 7.7 |
| 0.0125 | 40 | | 0.0 | 0.0 | 0.0 | 0.0 | 0.0 | 0.0 | 0.0 | 0.0 | 0.0 |

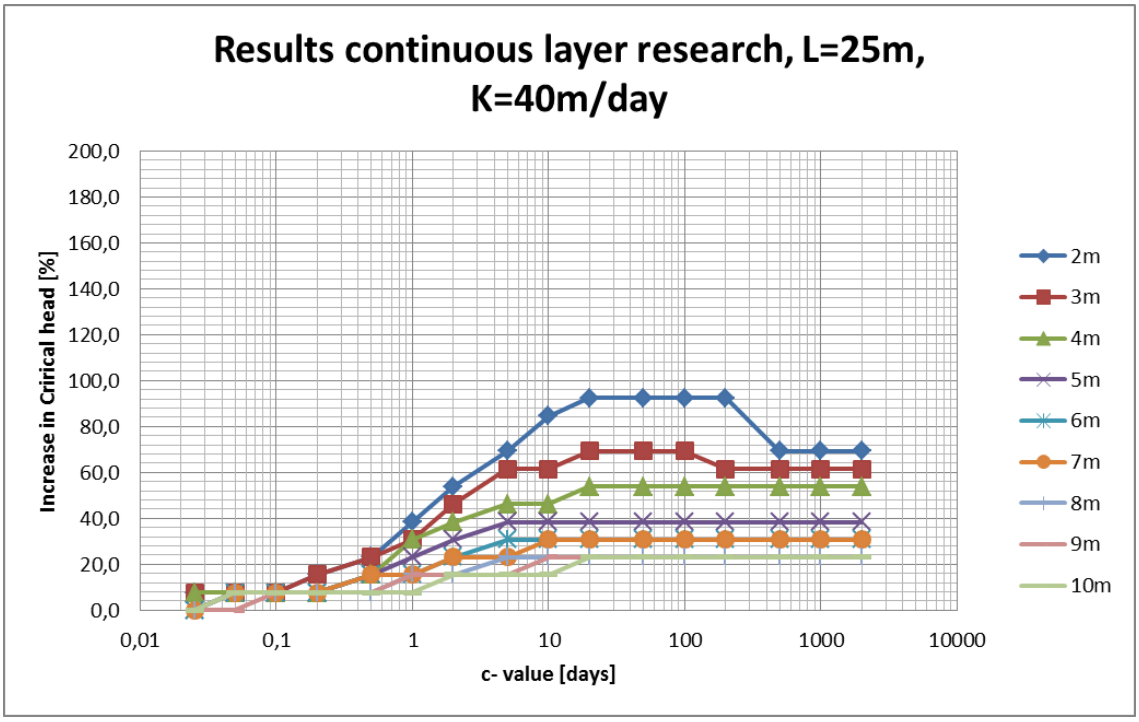


Figure I.4: Result: Seepage length=25m, Hydraulic conductivity aquifer = 40m/day

Seepage length =50m

Table I.5: Results continuous layer- Lseep=50m - Kaq=40m/day

| Layer depth m: | | 10 | 9 | 8 | 7 | 6 | 5 | 4 | 3 | 2 |
|---|---|---|---|---|---|---|---|---|---|---|
| C-value layer | K-value layer | | | | | | | | | |
| 2000 | 0.00025 | 25.0 | 29.2 | 33.3 | 41.7 | 45.8 | 58.3 | 66.7 | 70.8 | 104.2 |
| 1000 | 0.0005 | 25.0 | 29.2 | 33.3 | 41.7 | 45.8 | 58.3 | 66.7 | 70.8 | 104.2 |
| 500 | 0.001 | 25.0 | 29.2 | 37.5 | 41.7 | 50.0 | 58.3 | 66.7 | 70.8 | 108.3 |
| 200 | 0.0025 | 25.0 | 29.2 | 37.5 | 41.7 | 50.0 | 58.3 | 66.7 | 70.8 | 108.3 |
| 100 | 0.005 | 29.2 | 33.3 | 37.5 | 41.7 | 50.0 | 58.3 | 70.8 | 75.0 | 108.3 |
| 50 | 0.01 | 29.2 | 33.3 | 37.5 | 41.7 | 50.0 | 58.3 | 70.8 | 75.0 | 120.8 |
| 20 | 0.025 | 25.0 | 29.2 | 37.5 | 41.7 | 50.0 | 58.3 | 70.8 | 75.0 | 120.8 |
| 10 | 0.05 | 25.0 | 29.2 | 33.3 | 37.5 | 45.8 | 54.2 | 66.7 | 70.8 | 104.2 |
| 5 | 0.1 | 20.8 | 25.0 | 29.2 | 33.3 | 37.5 | 45.8 | 54.2 | 54.2 | 75.0 |
| 2 | 0.25 | 16.7 | 16.7 | 20.8 | 20.8 | 25.0 | 29.2 | 33.3 | 33.3 | 41.7 |
| 1 | 0.5 | 8.3 | 12.5 | 12.5 | 12.5 | 16.7 | 16.7 | 20.8 | 16.7 | 25.0 |
| 0.5 | 1.0 | 4.2 | 8.3 | 8.3 | 8.3 | 8.3 | 12.5 | 12.5 | 8.3 | 16.7 |
| 0.2 | 2.5 | 4.2 | 4.2 | 4.2 | 4.2 | 4.2 | 8.3 | 4.2 | 4.2 | 8.3 |
| 0.1 | 5 | 0.0 | 0.0 | 0.0 | 0.0 | 4.2 | 4.2 | 0.0 | 0.0 | 4.2 |
| 0.05 | 10 | 0.0 | 0.0 | 0.0 | 0.0 | 0.0 | 0.0 | 0.0 | 0.0 | 0.0 |
| 0.025 | 20 | 0.0 | 0.0 | 0.0 | 0.0 | 0.0 | 0.0 | 0.0 | 0.0 | 0.0 |
| 0.0125 | 40 | 0.0 | 0.0 | 0.0 | 0.0 | 0.0 | 0.0 | 0.0 | 0.0 | 0.0 |

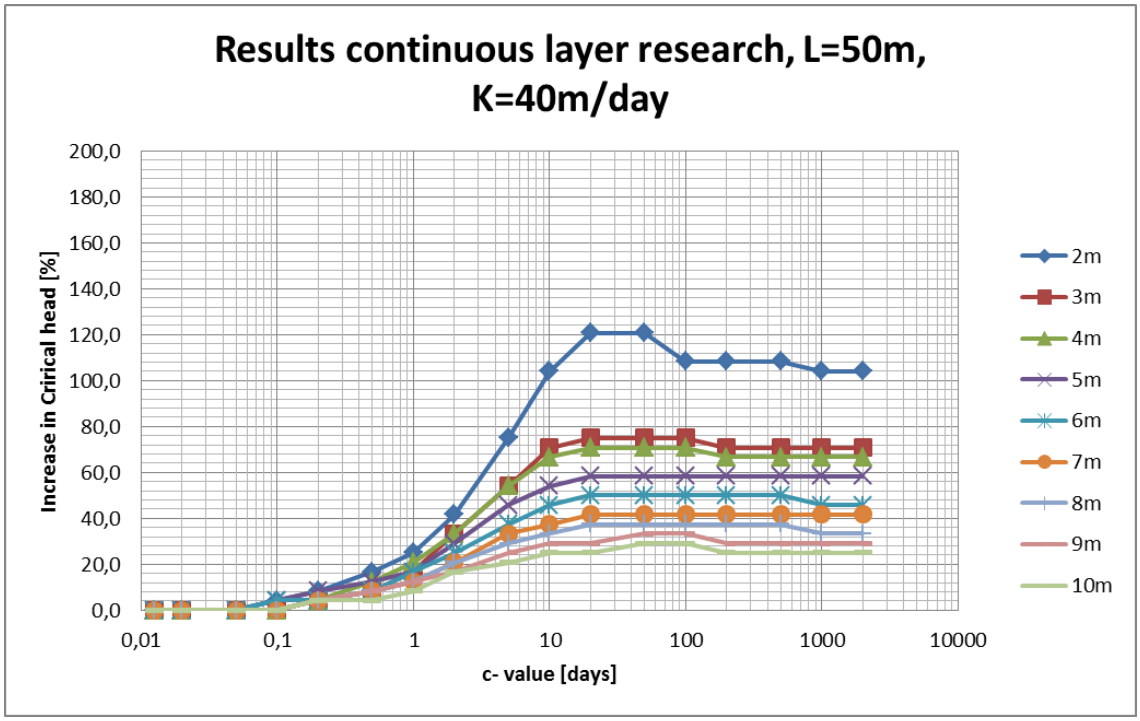


Figure I.5: Result: Seepage length=50m, Hydraulic conductivity aquifer = 40m/day

Seepage length =100m

Table I.6: Results continuous layer- Lseep=100m - Kaq=40m/day

| Layer depth m: | | 10 | 9 | 8 | 7 | 6 | 5 | 4 | 3 | 2 |
|---|---|---|---|---|---|---|---|---|---|---|
| C-value layer | K-value layer | | | | | | | | | |
| 2000 | 0.00025 | 34.1 | 45.5 | 47.7 | 56.8 | 65.9 | 70.5 | 88.6 | 106.8 | 136.4 |
| 1000 | 0.0005 | 34.1 | 45.5 | 47.7 | 56.8 | 65.9 | 70.5 | 88.6 | 109.1 | 138.6 |
| 500 | 0.001 | 38.6 | 45.5 | 50.0 | 54.5 | 65.9 | 75.0 | 90.9 | 111.4 | 140.9 |
| 200 | 0.0025 | 40.9 | 47.7 | 52.3 | 59.1 | 68.2 | 75.0 | 95.5 | 118.2 | 150.0 |
| 100 | 0.005 | 40.9 | 47.7 | 52.3 | 61.4 | 70.5 | 81.8 | 100.0 | 122.7 | 163.6 |
| 50 | 0.01 | 40.9 | 47.7 | 54.5 | 59.1 | 72.7 | 84.1 | 102.3 | 122.7 | 168.2 |
| 20 | 0.025 | 40.9 | 45.5 | 50.0 | 59.1 | 68.2 | 77.3 | 93.2 | 118.2 | 140.9 |
| 10 | 0.05 | 34.1 | 38.6 | 43.2 | 47.7 | 56.8 | 61.4 | 70.5 | 111.4 | 93.2 |
| 5 | 0.1 | 25.0 | 27.3 | 31.8 | 34.1 | 38.6 | 40.9 | 43.2 | 50.0 | 54.5 |
| 2 | 0.25 | 13.6 | 15.9 | 15.9 | 18.2 | 18.2 | 22.7 | 20.5 | 20.5 | 27.3 |
| 1 | 0.5 | 9.1 | 9.1 | 9.1 | 9.1 | 9.1 | 11.4 | 11.4 | 9.1 | 11.4 |
| 0.5 | 1.0 | 4.5 | 4.5 | 6.8 | 6.8 | 4.5 | 4.5 | 4.5 | 4.5 | 4.5 |
| 0.2 | 2.5 | 2.3 | 2.3 | 2.3 | 2.3 | 2.3 | 2.3 | 2.3 | 0.0 | 2.3 |
| 0.1 | 5 | 0.0 | 2.3 | 2.3 | 2.3 | 2.3 | 2.3 | 0.0 | 0.0 | 0.0 |
| 0.05 | 10 | 0.0 | 0.0 | 2.3 | 2.3 | 0.0 | 0.0 | 0.0 | 0.0 | 0.0 |
| 0.025 | 20 | 0.0 | 0.0 | 0.0 | 0.0 | 0.0 | 0.0 | 0.0 | 0.0 | 0.0 |
| 0.0125 | 40 | 0.0 | 0.0 | 0.0 | 0.0 | 0.0 | 0.0 | 0.0 | 0.0 | 0.0 |

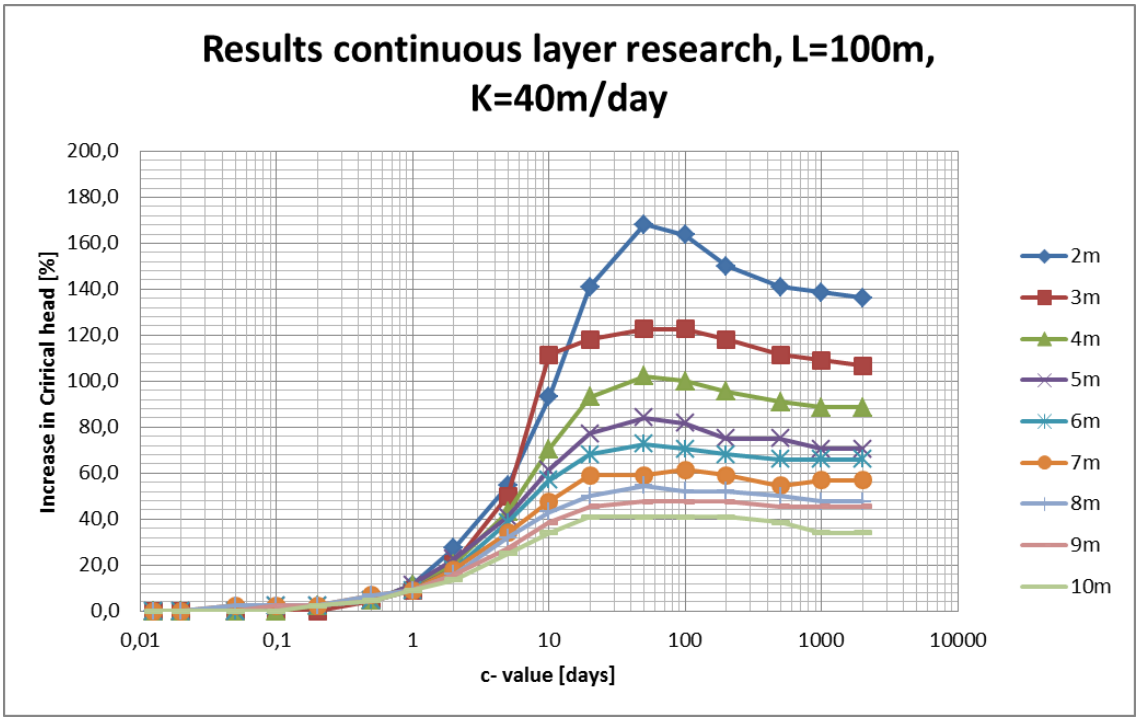


Figure I.6: Result: Seepage length=100m, Hydraulic conductivity aquifer = 40m/day

# J

# Appendix: Results heterogeneity models

## J.1. Salmsteke

Model Salmsteke 1

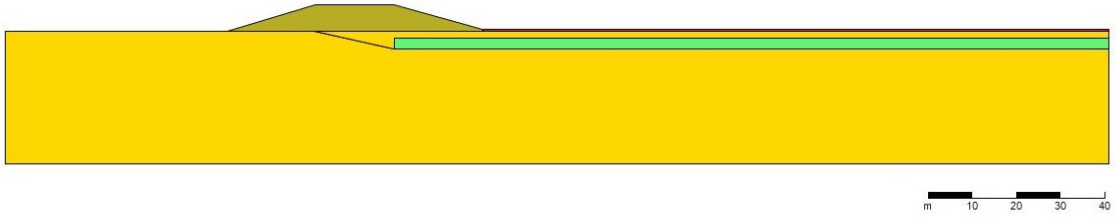


Figure J.1: D-Geo Flow model, Salmsteke model 1

Table J.1: Results case Salmsteke, model 1

| Hyd, cond, $[m/day]$ | Critical head $[m]$ | In-/decrease in Crit. head [%] |
|---|---|---|
| 0.002 | 4.1 | 20 |
| 0.15 | 3.7 | 9 |

Model Salmsteke 2

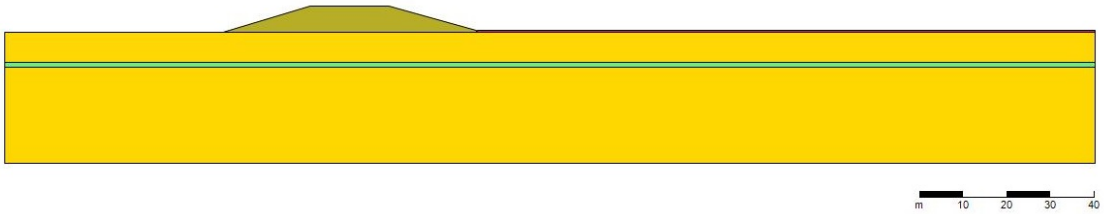


Figure J.2: D-Geo Flow model, Salmsteke model 2

Table J.2: Results case Salmsteke, model 2

| Thickness $[m]$ | Hyd, cond, $[m/day]$ | Critical head $[m]$ | In-/decrease in Crit. head [%] |
|---|---|---|---|
| 1.0 | 0.002 | 5.0 | 47 |
| | 0.15 | 4.5 | 32 |
| 2.0 | 0.002 | 5.0 | 47 |
| | 0.15 | 4.8 | 41 |

Model Salmsteke 3

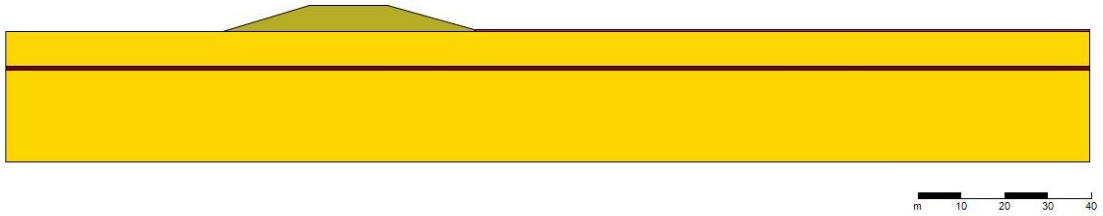


Figure J.3: D-Geo Flow model, Salmsteke model 3

Table J.3: Results case Salmsteke, model 3

| Thickness $[m]$ | Hyd, cond, $[m/day]$ | Critical head $[m]$ | In-/decrease in Crit. head [%] |
|---|---|---|---|
| 0.5 | 1 | 3.6 | 6 |
| | 5 | 3.5 | 3 |
| 1.0 | 1 | 3.7 | 9 |
| | 5 | 3.5 | 3 |

Model Salmsteke 4

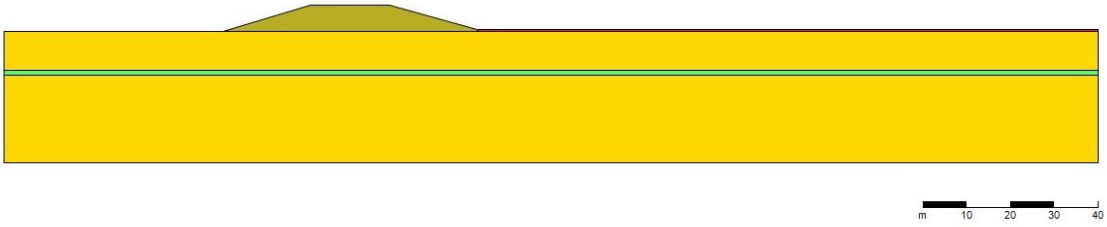


Figure J.4: D-Geo Flow model, Salmsteke model 4

Table J.4: Results case Salmsteke, model 4

| Thickness $[m]$ | Hyd, cond, $[m/day]$ | Critical head $[m]$ | In-/decrease in Crit. head [%] |
|---|---|---|---|
| 0.5 | 0.002 | 4.6 | 35 |
| | 0.15 | 4.0 | 17 |
| 1.0 | 0.002 | 4.6 | 35 |
| | 0.15 | 4.3 | 26 |

## J.2. Honswijk

Model 1 Honswijk

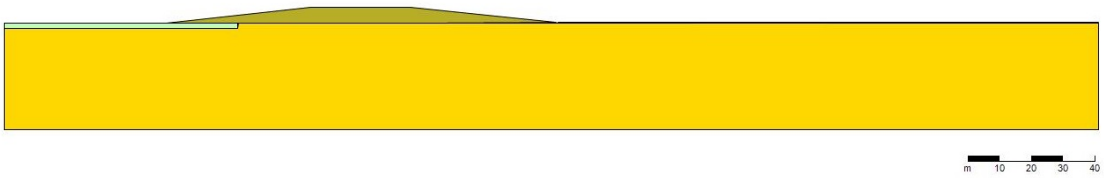


Figure J.5: D-Geo Flow model, Honswijk model 1

Table J.5: Results case Honswijk, model 1

| Hyd, cond, $[m/day]$ | Critical head $[m]$ | In-/decrease in Crit. head [%] |
|---|---|---|
| 0.1 | 14.8 | 139 |
| 0.5 | 8.3 | 34 |

Model 2 Honswijk

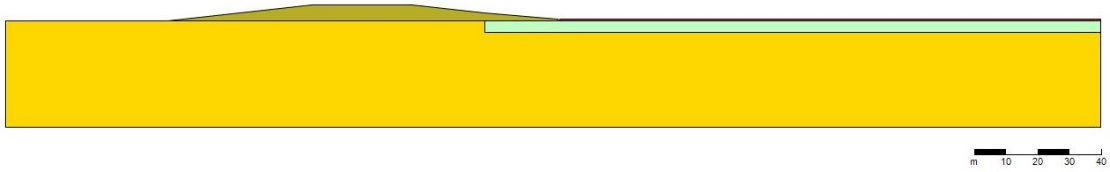


Figure J.6: D-Geo Flow model, Honswijk model 2

Table J.6: Results case Honswijk, model 2

| Hyd, cond, $[m/day]$ | Critical head $[m]$ | In-/decrease in Crit. head [%] |
|---|---|---|
| 0.1 | 5.7 | -8 |
| 0.5 | 4.6 | -26 |

Model 3 Honswijk

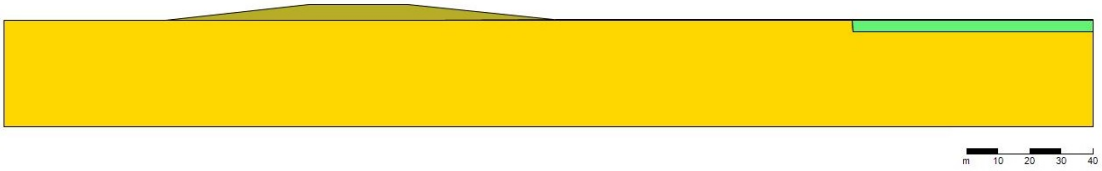


Figure J.7: D-Geo Flow model, Honswijk model 3

Table J.7: Results case Honswijk, model 3

| Hyd, cond, $[m/day]$ | Critical head $[m]$ | In-/decrease in Crit. head [%] |
|---|---|---|
| 0.002 | 6.2 | 0 |
| 0.15 | 6.2 | 0 |

Model 4 Honswijk

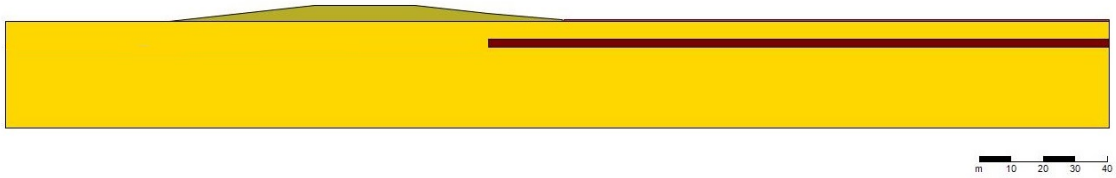


Figure J.8: D-Geo Flow model, Honswijk model 4

Table J.8: Results case Honswijk, model 4

| Thickness $[m]$ | Hyd, cond, $[m/day]$ | Critical head $[m]$ | In-/decrease in Crit. head [%] |
|---|---|---|---|
| 2.5 | 1.0 | 5.7 | -8 |
| | 5.0 | 5.7 | -8 |
| 3.0 | 1.0 | 5.7 | -8 |
| | 5.0 | 5.6 | -10 |

Model 5 Honswijk


Figure J.9: D-Geo Flow model, Honswijk model 5

Table J.9: Results case Honswijk, model 5

| Depth $NAP-[m]$ | Thickness $[m]$ | Hyd, cond, $[m/day]$ | Critical head $[m]$ | In-/decrease in Crit. head [%] |
|---|---|---|---|---|
| -4 | 1.5 | 0.002 | 10.8 | 74 |
| | | 0.15 | 9.0 | 45 |
| | 2.5 | 0.002 | 10.6 | 71 |
| | | 0.15 | 10.2 | 65 |
| -5 | 1.5 | 0.002 | 10.1 | 63 |
| | | 0.15 | 8.6 | 39 |
| | 2.5 | 0.002 | 10.3 | 66 |
| | | 0.15 | 9.4 | 52 |